

# Comparison of human alternatives to foetal bovine serum for osteogenic differentiation of mesenchymal stem/stromal cells

Jamie Mollentze,<sup>1</sup> Chrisna Durandt,<sup>1</sup> and Michael S. Pepper<sup>1</sup>

<sup>1</sup> Institute for Cellular and Molecular Medicine, Department of Immunology; SAMRC Extramural Unit for Stem Cell Research and Therapy, Faculty of Health Sciences, University of Pretoria, Pretoria, South Africa

Correspondence should be addressed to Michael Pepper: michael.pepper@up.ac.za

## 1. Introduction

Over the years, the use of adipose-derived stem/stromal cells (ASCs) in clinical applications have increased, especially in the field of regenerative medicine. As mentioned before, one of the main reasons why ASCs are preferred over bone marrow mesenchymal stem/stromal cells (BM-MSCs), is the fact that isolation from adipose tissue yields more stem/stromal cells when compared to isolation from bone marrow. The ability of ASCs to differentiate into various cell types, including adipocytes, osteoblasts, chondrocytes and myocytes, makes them attractive for use in regenerative medicine [1]. However, the clinical use of ASCs requires more research, and optimization, and standardization of isolation and differentiation methods before they can be considered as a therapeutic product.

The attachment, growth, maintenance and proliferation of ASCs is dependent on components present in FBS such as amino acids, hormones, various growth factors, vitamins, attachment factors like fibronectin, collagen and other trace elements like copper, zinc, tin and lead to name a few [2,3]. FBS has commonly been used in medium supplementation for cell culture despite all the associated disadvantages with. Some of these disadvantages include batch-to-batch variation, possibility of mycoplasma infection, prions and viral contamination, introduction of xenogeneic antigens causing immune activation during cell expansion, ethical concerns about animal welfare, and prolonged proliferation rates of ASCs [3–7]. These factors make the use of FBS in a cell culture setting non-compliant with Good Manufacturing Principles (GMP). One of the greatest disadvantages of FBS is the fact that it does not mimic the human environment which can lead to inaccurate results when measuring any cellular

response [8]. Researchers therefore are continuously seeking alternatives to FBS that will result in cell therapy products that are GMP compliant and are more physiologically compatible with the human body. Alternatives to FBS include chemically defined medium, or supplementing culture medium with additional growth factors, human serum albumin, human serum, platelet poor plasma (PPP), platelet rich plasma (PRP), fresh frozen plasma (FFP) or pooled human platelet lysate (pHPL). Using these human alternatives to FBS, the culture environment is more physiologically compatible with the human body and will likely result in a more accurate and reliable translation to the clinic [9]. The use of human blood products also reduces the risk of immune activation due to the absence of xenogeneic proteins [5].

In this study we investigated the effect of two human alternatives, PRP and pHPL, on osteogenic differentiation of ASCs. PRP is produced through the centrifugation of whole blood at reduced speeds to prevent platelets clumping. However, the platelets remain in the plasma, resulting in plasma that is enriched in platelets [10]. Platelets release growth factors upon activation that promote cell proliferation. This platelet-mediated activation can be achieved in three ways *in vitro*, namely through a single freeze thaw cycle, addition of thrombin or addition of  $Ca^{+2}$  [5]. The classic spindle-shape morphology of ASCs and phenotype is maintained when these cells are exposed to PRP-supplemented media. However, the proliferation rate of ASCs is significantly increased in PRP-supplemented media when compared to FBS-supplemented media [11]. Several studies have shown improved osteogenic differentiation of ASCs when PRP was used as a supplement in the culture medium [12–16]. Some of the disadvantages associated with PRP include batch-to-batch variation due to biological differences between donors and the absence of a standardised protocol in the production of PRP, which may lead to inconsistency and variability in results [17].

Another promising human alternative to FBS is pHPL, as it is associated with lower biological variability and higher yield quantities per batch for clinical applications [12]. pHPL is produced by pooling various donor platelet concentrates, routinely manufactured by blood banks, and subjecting these pooled concentrates to multiple freeze thaw cycles. The multiple freeze thaw cycles lyse the platelets which results in the release of growth factors [3]. Consequently, growth factor concentrations are much higher in pHPL compared to PRP [18]. pHPL is readily

available as it is manufactured worldwide by blood banks for the treatment of various disorders [4]. Like PRP, pHPL supplementation seems to influence the morphology and phenotype of ASCs. As reported for PRP, the proliferation rate of ASCs expanded in pHPL is also significantly higher than ASCs expanded in FBS [4,8,19]. Studies have shown that ASCs are capable of successful osteogenic differentiation in the presences of pHPL and that osteogenesis is enhanced when compared to ASCs differentiated in FBS [20–24]. There may also be variability in the production of pHPL, especially regarding the concentration of cytokines and growth factors present in the various batches produced.

*In vitro*, ASCs can be differentiated into osteoblasts through the addition of dexamethasone,  $\beta$ -glycerophosphate and ascorbate-2-phosphate to the complete growth/culture medium. Ascorbic acid and dexamethasone upregulate the activity of alkaline phosphatase (ALP), and therefore increase the rate at which osteogenesis occurs [25]. In the early stages of osteogenesis, ascorbic acid is responsible for the synthesis of the collagen matrix, which is later mineralized to form bone [26].  $\beta$ -glycerophosphate plays a role in this mineralization process [27]. Dexamethasone,  $\beta$ -glycerophosphate and ascorbate-2-phosphate act on genes that play an important role during osteogenic differentiation [25–28]. In this study, osteogenic differentiation of ASCs maintained in CGM supplemented with FBS was compared to the osteogenic differentiation of ASCs maintained in CGM supplemented with pHPL or PRP.

## 2. Methods

### 2.1. Isolation of ASCs

The lipoaspirate was collected from informed and consenting female patients undergoing liposuction or abdominoplasty procedures. All samples in this study tested negative for HIV, Hepatitis B and C and were free of mycoplasma. The protocol described by Zuk et al. [29] was used to isolate ASCs from lipoaspirate. Cells were cryopreserved until needed.

### 2.2. ASC Maintenance and Passaging

Cryovials containing ASCs were removed from the liquid nitrogen dewar and allowed to thaw slightly on ice. The thawed cells were maintained in a 37°C/5% CO<sub>2</sub> water-jacketed incubator and were assessed 2-3 times a week during which the culture medium was replaced with fresh

CGM. The cultures were passaged once the cells reached 80-90% confluency. To passage cells, the cells in the culture flasks were first washed with 4 mL pre-warmed PBS (2% pen/strep), after which 2-3 mL 0.25% of Trypsin-EDTA was added and incubated for 7 min at 37°C. The trypsin was neutralized by adding CGM (2-3 mL) to the cell suspension, and the contents was swirled gently to mix. The cell suspension was transferred to centrifuged tubes (each sample in a separate tube; tube size dependant on the number of culture flasks per culture) and centrifuged at 300 x *g* for 5 min. The supernatant was aspirated, and the cell pellet was re-suspended in CGM (1 mL per flask). To count the number of cells, 100  $\mu$ l of cell suspension, 5  $\mu$ l of 7-actinomycin D (7-AAD), 100  $\mu$ l of Flow-Count™ Fluorospheres and 400  $\mu$ l of PBS was added to a flow cytometry test tube (referred to as flow tube from hereon) and analysed on a CytoFLEX flow cytometer (Beckman Coulter, California, United States) (Supplementary Information A, Figure A1). Cells were reseeded at 5000 cells/cm<sup>2</sup> and the CGM was replaced every 3-4 days.

### 2.3. Characterization of ASCs

The International Society for Cell and Gene Therapy (ISCT) guidelines recommended that ASCs should express certain pre-defined cell surface markers. To confirm the immunophenotypic profiles of ASCs, the cells were stained with a panel of monoclonal antibodies consisting of CD34, CD36, CD44, CD45, CD73, CD90 and CD105 (Supplementary Information A, Table A1).

Compensation experiments were set up for FBS, pHPL and PRP. Compensation experiments and immunophenotyping experiments are described in the supplementary information (A).

### 2.4. Production of Human Alternatives

#### 2.4.1. Pooled Human Platelet Lysate (pHPL)

Platelet concentrates (4 bags; independent donors) and one bag of plasma were donated by the South African National Blood Service (SANBS). On receipt, the bags were frozen for 24 hours at -20°C, after which pHPL was manufactured according to the protocol described by Schallmoser & Strunk protocol [30] with minor modifications. In summary, platelet concentrates were thawed after 24 hours in a 37°C water bath and the platelet concentrates from the four independent donors were pooled. The pooled platelet concentrates were again

frozen for 24 hours at -20°C. After 24 hours, the frozen pooled platelet lysate was thawed in a 37°C water bath. At this point the product is referred to as pHPL. The pHPL was aliquoted into 50 mL conical tubes and centrifuged at 4 000 x *g* at 4°C for 15 min. The supernatant was transferred into new 50 mL conical tubes and stored at -20°C for future use.

#### *2.4.2. Platelet Rich Plasma (PRP)*

Platelet rich plasma was collected by SANBS via the Spectra Optia® Apheresis system (Terumo Coporation, Tokyo, Japan). As per the SANBS protocol, the calcium, magnesium, and potassium levels in the donor's blood was assessed before donation. Some patients might experience hypocalcaemia during PRP donation and therefore it is important to confirm that the patients' calcium, magnesium, and potassium levels are within normal ranges before collection starts [31]. Sterility tests and pH levels were also determined as per the SANBS protocol. All results were within expected ranges and is available in supplementary Information (B).

On receipt of the PRP bags from SANBS, samples were aliquoted into 15 ml tubes and frozen at -20°C. One freeze-thaw cycle was allowed to activate the platelets before use of the PRP. Before freezing the products, an aliquot was taken to determine the number of platelets/ $\mu\text{l}$  (CD42a -positive), if the platelets were inactive/active (CD61-positive) and the percentage of white blood cells (WBC; CD45-positive) present in the sample. Briefly, a 100x dilution was made of the PRP product using PBS and stained with CD42a, CD61 and CD45 (5  $\mu\text{l}$  of each antibody). Stained samples were incubated for 20 min in the dark. After incubation, 400  $\mu\text{l}$  PBS was added, and the results were analysed on the CytoFLEX flow cytometer. Unstained samples were also run to determine the negative/positive staining boundaries.

When aliquots were thawed for use, the samples were again stained with CD42a and CD61 to determine if the platelets were activated by the freeze-thaw cycle.

#### 2.5. Osteogenic differentiation

Cells were seeded in 6-well (9.6cm<sup>2</sup>/well) plates at 5000 cells/cm<sup>2</sup> and grown to 70-80% confluence after which the CGM was removed and replaced with osteogenic induction

medium (10nM Dexamethasone, 50mg/mL ascorbate-2-phosphate, 10mM  $\beta$ -glycerophosphate). ASCs that were not exposed to osteogenic induction medium were maintained in CGM and served as negative (undifferentiated) controls. The experimental layout is depicted in Supplementary Information C, Figure C1 - C2. Osteogenic differentiation was assessed on day 0 (baseline measurements) and on day 21 (PRP and pHPL samples)/28 (FBS samples). The reason for using different termination days for FBS and the two human alternatives is based on initial observations in which we found no/poor osteogenic differentiation at day 21 for the cultures maintained in CGM (FBS). Our findings were aligned with the findings described by Mohamed-Ahmed et al. 2018 which reported a longer proliferation period, with the ASCs cultured in the presence of FBS only starting to differentiate on day 21 [32]. RNA was isolated at four different time points (day 0, 7, 14 and 21) to determine the kinetic expression of osteogenic genes during the differentiation process (Supplementary Information, Figure C3).

#### 2.5.1. Assessment of Osteogenic Differentiation

##### *Alizarin Red S (ARS) Staining Assay*

On the day of termination, the ASCs monolayer cultured in 6 well plates (9.6 cm<sup>2</sup>/well) was washed with PBS (2% pen/strep) after which the cells were fixed by adding 2 mL paraformaldehyde (4%) per well to the cells followed by incubation for 15 min at room temperature. The paraformaldehyde was removed, and the cells were washed with PBS. The PBS was removed completely before adding 2 mL of a 2% ARS staining solution(w/v) to the wells followed by incubation at room temperature for 10 min. After aspirating the unincorporated staining solution, cells were washed four times with PBS (2% pen/strep). Excess PBS was removed by incubating the plates at an angle to drain and remove any excess PBS. Plates were air dried overnight, and the stained monolayer was visualized using light microscopy (Carl Zeiss Werke, Göttingen, Germany). Images were captured using a Zeiss Axiocam digital camera (Carl Zeiss Werke, Göttingen, Germany).

To quantify the ARS concentration, 2 mL of acetic acid (10%) was added to each well followed by incubation for 30 min at room temperature. The reaction was stopped by adding 200  $\mu$ l of ammonium hydroxide (10%) to each well. An aliquot (100  $\mu$ l) from each well was then read

on a spectrophotometer (PowerWave X, BioTek Instruments Inc, Winooski, USA) at 405nm and 650 nm (reference) to determine the ARS concentration in mM (see Supplementary Information D)

The acetic acid was aspirated, and the cells were washed with PBS (2% pen/strep). PBS (2% pen/strep) was added and 1 µl of DAPI (0.02 µg/ml in molecular H<sub>2</sub>O) was added to each well to perform a cell count for normalization. The DAPI was incubated for 5 min and images were taken on the Zeiss AxioVert A1 fluorescence microscope (Carl Zeiss Werke, Göttingen, Germany) using the Zeiss AxioCam digital camera (Carl Zeiss Werke, Göttingen, Germany). The ARS concentrations were adjusted (normalized) to the relative number of cells using the following formula.

$$\text{Normalization} = \frac{\text{OD value or Concentration}}{\text{Cell number}} \times \text{Value}$$

**Equation 1.** Formula used to normalize level of ALP activity or ARS concentration to the amount of cells.

#### *Alkaline Phosphatase Assay*

As described for the ARS assay, the cultures were washed and fixed using paraformaldehyde (4%). An ALP buffer (2 mL/well) was then added to the cells and incubated for 60 min at 37°C. The composition of the ALP buffer was 4-nitrophenylphosphate (5 mM), MgCl hexahydrate (0.5 mM), Tris-HCl (50 mM) and Triton X-100 (0.01%). An aliquot (100 µl) of each reaction was read at 405 nm and 650 nm (reference) on a spectrophotometer. Like with the ARS assay, the ALP assay solution was aspirated, and the cells were stained with DAPI to determine the average number of cells/well.

As for the ARS assay, the ALP concentrations were also normalized to the relative number of cells/well using the formula above (Equation1).

## 2.6. Microscopy

### *Light microscopy*

Bright field microscopy images were captured on day 0 and day 21 or 28 using the Zeiss Primo Vert inverted light microscope (Carl Zeiss Werke, Göttingen, Germany) and Zeiss AxioCam

digital camera. The ZEN software (version 2.6) was used to capture the images. Bright field images were used to compare the morphology of cells grown in different osteogenic differentiation media. Images were also taken after the cells had been stained with ARS to visually assess the degree of osteogenic differentiation. A 5x objective lens magnification was used.

#### *Fluorescence microscopy*

To normalize the levels of ARS and ALP to the relative number of cells (calculated as the average number of nuclei per well), cells were stained with DAPI and imaged using the Zeiss AxioVert A1 fluorescence microscope (blue filter) and Zeiss AxioCam digital camera. A 5x/10x/20x/40x objective lens magnification was used depending on the number of cells present in each well. The more cells there were the more difficult it was to accurately determine the relative number of cells. For this reason, a higher magnification was used to decrease the number of cells per field of vision making the identification of single cells easier for downstream counting analysis. The scale bar was used to calculate the area of the field of vision. The average number of cells of five fields of vision were used as a representative count per well (Figure 1). The following equation was used to calculate an approximate cell count per well (9.6 cm<sup>2</sup>) thus allowing for the comparison of counts even if different magnifications were used. Protocol for obtaining the cell number within a well using ImageJ is described in the supplementary information E.

#### *Approximate cell count*

$$= \frac{\text{Average cells from the 5 representative images} \times 9.6 \text{ cm}^2}{\text{Area of field of vision}}$$

**Equation 2.** Formula used to calculate the approximate cell count in each well.



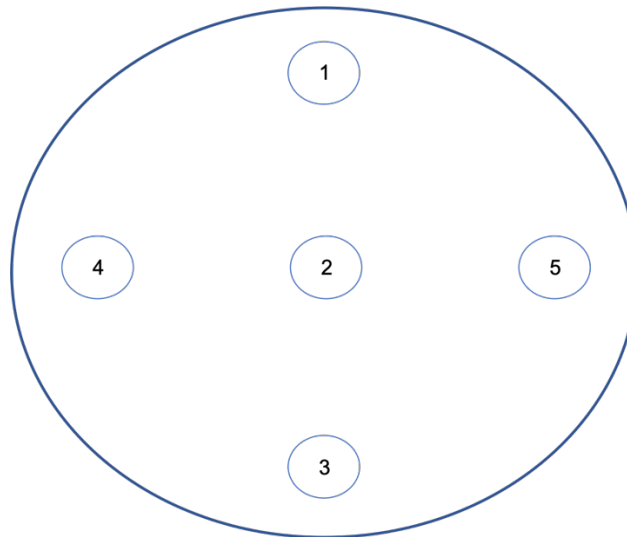


**Figure 1.** Schematic illustration of the fields of visions used to calculate a representative cell count per well.

## 2.7. RNA isolation

Cells were washed with ice cold PBS (2% pen-strep) and lysed using TriZol (1 mL for every 10cm<sup>2</sup>). After 3 min incubation, the lysate was transferred into Eppendorf tubes and placed on ice for a further 5 min to permit complete dissociation of the nucleoprotein complex. Chloroform was added to the lysate (0.2mL for 1 mL of Trizol), vortexed and incubated at room temperature for 2-3 min after which samples were centrifuged at 12 000 x g for 15 min. The mixture separated into 3 layers; a lower red phenol-chloroform layer, an interphase layer, and an upper aqueous layer. The aqueous layer was transferred into a new Eppendorf tube and ice-cold isopropyl alcohol was added (0.5 mL for every 1 mL of TriZol). Tubes were inverted several times and incubated at room temperature for 10 min. Samples were then centrifuged for 20 min at max speed. The supernatant was removed, and the RNA precipitate was re-suspended in 75% ice cold ethanol. The RNA was further purified using the PureLink<sup>®</sup> RNA Mini Kit from Thermo Fischer. The concentration, A<sub>260/280</sub> and A<sub>260/230</sub> values were measured on a NanoDrop<sup>®</sup> ND 1000 spectrophotometer (Thermo Fisher Scientific; Waltham, MA, USA).

## 2.8. RNA integrity

The RNA integrity was tested using the 2200 Tape Station (Agilent Technologies, California, United States). Representative samples from each time point were selected at random to test the RIN values. In summary, samples were diluted to achieve a concentration between 25 and

500 ng/ $\mu$ L. Sample buffer (5  $\mu$ L) was added to 1  $\mu$ L RNA sample and vortexed. The samples were denatured for 3 min at 72°C and placed on ice for 2 min. The samples were loaded into strips and analysed on the instrument.

## 2.9. cDNA synthesis

Any sample with a RIN<sup>e</sup> value lower than 6.5 was excluded from downstream experiments. The RNA with RIN<sup>e</sup> values above 6 were converted into cDNA using the Sensifast™ cDNA conversion kit from Celtic (Bioline, London, England). For every different expansion condition, 3 random samples were selected as no reverse transcriptase (NRT) controls, to determine if the samples or the buffers contained any genomic DNA contamination.

**Table 1. Composition and volume of reaction mixture for cDNA synthesis**

Reagent	Sample	NRT Control
5x TransAmp buffer	4 $\mu$ L	4 $\mu$ L
Reverse Transcriptase	1 $\mu$ L	None
Molecular grade water	Variable	Variable
RNA	Variable	Variable
<b>Total reaction volume</b>	20 $\mu$ L	20 $\mu$ L

Sample mixes were placed in a thermal cycler (Gene Amp® PCR system 9700 from Applied Biosystems, Life Technologies®/Thermo Fisher Scientific, Carlsbad, California, USA) and processed according to the following cycling conditions; 10min at 25°C, 15 min at 42°C for reverse transcription, 5 min at 85°C to inactivate the reverse transcriptase enzyme, followed by cooling of the reaction for 5min at 4°C. The cDNA was stored at -20°C until it was used.

## 2.10. Quantitative Polymerase Chain Reaction (qPCR)

Appropriate reference genes should show stable expression regardless of the experimental conditions. Four reference genes were tested for use in the study. Representative samples from each experimental group were selected to test for appropriate reference genes.

To test the efficiency of the primers, standard curve experiments were setup. In short, DNA samples were subjected to at least 5, 2-fold dilutions (in triplicate) using an optimised SYBR green protocol (see Supplementary Information F, Table F11). The Ct value was recorded and

plotted on the y-axis while the concentration of cDNA was plotted on the x-axis. The primer efficiency was determined using the LightCycler 480 II software (Abs Quant/2<sup>nd</sup> Derivative Max function).

All samples were prepared in triplicate and 10  $\mu$ L reaction volumes were used. The LightCycler 480 II instrument (Roche, Basel, Switzerland) was used for qPCR amplification and detection. Each plate also included (in triplicate) no template controls (NTC), 3 reference genes (*TBP*, *GUSB* and *YWHAZ*), representative samples from the two time points (Day 0 and Day 21 or Day 28) and standards from standard curve experiments. By including standards on each plate, we can use the primer efficiency calculated using the standard curves to calculate relative gene expression values using the comparative Ct method.

Primers were made up to a stock concentration of 100  $\mu$ M using TE Buffer, according to manufacturer's instructions. Stock solutions were then diluted with molecular grade water into working solutions of 10  $\mu$ M and stored at -20°C. The osteogenic primers RUNX2, ALP and Osteocalcin were used to determine at which stage of osteogenesis the samples were at the time of termination. Two adipogenic genes (*PPAR $\gamma$*  and *FABP4*) were included as the osteogenic differentiation and the adipogenic differentiation processes are mutually exclusive. Reference genes included in the study were *TBP*, *GUSB* and *YWHAZ*. All primers were purchased from Integrated DNA Technologies (IDT, Coralville, Iowa USA) and are listed in Table 2.

All reactions contained between 25 – 50 ng of template cDNA, 400 nM of forward and reverse primer respectively, 5  $\mu$ L of 1x SYBR Green Master Mix. The following cycling conditions were used; a one-step denaturation at 95°C for 5 min, an amplification series of 45 cycles consisting of the following 3 steps; 95°C for 30s, 62°C for 30s and 72°C for 30s. Following the amplification step, a two-step melt curve was performed; 95°C for 30s and 40°C for 30s. The average ramp rate for the qPCR reaction was 0.1°C/s.

Melt curves were analysed after each run to determine the specificity of each primer and that the product amplified was homogenous.

**Table 2. Primer sequences used in the study.**

Abbreviation	Description	Forward primer sequence	Reverse primer sequence
<b>RUNX2</b>	Runt-related transcription factor 2	ACCCATATCAGAGTCCAG	GACCGTCTAAAGAGCAAAC
<b>ALP</b>	Alkaline phosphatase	GCAACTCTATCTTTGGTCTG	GGTAGTTGTTGTGAGCATAG
<b>OCN</b>	Osteocalcin	ACCCTTCTTTCCTCTCC	CCCACAGATTCCTCTTCT
<b>PPAR<math>\gamma</math></b>	Peroxisome proliferator-activated receptor gamma	CGTGGATCTCTCCGTAAT	TGGATCTGTTCTTGTGAATG
<b>FABP4</b>	Fatty acid binding protein 4	ATCAACCACCATAAAGAGAAA	ACCTTCAGTCCAGGTCAA
<b>TBP</b>	TATA binding protein	CCGAAACGCCGAATATAA	GGACTGTTCTTCACTCTTG
<b>GUSB</b>	Glucuronidase, beta	GATCGCTCACACCAAATC	TCGTGATACCAAGAGTAGTAG
<b>YWHAZ</b>	Tyrosine 3-Monooxygenase/Tryptophan 5-Monooxygenase Activation Protein, Zeta	TGACATTGGGTAGCATTAAAC	GCACCTGACAAATAGAAAAGA

Primers were designed and assessed on the IDT website (*see MIQE guidelines, Supplementary Information E*)

### 2.11. Statistical Analysis

Statistical analysis of data was performed in R (Version 4.0.1) and RStudio (Version 1.3.959). Data is reported as mean  $\pm$  standard deviation (SD). Gene expression data is reported as standard error of mean (SEM). To test statistical significance, a one-way ANOVA was performed. This test was followed by a Tukey's test to determine the individual significance between each treatment group. A p-value  $\leq 0.05$  was considered statistically significant.

## 3. Results

### 3.1. Platelet rich plasma characterization

Platelet rich plasma (PRP) was collected from 3 male donors and was labelled as PRP070821, PRP240821 and PRP260821. On the day of collection, the PRP was characterized as follows: cells were stained with CD42a to identify and enumerate the platelets, CD61 to determine the percentage of activated platelets and CD45 to check for WBC contamination. After assessing the above-mentioned parameters, the PRP was stored at  $-20^{\circ}\text{C}$  until needed. Immunophenotypic characterisation was repeated once the PRP was thawed. PRP070821 had a platelet count of 22 482.3 platelets/ $\mu\text{l}$  and a WBC count of 30.11 cells/ $\mu\text{l}$ . Almost all the

platelets were resting (not activated) as only 0.01% of the platelets expressed CD61. PRP240821 had a platelet count of 16 939.99 platelets/ $\mu$ l and WBC count of 7.87 cells/ $\mu$ l. Again, the majority of the platelets were not active with only 0.43% of platelets expressing CD61. PRP260821 had a platelet count of 35 918.37 platelets/ $\mu$ l and a WBC count of 141.6 cells/ $\mu$ l. As with the two previous collections, the majority of the platelets were not active with only 0.11% of the platelets expressing CD61. After thawing, 0.21% (PRP070821), 3.33% (PRP240821) and 48.29% (PRP260821) of the platelets expressed the activation marker CD61 (Figure 2).

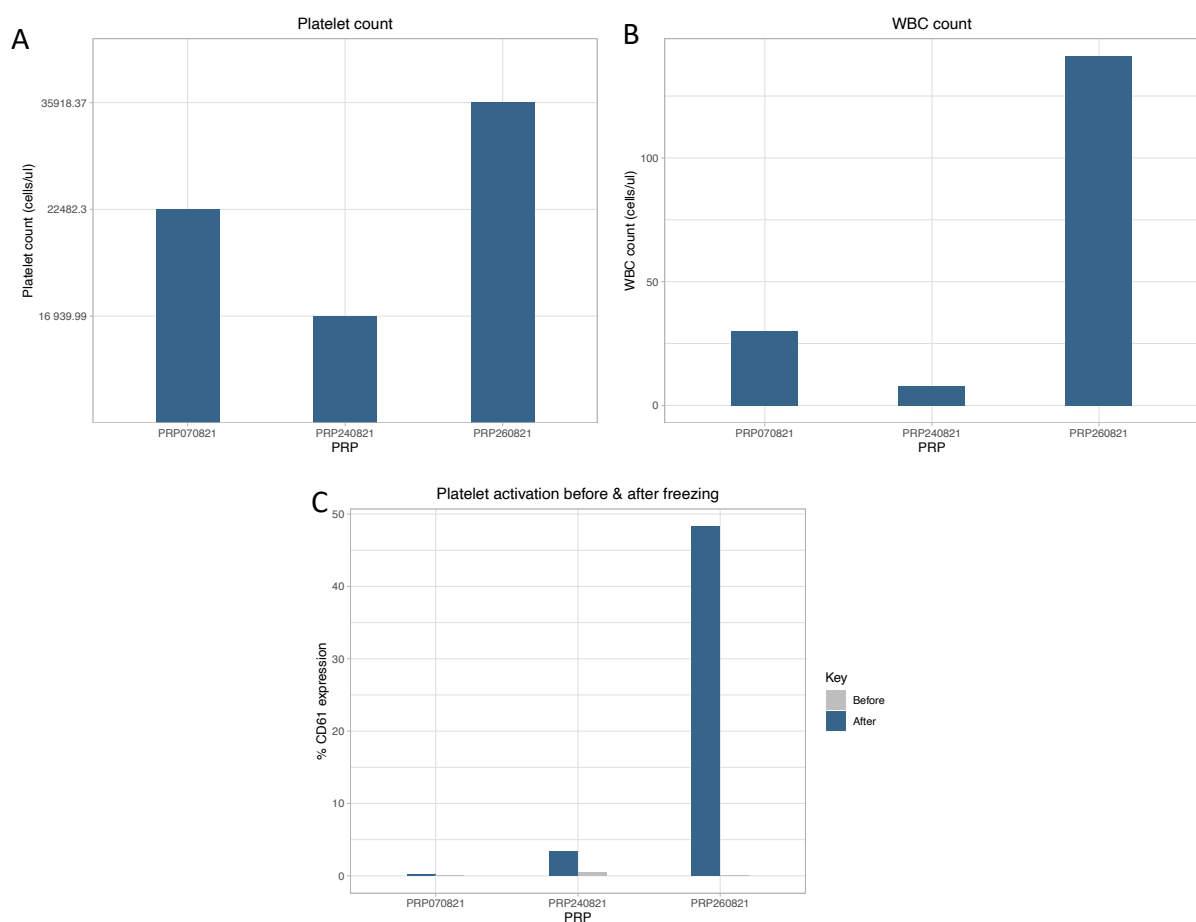


**Figure 2. Summary of platelet data.**

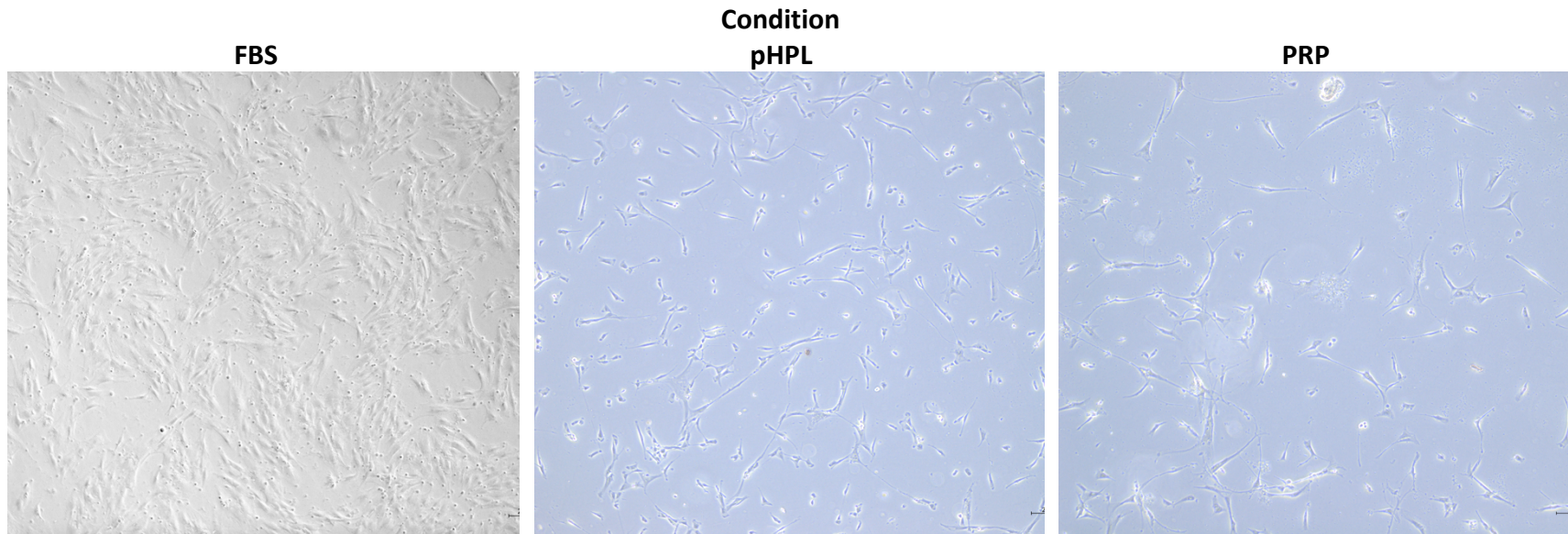
A. Platelet count after collection of platelet-rich plasma. B. White cell contamination in platelet product. C. Percentage activation of platelets, expressed as a percentage of CD61-positive platelets, before and after one freeze-thaw cycle.

### 3.2. ASC Isolation and Characterisation

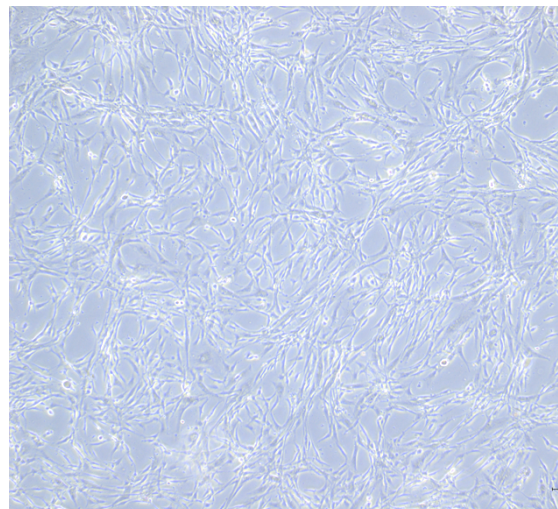
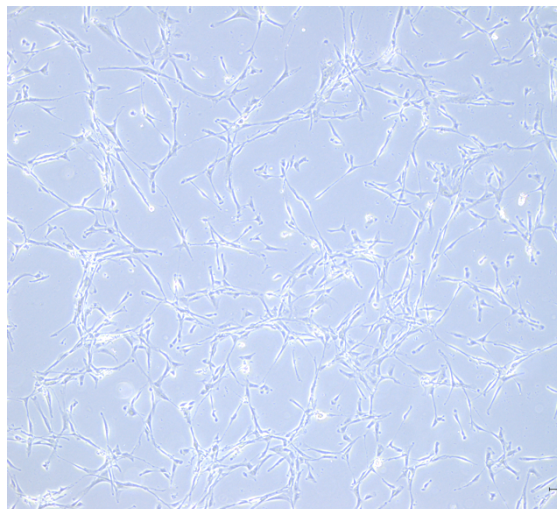
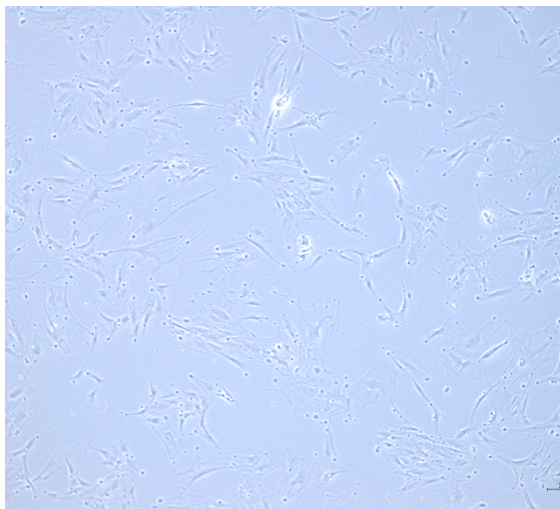
Representative micrographs of ASCs cultured in media supplemented with either FBS, pHPL or PRP are displayed in Figure 3. Plastic adherent ASCs had a typical fibroblastic morphology. Cells grown in medium supplemented with FBS revealed a more flattened, broader spindle morphology when compared to the morphology of ASCs grown in a medium supplemented with a human alternative (either pHPL or PRP), which were smaller in size, more elongated and had a tighter spindle shape. The size difference between ASCs grown in FBS vs ASCs grown in pHPL or PRP correlated to flow cytometry forward scatter measurements, which measures relative cell size. The forward scatter of ASCs grown in FBS was slightly larger than ASCs grown in pHPL or PRP (Figure 4).

**Culture**

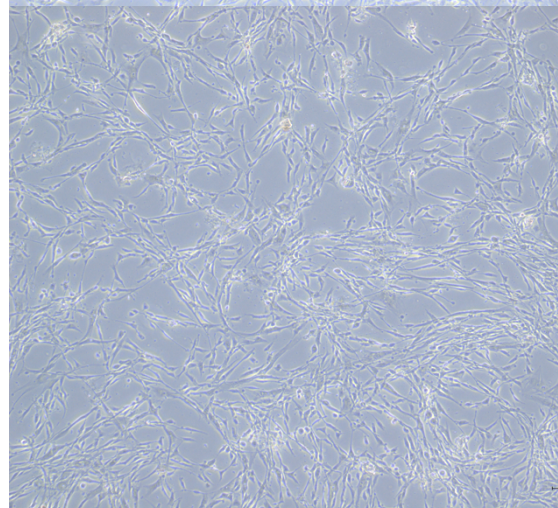
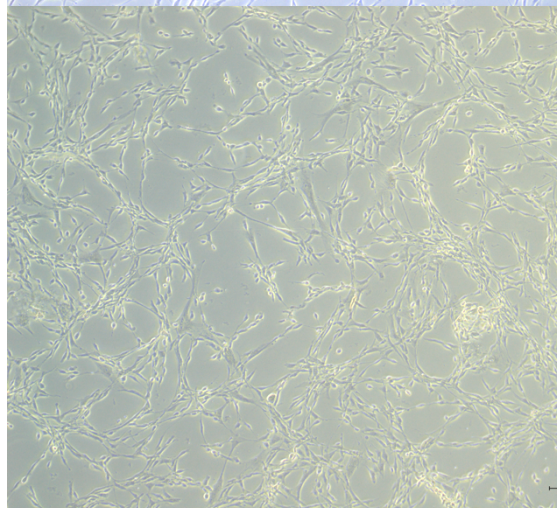
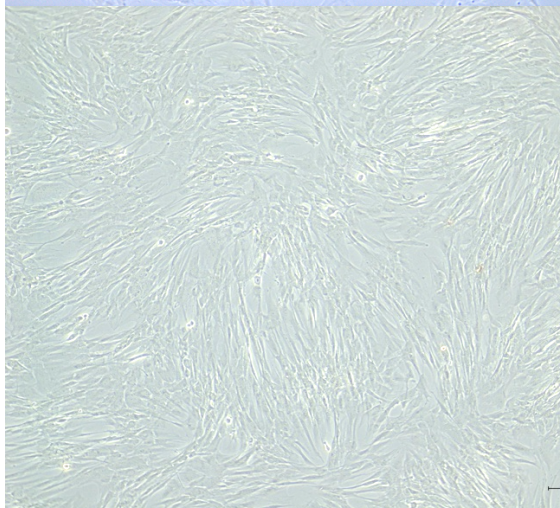
**A31101  
9-01A**



**A31101**  
**9-02T**



**A28062**  
**1-01R**



**A15022  
1-01A**

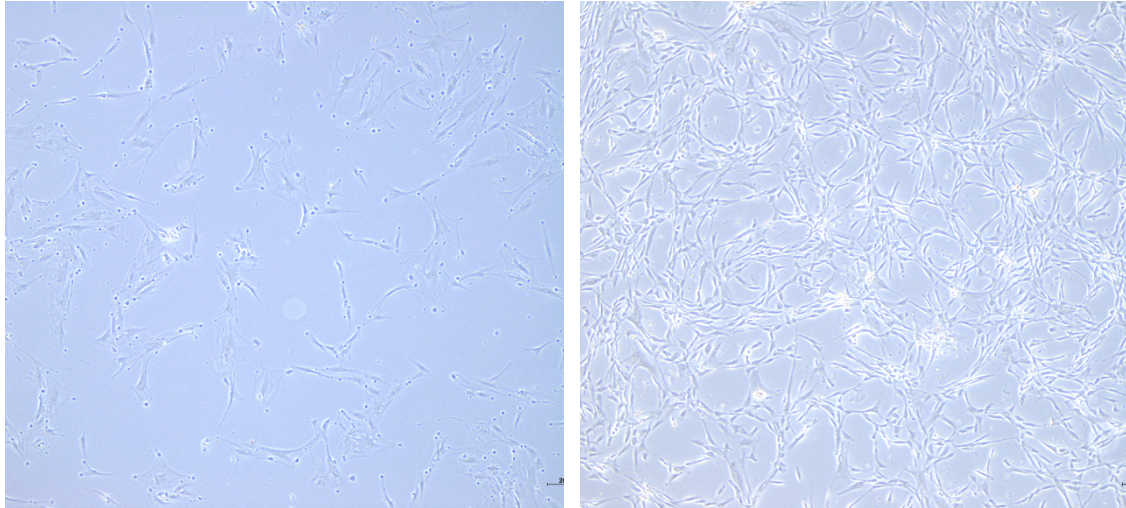


**Figure3. Morphology of primary ASCs cultured in the three different media formulations.**

Slight differences can be seen in the morphology of ASCs cultured using FBS versus ASCs cultured using either pHPL or PRP. Cells grown in medium supplemented with FBS has a more flattened appearance while ASCs cultured in either pHPL or PRP displayed a more elongated and smaller cell size.



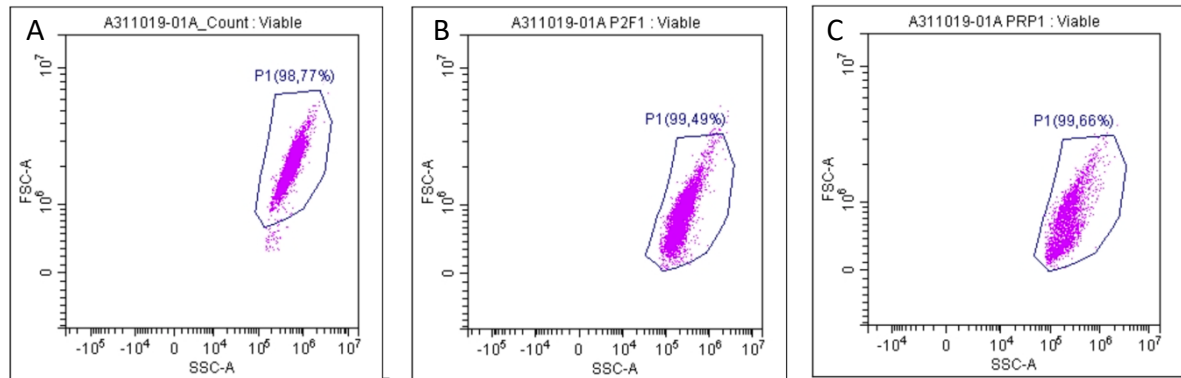


**Figure 4. Differences in forward scatter profiles of ASCs cultured in FBS, pHPL and PRP.** ASCs cultured using FBS (A) show a slightly higher forward scatter compared to ASCs cultured using pHPL and PRP (respectively B & C). Forward scatter is representative of cell size. An increase in forward scatter (upwards shift on y-axis; A) suggests an increase in cell size

Prior to plating for each experiment, ASCs were counted and cell viability and phenotypic profiles were assessed. Absolute cell numbers were determined on the CytoFlex flow cytometer using Flow-Count™ fluorospheres. The average cell viability was  $38.17\% \pm 6.72\%$  in FBS,  $54.6\% \pm 11.12\%$  in pHPL, and  $19.22\% \pm 1.21\%$  in PRP (Figure 9). The low cell viability in the human alternative supplemented expansion medium could be attributed to the fact the cells proliferated at a faster rate and that the cells started detaching from the culture vessel surface. ASCs cultured in medium supplemented with FBS took longer to proliferate and to reach the desired cell numbers and thus were kept in culture for extended periods. The low cell viability observed for last-mentioned ASCs is likely due to long expansion periods. The ASCs were stained with a panel of monoclonal antibodies (CD34, CD36, CD44, CD45, CD73, CD90 and CD105). The expression of the individual markers was determined (Figure 10). In FBS; CD90 was expressed on  $97.02\% \pm 3.38\%$ , CD44 was expressed on  $99.66\% \pm 0.2\%$  and CD73 was expressed  $81.69\% \pm 19.67\%$  of ASCs. CD36 was present on  $31.5\% \pm 25.61\%$  of the cells and  $3.51\% \pm 3.4\%$  of the ASCs expressed detectable levels of CD105. CD34 and CD45 were only expressed on  $0.43\% \pm 0.38\%$  and  $0.3\% \pm 0.31\%$  of the cells respectively. In pHPL; CD44 was expressed on  $99.23\% \pm 0.57\%$  and CD73 was expressed on  $98.61\% \pm 0.88\%$  of ASCs. Interestingly the percentage of cells that expressed CD90 on ASCs cultured and maintained in medium supplemented with pHPL was lower ( $43.78\% \pm 33.35\%$ ) compared to the expression levels of the same marker on ASCs cultured in medium supplemented with FBS. In contrast to CD90, a higher percentage of the ASCs expressed CD105 ( $23.65\% \pm 44.55\%$ ) and CD34 ( $18.83\% \pm 32.23\%$ ). CD36 was present on  $47.42\% \pm 38.32\%$  of the cells,

while an almost negligible percentage ( $0.38\% \pm 0.88\%$ ) of ASCs expressed CD45. In PRP; CD44 was expressed on  $85.99\% \pm 8.49\%$  and CD73  $80.01\% \pm 6.1\%$  of the ASCs. The percentage of ASCs expressing CD90, CD105 and CD34 were  $16.47\% \pm 11.56\%$ ,  $28.4\% \pm 23.41\%$  and  $5.22\% \pm 1.57\%$  respectively. CD36 was present on  $66.6\% \pm 10.7\%$  of cells, and CD45 on  $0.35\% \pm 0.35\%$  (Figure 10). In both human alternative supplemented media, CD90, CD105 and CD36 expression had a very high standard deviation, and this was due to half of the biological repeats expressing the relative cell surface marker and the other half of the biological replicates not expressing the relative cell surface marker.

In summary, in all three cultures ASCs expressed CD44, CD73 and CD90 and were negative for CD45. Interestingly, only a small percentage of ASCs cultured/maintained in FBS-supplemented medium did not express detectable levels of CD105 while CD105 expression was observed in a larger percentage of ASCs cultured/maintained in human alternative-supplemented medium (not significant). CD34 and CD36 expression was variable in all three culture conditions. FBS cultured cells showed the highest percentage expression of CD90, followed by pHPL and PRP (FBS vs, PRP;  $p=0.0000158$ ).

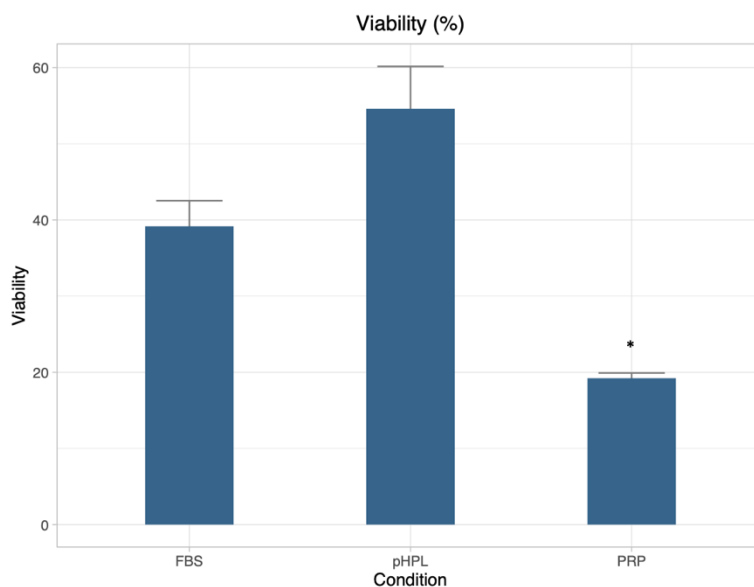


**Figure 5. Cell viability in the different culture condition.**

pHPL samples showed the highest cell viability percentage followed by FBS and then PRP ( $p<0.05$ ). Significant codes:\*\*\*:  $p < 0.001$ ; \*\*:  $p<0.01$ , \*:  $p<0.05$ .

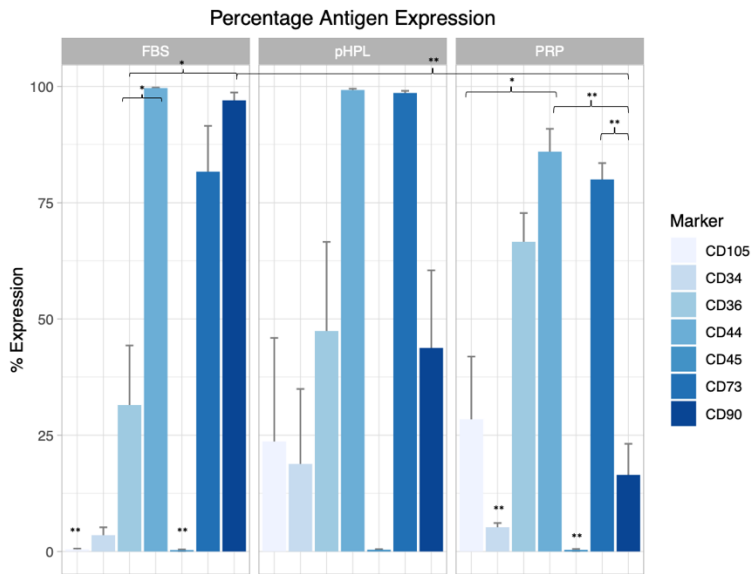


**Figure 6. Percentage expression of surface antigens on ASCs in the different culture condition.**

The data represent the average percentage of ASCs expressing the different cell surface markers  $\pm$  standard deviation (SD). ASCs did not express CD45 in all three the culture conditions. CD44, CD73 and CD90 expression was seen in all three culture conditions. Higher percentages of ASCs expressed CD105 when cultured/maintained in human alternative-supplemented media. The percentage of ASC expressing CD90 decreased when cultured in the presence of pHPL and PRP compared to FBS. Significant codes:\*\*\*:  $p < 0.001$ ; \*\*:  $p < 0.01$ , \*:  $p < 0.05$ .

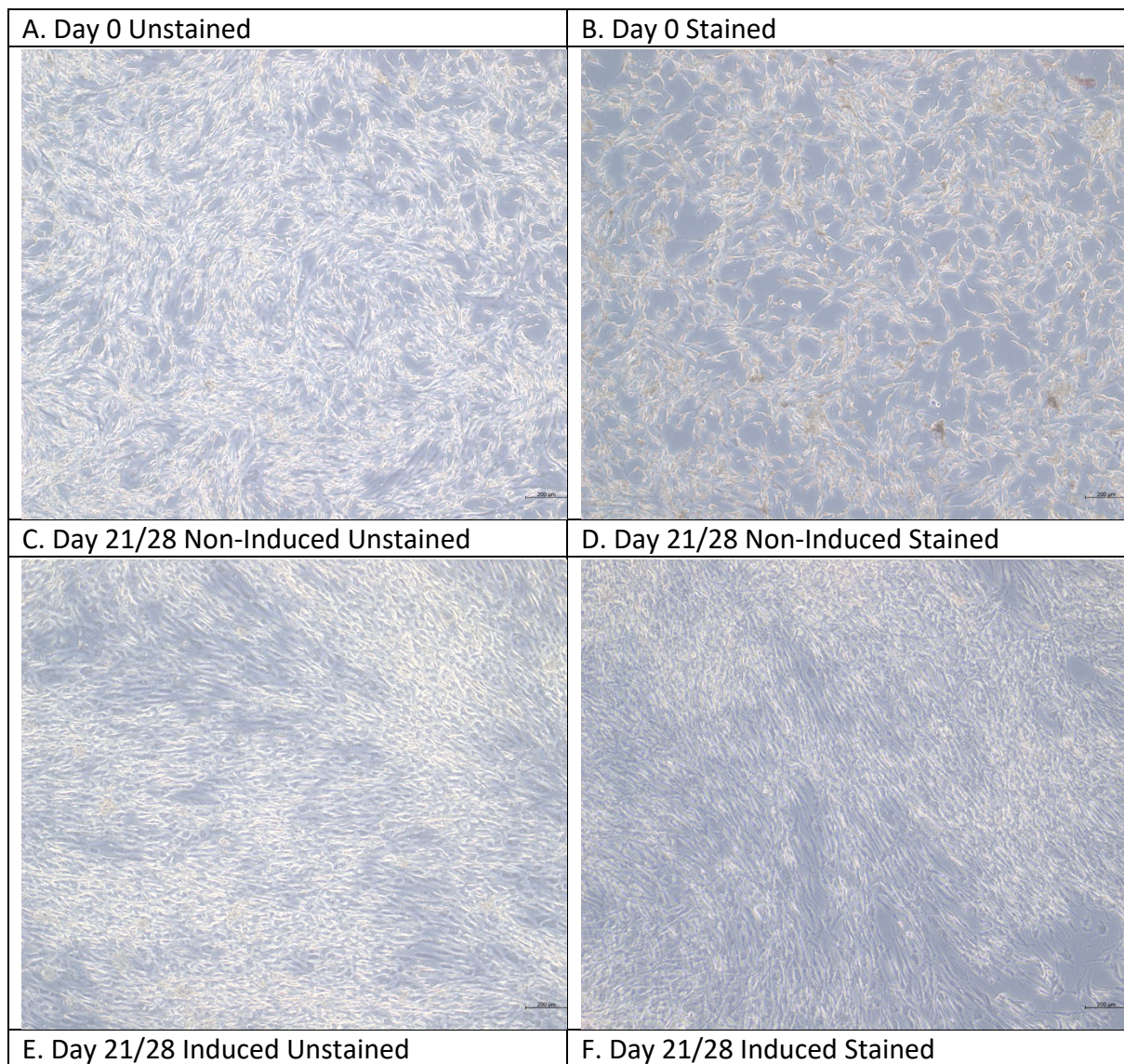
### 3.3. Assessment of Osteogenic Differentiation

Osteogenic differentiation was assessed using two semi-quantitative assays namely, an ARS stain, that was quantified on a spectrophotometer and secondly an ALP assay that was also measured on a spectrophotometer. Brightfield images were taken of the ARS assays to visually confirm the success of osteogenic differentiation. Fluorescent images were taken of both the ARS and ALP assays where cells were stained with DAPI to quantify the number of cells by staining the nuclei. These images were used to quantify the number of cells per well as explained in the methodology section for normalization. Lastly, RNA was extracted from ASCs expanded in growth medium and ASCs undergoing osteogenic differentiation in T24 flasks at 4 different time points. The relative gene expression of 3 osteogenic genes and 2 adipogenic genes was assessed.

#### 3.3.1. Alizarin Red S Assay

At day 21/28 post induction of osteogenesis, cells were fixed with 2% and stained with ARS. Two different controls were included (in triplicate): (1) samples not stained with ARS (Figure 7A, C & E) and (2) non-induced samples that were maintained in CGM (Figure 7D). No

ARS staining was observed on day 0 (Figure 7A & B). On day 21/28, the non-induced controls showed little to no ARS staining in FBS, pHPL and PRP supplemented media (Figure 7C & D), whereas clear ARS staining was observed in the induced samples indicating the presence of calcium deposition (Figure 7F). Induced samples supplemented with FBS showed noticeably less ARS staining when compared to ARS staining present in induced samples supplemented with either pHPL or PRP medium (Supplementary Information, Figure F1).



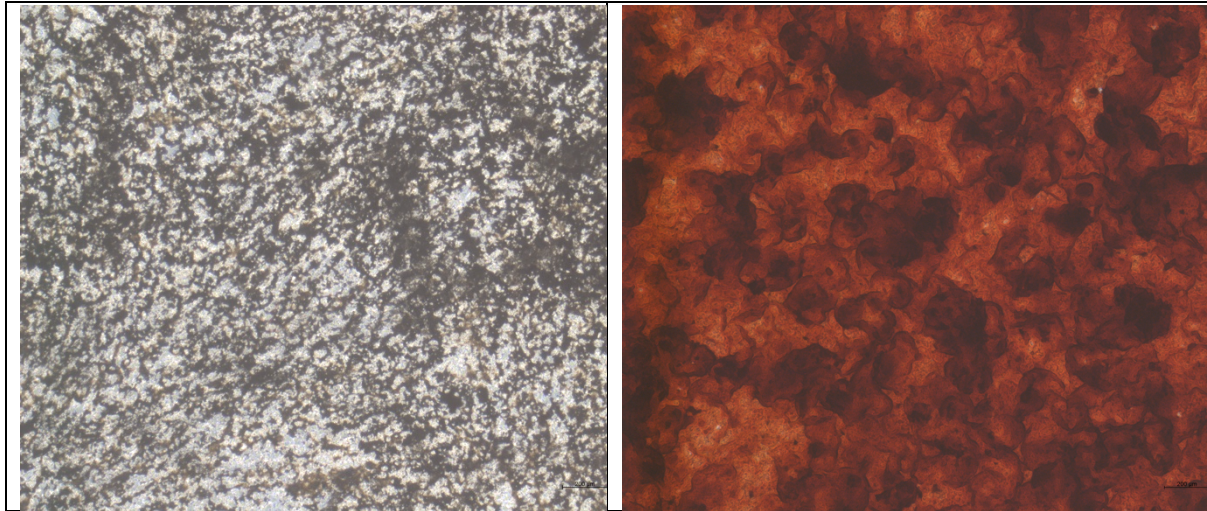


**Figure 7. Representative images of the different controls used in the Alizarin Red assay.**

A & B: Day 0 samples refer to samples on the day of osteogenic induction and were divided into unstained control samples (A) and stained samples (B). C-F: On day 21/28 samples were divided into non-induced (C & D) and induced samples (E & F). Non-induced and induced samples (day 21/28) were further divided into unstained controls (C & E) and stained samples (D & F).

The ARS was eluted with a solution of acetic acid (10% v/v) and the amount of stain was quantified on a spectrophotometer and results are displayed in Figure 8. Differentiated ASCs cultured in pHPL-supplemented osteogenic differentiation medium showed significantly more ( $p < 0.05$ ) osteogenic differentiation (significantly higher levels of ARS per well) on the day of termination when compared to the levels of osteogenic differentiation achieved in PRP- and FBS-supplemented media. The level of osteogenic differentiation achieved in osteogenic differentiation medium, supplemented with PRP samples was lower than the differentiation levels achieved using pHPL supplementation ( $p < 0.05$ ), but significantly higher than the osteogenic differentiation achieved when ASCs were cultured in supplemented with FBS ( $p < 0.001$ ). In summary, more ARS staining was present in both human alternative samples compared to FBS, suggesting more calcium deposition and thus higher levels of osteogenic differentiation was achieved using human alternative supplementation.

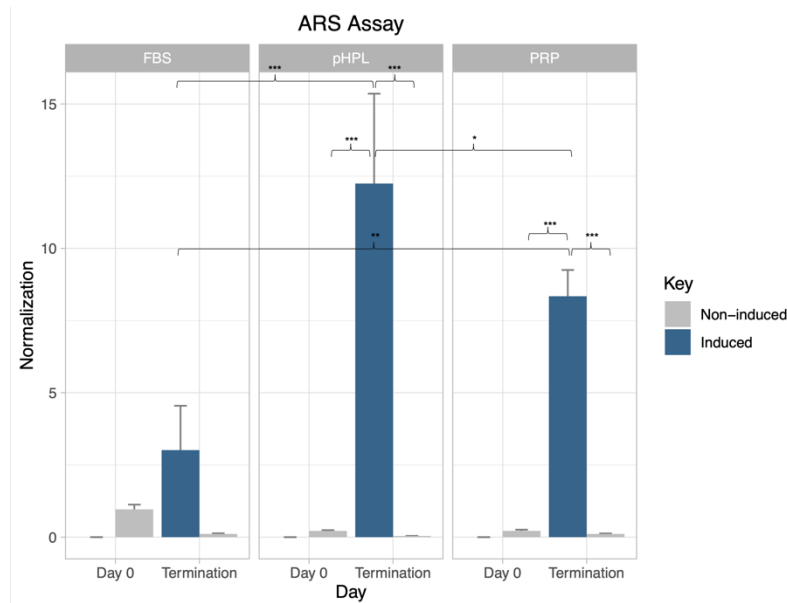


**Figure 8. ARS concentrations eluted from various samples normalized to cell number and to unstained controls.**

ASCs cultured in the presence of pHPL had the most amount of calcium deposition present followed by PRP. Samples cultured in FBS supplementation had the least amount of ARS stain present indicating lower levels of calcium deposition in ASCs cultured in FBS-supplementation. Results from the unstained controls were also included and showed little to no stain present and were also used to normalize the stained results. Significant codes:\*\*\*:  $p < 0.001$ ; \*\*:  $p < 0.01$ , \*:  $p < 0.05$ . Day of termination refers to day 28 post induction in FBS supplemented medium and day 21 post induction in pHPL/PRP supplemented media.

### 3.3.2. Alkaline Phosphatase Assay

The activity of ALP was measured at day 0 and on the day of termination in non-induced and induced samples. ASCs cultured/maintained in FBS-supplemented osteogenic medium showed the highest activity of ALP on day 0 compared to ALP activity levels measured for ASCs differentiated in pHPL- and PRP-supplemented medium (Figure 9). At termination (day 21/28) the level of ALP activity was higher in the non-induced samples compared to the induced samples for all three the culture conditions (Figure 9). For ASCs cultured in FBS-supplemented CGM, the level of ALP activity decreased in both non-induced and induced at day 28 when compared to day 0 ALP levels (not significant). For ASCs cultured/maintained in either pHPL or PRP the level of ALP activity, increased significantly (pHPL:  $p < 0.0001$ ; PRP:  $p < 0.0001$ ) in the non-induced samples when compared to the on day 0 (Figure 9). In contrast, the ALP levels were significantly decreased (pHPL:  $p < 0.001$ ; PRP:  $p < 0.001$ ) in the induced samples of pHPL and PRP supplemented media compared to the ALP levels recorded at day 0 (Figure 9). For the induced samples, the level of ALP activity was significantly higher ( $p < 0.01$ ) in ASCs cultured in FBS-supplemented CGM than the ALP activity observed for both

pHPL and PRP samples. In both pHPL and PRP samples there was a significant difference between the level of ALP activity in the non-induced and induced samples on the day of termination (pHPL:  $p < 0.001$ ; PRP:  $p < 0.001$ ) (Figure 9).

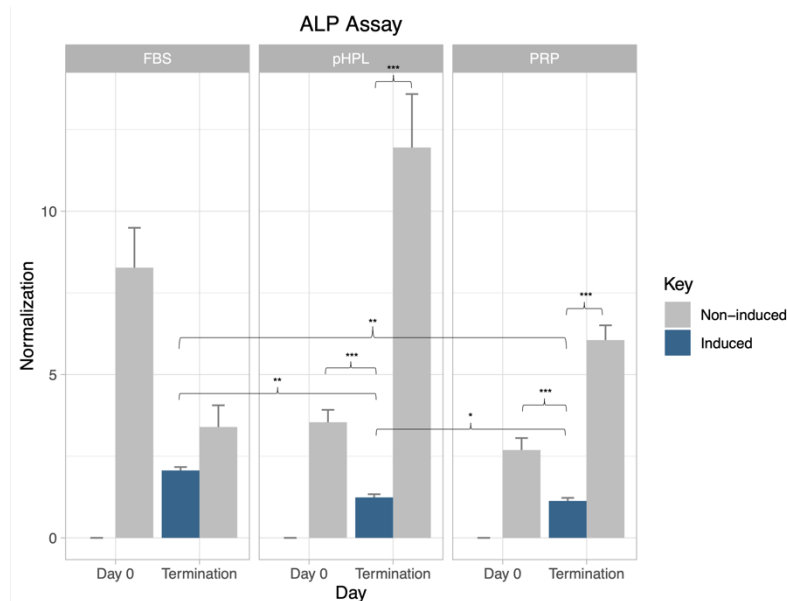


**Figure 9. Level of alkaline phosphatase activity in various samples.**

When looking at FBS samples, the level of ALP activity decreased from day 0 to the day of termination in both non-induced and induced samples. In both pHPL and PRP samples, the level of ALP activity decreased from day 0 to day of termination in induced samples and increased in the non-induced samples. The level of ALP activity in FBS samples on the day of termination was significantly higher in FBS samples when compared to pHPL and PRP samples. Significant codes:\*\*\*:  $p < 0.001$ ; \*\*:  $p < 0.01$ , \*:  $p < 0.05$ .

### 3.4. Relative gene expression

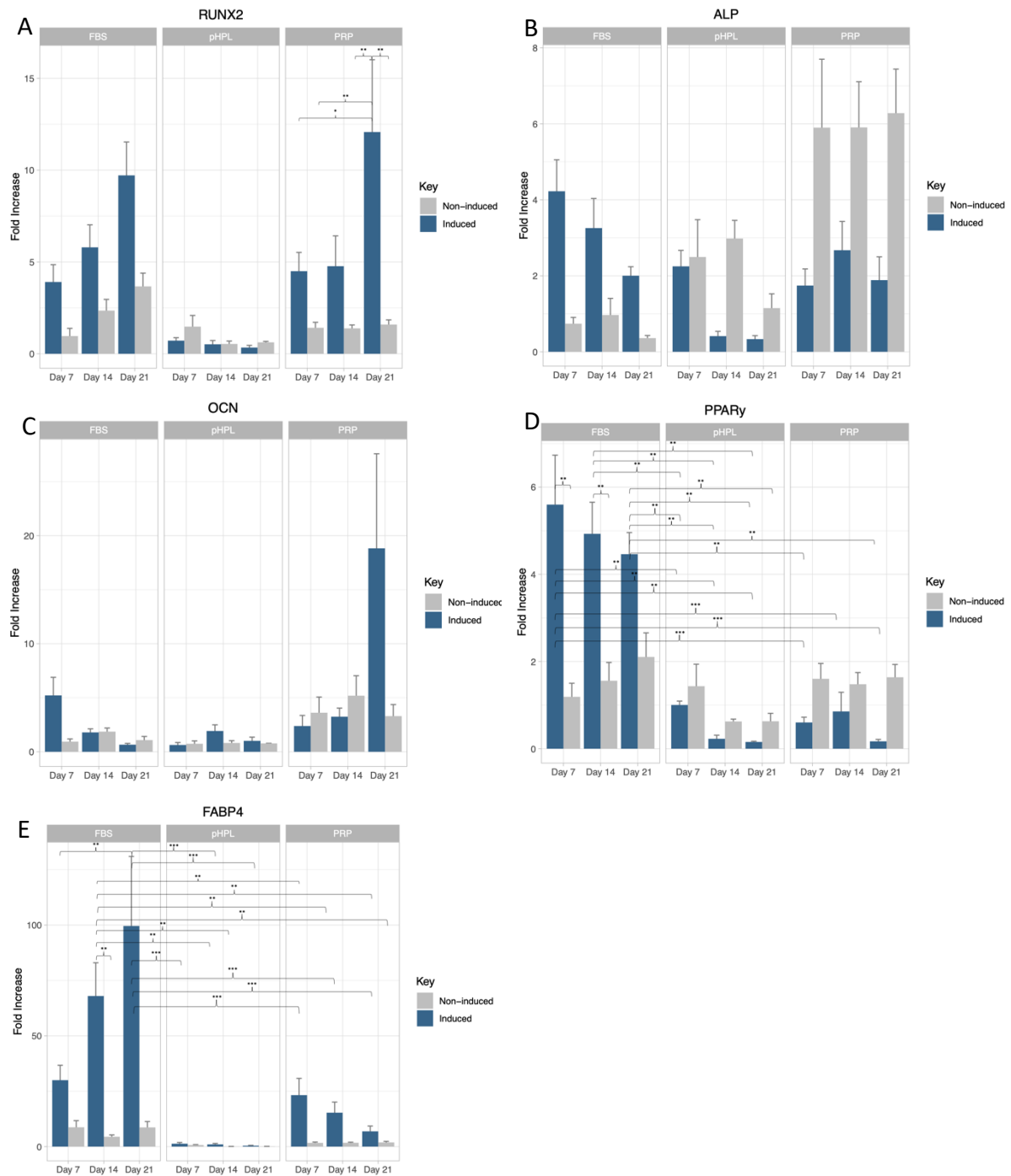
We also investigated the kinetics of osteogenic gene expression at various time points during the differentiation process. RNA was isolated at 4 time points throughout the differentiation process namely day 0, 7, 14 and 21. Once the RNA was isolated, RIN values were obtained to ensure that only RNA samples of acceptable quality were used in downstream applications. Samples with RIN values below 5 were excluded from downstream testing. Samples excluded were the A311019-01A pHPL Day 14 induced sample as well as A311019-01A pHPL Day 21 induced sample as their RIN values were 3.7 and 2.7 respectively. The corresponding non-induced samples were also not used in downstream experiments. The expression of three osteogenic genes (RUNX2, ALP and OCN) were monitored in both non-induced and induced samples. The relative expression of target genes normalized to the three reference genes over the 21-day differentiation period is summarized in Figure 10.

The stability of the reference genes was tested over the 21-day culture period in both non-induced and induced samples.  $\Delta C_t$  values comparing three potential reference genes were calculated and the total standard deviation in comparison was as follows: TBP vs GUSB = 1.18; TBP vs YWHAZ = 1.19 and GUSB vs YWHAZ = 1.02, all below a standard deviation of 2, which indicates that all three reference genes are acceptable to use in the study (Supplementary information E, Table E11) [33]. When testing the stability of the reference genes, a slight up-regulation of all three reference genes were observed on day 21. For this reason, two sets of samples for each reference gene were included on each experimental plate: one sample from day 7 and one sample from day 21. The average  $C_t$  value between these two-time points was used as reference samples.

Standard curves were generated for all target genes as well as the three reference genes. Standard curves generated using samples from two time points (an early timepoint and a late timepoint), reason described above, for the three reference genes. An efficiency of 100% is equal to 2 and the optimal efficiency ranges from 90% - 100% (1.8 – 2). ALP standard curve had an efficiency of 1.72 (86%) and might be indicative of the presence of PCR inhibitors or that the primer sequence might not be optimal. OCN, TBP and YWHAZ had an efficiency of 2.144 (107.2%), 2.090 (104.5%) and 2.111 (105.55%) which might indicate the presence of PCR inhibitor or non-specific binding of the primers. Although these values are outside the optimal ranges they are still acceptable [34].

The comparative  $C_t$  method was used to represent gene expression as relative fold changes. When analysing the mRNA expression level, three different strategies were used. Firstly, the relative gene expression of target genes was normalized to reference genes (the average  $C_t$  value of 3 reference genes which each had 2 time points, an early timepoint and a late timepoint), next the relative gene expression was normalized to day 0 (Figure 10). Lastly, the relative gene expression of target genes was double normalized, first to day 0 samples then to NI samples (Figure 11).





The non-induced ASCs cultured in the presence of either FBS, pHPL and PRP did not show significant changes in any genes of interest over the 21-induction period (Figure 10 A-E). For induced ASCs cultured in FBS supplemented ODM; a gradual increase in *RUNX2* expression levels were observed over the 21-day induction period, there was a gradual decrease in *ALP* expression and, *OCN* expression levels decreased over the 21-day culture period with the

highest expression levels observed on day 7. In induced ASCs culture in FBS-supplemented ODM, *PPAR $\gamma$*  gradually decreased, while the *FABP4* expression levels (Figure 10 E) increased over the 21-day culture period (Figure 10D). The expression levels of both *PPAR $\gamma$*  (days 7,  $p=0.0000005$ ; day 14,  $p=0.0006142$ ) and *FABP4* (day 14,  $p = 0.0000303$ ; day 21,  $p = 0.00000001$ ) were significantly higher in the induced ASCs cultured in FBS-supplemented ODM compared to the non-induced ASCs cultured in FBS supplemented ODM. ASCs grown in pHPL supplemented ODM did not show significant differences between the non-induced and the induced samples when looking at *RUNX2*, *OCN*, *PPAR $\gamma$*  and *FABP4*. The expression of *ALP* in ASCs grown in pHPL supplemented ODM did decrease after day 7 in the induced samples compared to the non-induced samples. For the ASCs grown in PRP; *RUNX2* was significantly higher in the induced samples compared to the non-induced samples (Day 21,  $p = 0.0001499$ ). ASCs grown in PRP-supplemented osteogenic differentiation medium did show a higher expression of *ALP* over the 21-day induction period, this difference was not significant due to the high standard deviation from one biological repeat expressing high levels of *ALP* and the other two biological repeats not expressing *ALP* (Figure 10B). The expression of *OCN* and *PPAR $\gamma$*  in ASC grown in PRP-supplemented ODM was not significantly different when comparing non-induced and induced samples. Lastly, *FABP4* had a higher level of expression in the induced ASCs grown in PRP supplemented ODM but gradually decreased over the 21-day induction period.

When the results were normalized to day 0 then to the non-induced samples for the respective experimental groups, the differences were highlighted more (Figure 11). There were no significant findings when looking at *RUNX2* expression in all three experimental groups, but it is worthy to note that in ASCs grown in FBS and PRP showed a gradual increase in *RUNX2* expression over the 21- day differentiation period. *RUNX2* is down regulated in pHPL samples from as early as day 7. ASCs grown in FBS show a significantly higher *ALP* expression when compared to PRP ( $p = 0.0058226$ ). Both ASCs grown in pHPL and PRP supplemented media show a down regulation of *ALP* from as early as day 7. When looking at *OCN* expression, there was no significant differences however it can be seen that there is an upregulation of *OCN* on day 21 of ASCs grown in PRP. When looking at the two adipogenic genes, FBS samples showed significant expression of both these genes in induced samples when compared to pHPL and PRP samples ( $p<0.01$ ). *PPAR $\gamma$*  and *FABP4* were both down

regulated in pHPL and PRP samples whereas these two genes were upregulated in ASCs grown in FBS. These findings are of interest as adipogenic genes need to be down regulated for osteogenesis to occur which was observed in pHPL and PRP samples but not in FBS samples.

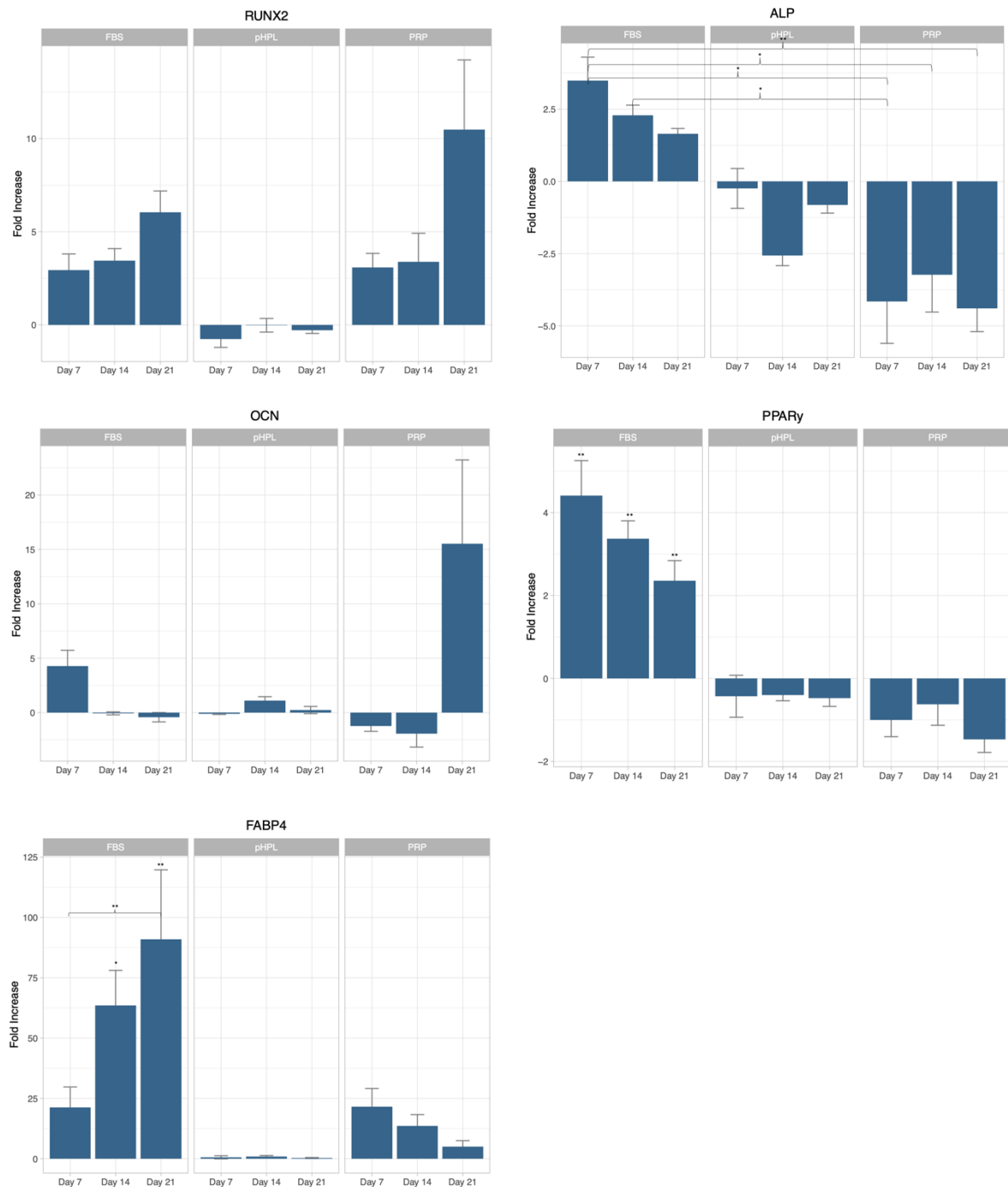


**Figure 11. Relative fold increase of gene expression normalized to day 0 then non-induced samples.**

RUNX2, ALP, OCN, PPAR $\gamma$  and FABP4 expression kinetics over a 21 day differentiation period in samples supplemented with either FBS, pHPL or PRP. Significant codes:\*\*\*: p < 0.001; \*\*: p < 0.01, \*: p < 0.05.

#### 4. Discussion

The use of ASCs in regenerative medicine holds the potential for many applications. Expanding and differentiating ASCs in the presence of FBS, which is currently the gold standard, does not comply with GMP regulations [35]. Not only does the use of FBS not comply with GMP guideline, FBS also has many disadvantages such as batch-to-batch variations, possibility of transmitting zoonotic agents and complications with animal welfare [8,36–38]. To date there has been a lot of research done in finding the best suited alternative to FBS that does in deed comply to GMP regulations [5,8,38–40]. Two attractive alternatives to FBS that stand-out are pHPL and PRP. Although PRP may be superior to FBS, large biological variance can be seen between different PRP samples, making pHPL more advantageous over PRP because pHPL reduces biological variance through pooling multiple donors [10,41]. There are clinical trials underway that have started expanding ASCs in pHPL [42,43]. In this study we investigated the osteogenic potential of ASCs supplemented with either FBS, pHPL or PRP. The composition of the osteogenic differentiation remained the same except for the serum/plasma/growth factor supplementation (FBS, pHPL or PRP). Previously collected pHPL was used in the study and met the quality controlled criteria set out by Schallmoser & Strunk [30].

Both pHPL and PRP use platelet concentrates to get to the final product. Blood donation centres worldwide collect and manufacture these platelet concentrates for the treatment of multiple disorders. [44–47]. Not only is the collection of platelet concentrates routinely done but platelet concentrates are also discarded after 5 days and thus an attractive alternative to FBS [48]. Platelets are found in circulating human blood and their primary functions involve coagulation and haemostasis. Platelets play an important role in cell culture because they have the ability to release growth factors and cytokines. These growth factors and cytokines can stimulate multiple biological processes, differentiation, cell recruitment cellular communication etc. [49].

ASCs grown in either FBS, pHPL or PRP maintained the classic fibroblast morphology [50,51]. It was noted that ASCs grown in pHPL and PRP were not only smaller in size but also thinner and more elongated. ASCs grown in FBS on the other hand were larger in size and flatter in

their morphology. Bieback et al. [39] suggests this may be due to pHPL or PRP selecting for a more primitive ASC.

Other studies have found that there were no major differences when it came to the viability of cells grown in different supplemented media and that cells grown in media supplemented with a human alternative to FBS actually enhanced proliferation rates and cell viabilities [4,11,19,52]. In this study, cells grown in pHPL had the highest viability followed by FBS and then PRP. The low cell viability in PRP can be attributed to rapid cell proliferation, leading to cells reaching confluency much quicker. ASCs have contact inhibition property that causes ASCs to lift off culture dishes leading to the decrease in viability that was noticed [53,54].

ASCs were immunophenotyped based on the recommendations of Bourin et al. 2013 [55]. The ASCs displayed a highly variable immunophenotype, especially when it came to CD105, CD36 and CD34. This variability has been reported by multiple research groups and is due to the heterogenous population of cells that make up the SVF. The immunophenotype of ASCs can also vary between different donors and different tissue sites [56,57]. No consensus has been reached to what panel of cell surface markers is ideal for the classification of ASCs. Positive markers included were CD90, CD73 and CD44. The most common negative marker that was included was CD45, as CD45 is a common haemopoietic (pan leukocyte) marker and was observed in less than 2% of ASCs across all the different media [58]. It is recommended by the ISCT that additional markers should be added to better characterize ASCs [55]. In this study we included CD105, CD34 and CD36. CD44 and CD73 were expressed in more than 80% of ASCs across all the different media. CD90 expression was positive in more than 80% of ASCs grown in the presence of FBS but we observed a decrease in CD90 expression in ASCs grown in the human alternative supplemented media that has not been documented before. A study done by Park et al. described a population of pericytes that were found to have decreased CD90 expression and could explain the decrease we saw as pericytes are in the SVF and have similar plastic adherent properties like ASCs [59–61]. CD34 expression is variable and unstable in ASC cultures and there is contradictory research available that both supports the argument that ASCs should be CD34 positive and arguments that support ASCs being CD34 negative [55,57,62,63]. Bourin et al. describe the differences between a CD36 positive and CD36 negative population [55], namely that MSCs isolated from adipose tissue are CD36 positive,

while MSCs isolated from bone marrow are CD36 negative. We saw variable CD36 expression across the various supplemented media. CD105 was another variable marker seen in this study, with an increase in CD105 expression seen in media supplemented with human alternative. Again, Bourin et al. characterize ASCs as either CD105 positive or CD105 negative [55]. The use of anti-fungal treatment, especially the use of Amphotericin, has been seen to negatively impact the expression of CD105 [64]. The use of trypsin has also been associated with the loss of CD105 expression as trypsin damages cell surface proteins like CD105 [65]. This can explain the difference we observed between FBS cultures and human alternative cultures as we used tryple and not trypsin in human alternative cultures.

ASCs possess the ability to differentiate into osteoblasts which are bone forming cells. We observed that both pHPL and PRP supplemented ODM promoted osteogenesis when compared to FBS. This was assessed using microscopy, spectrophotometry, and gene expression analysis. Our results were in line with what others have found [66–68]. Chignon-Sicard and colleagues showed that PRP inhibits adipogenesis by down regulation of the adipogenic genes. *PPAR $\gamma$*  and *FABP4* [69]. EGF and PDGF are growth factors that are abundant in PRP. It is these growth factors that specifically inhibit the transcription of *PPAR $\gamma$*  and *FABP4* via the MAP kinase cascade [69]. Adipogenesis and osteogenesis are two mutually exclusive processes. For osteogenesis to take place, adipogenesis needs to be inhibited. This is mainly achieved through the inhibition of *PPAR $\gamma$*  [70]. Therefore, the use of PRP in osteogenesis proves to be superior to the use of FBS as growth factors found in PRP inhibit adipogenesis.

Osteogenesis is comprised of four sequential phases namely lineage commitment, proliferation, synthesis of the matrix and lastly mineralization of the matrix [71]. Successful mineralization was measured using ARS assays, where ARS stains calcium deposits [72]. Some mineralization was seen in FBS samples but was very variable. ASCs differentiated in both pHPL and PRP showed greater and more consistent mineralization. ALP is an early-stage osteogenic marker and is expressed during the proliferation period of osteogenesis. On the day of termination, the level of ALP activity in the induced samples was significantly higher in FBS samples when compared to pHPL or PRP samples and can thus explain why mineralization has not occurred in FBS samples because FBS samples were still in the proliferation phase of osteogenesis and not the mineralization phase [32].

To examine the kinetics of the osteogenic process, expression of 3 osteogenic genes was monitored namely *RUNX2*, *ALP* and *OCN*. *RUNX2* is the master regulator when it comes to osteogenesis and is mainly responsible for the differentiation of ASCs into preosteoblasts [73]. *RUNX2* is down-regulated in the later stages of osteogenesis [73]. FBS and PRP induce an increase in *RUNX2* expression over the differentiation period, while pHPL induces a down regulation of *RUNX2* as early as day 7, indicating that ASC differentiation to preosteoblasts had to have happened before day 7 already. Both FBS and PRP samples had less calcium deposition than pHPL, suggesting that because pHPL samples differentiated into preosteoblasts earlier, they had more time to calcify the extra cellular matrix. *ALP*, like *RUNX2*, is an early osteogenic gene that plays an important role in matrix formation through the hydrolysis of inorganic phosphate [74]. *ALP* expression slowly decreased in FBS samples indicating that matrix formation was still taking place at the day of termination. The level *ALP* expression in both pHPL and PRP samples was downregulated indicating that matrix formation had already occurred as early as day 7. *OCN* is used as a biochemical marker for bone formation, as it is the most abundant non-collagenous protein in bone tissue [75]. FBS samples showed almost no expression of *OCN* on the day of termination which correlates with ARS assay results. pHPL samples also showed no expression of *OCN* on the day of termination; however, ARS assay results showed that pHPL samples had the highest amount of calcified bone product. PRP samples showed an increased expression of *OCN* on the day of termination which coincides with ARS assay results as PRP samples did show calcified bone product on the day of termination. Two adipogenic genes were included as controls. As mentioned previously, *PPAR $\gamma$*  is the main transcription factor in adipogenesis and needs to be inhibited for osteogenesis to occur [70]. In both pHPL and PRP samples, *PPAR $\gamma$*  is down-regulated as early as day 7. This however was not true for FBS samples. *PPAR $\gamma$*  gradually decreases over the differentiation period but is never fully downregulated. *FABP4* is a late adipogenic marker and plays a role in lipid formation [76]. FBS samples show a gradual increase in *FABP4*, with the highest expression of *FABP4* on the day of termination. In pHPL samples, *FABP4* is downregulated across the entire differentiation period. PRP samples show little *FABP4* expression, and the expression decreases until the day of termination. Results from both adipogenic genes explains why there is little to no osteogenesis taking place in FBS

samples as adipogenic genes are being expressed. In both pHPL and PRP samples both the adipogenic genes are downregulated allowing for osteogenesis to take place.

## 5. Conclusion

For ASCs to be a GMP compliant therapeutic product, the standardization of isolation, expansion and differentiation protocols needs to be done as well as the replacement of FBS as a supplementation factor. FBS is seen as a xenogeneic contaminant and therefore the use of FBS in culture medium does not meet GMP standards. In the current study, we looked at two possible alternatives to FBS namely pHPL and PRP. Our results show that not only were the two human alternatives able to sustain and differentiate ASCs into osteoblasts, they also out-performed ASCs differentiated in FBS. According to the gene expression kinetics of the osteogenic genes, ASCs also differentiated at a higher rate in pHPL and PRP supplemented media when compared to FBS. This fact is especially important when it comes to clinical applications as it shortens the time required for differentiation. ASC's osteogenic differentiating capacity make them attractive in treating bone defects/disorders. It is important to keep in mind that multiple *in vitro* discrepancies exist and it is therefore important to further test this work *in vivo*.



## 6. References

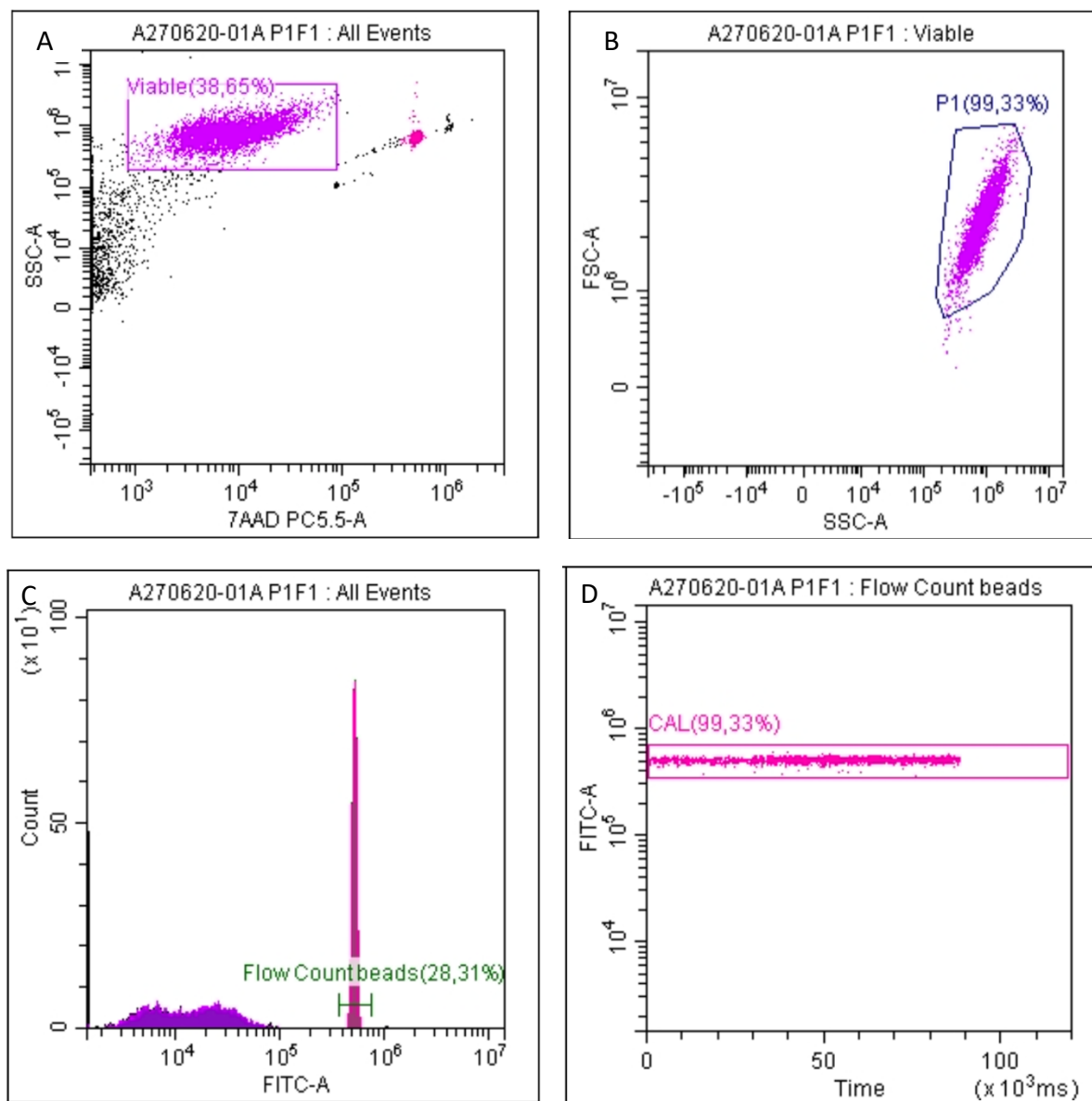
1. Ambele, M.A.; Dessels, C.; Durandt, C.; Pepper, M.S. Genome-wide analysis of gene expression during adipogenesis in human adipose-derived stromal cells reveals novel patterns of gene expression during adipocyte differentiation. *Stem Cell Res.* **2016**, *16*, 725–734, doi:10.1016/j.scr.2016.04.011.
2. van der Valk, J.; Brunner, D.; De Smet, K.; Fex Svenningsen, A.; Honegger, P.; Knudsen, L.E.; Lindl, T.; Noraberg, J.; Price, A.; Scarino, M.L.; et al. Optimization of chemically defined cell culture media--replacing fetal bovine serum in mammalian in vitro methods. *Toxicol. In Vitro* **2010**, *24*, 1053–1063, doi:10.1016/j.tiv.2010.03.016.
3. van der Valk, J.; Bieback, K.; Buta, C.; Cochrane, B.; Dirks, W.G.; Fu, J.; Hickman, J.J.; Hohensee, C.; Kolar, R.; Liebsch, M.; et al. Fetal Bovine Serum (FBS): Past - Present - Future. *ALTEX* **2018**, *35*, 99–118, doi:10.14573/altex.1705101.
4. Dessels, C.; Durandt, C.; Pepper, M.S. Comparison of human platelet lysate alternatives using expired and freshly isolated platelet concentrates for adipose-derived stromal cell expansion Comparison of human platelet lysate alternatives using expired and freshly isolated platelet concentrates. *Platelets* **2019**, *30*, 356–367, doi:10.1080/09537104.2018.1445840.
5. Shih, D.T.-B.; Burnout, T. Preparation, quality criteria, and properties of human blood platelet lysate supplements for ex vivo stem cell expansion. *N. Biotechnol.* **2015**, *32*, 199–211, doi:10.1016/j.nbt.2014.06.001.
6. Fekete, N.; Gadelorge, M.; Fürst, D.; Maurer, C.; Dausend, J.; Fleury-Cappellesso, S.; Mailänder, V.; Lotfi, R.; Ignatius, A.; Sensebé, L.; et al. Platelet lysate from whole blood-derived pooled platelet concentrates and apheresis-derived platelet concentrates for the isolation and expansion of human bone marrow mesenchymal stromal cells: production process, content and identification of active com. *Cytotherapy* **2012**, *14*, 540–554, doi:10.3109/14653249.2012.655420.
7. Trojahn Kølbe, S.-F.; Oliveri, R.S.; Glovinski, P. V.; Kirchhoff, M.; Mathiasen, A.B.; Elberg, J.J.; Andersen, P.S.; Drzewiecki, K.T.; Fischer-Nielsen, A. Pooled human platelet lysate versus fetal bovine serum--investigating the proliferation rate, chromosome stability and angiogenic potential of human adipose tissue-derived stem cells intended for clinical use. *Cytotherapy* **2013**, *15*, 1086–1097, doi:10.1016/j.jcyt.2013.01.217.
8. Bieback, K. Platelet lysate as replacement for fetal bovine serum in mesenchymal stromal cell cultures. *Transfus. Med. Hemotherapy* **2013**, *40*, 326–335, doi:10.1159/000354061.
9. Ben Azouna, N.; Jenhani, F.; Regaya, Z.; Berraëis, L.; Ben Othman, T.; Ducrocq, E.; Domenech, J. Phenotypical and functional characteristics of mesenchymal stem cells from bone marrow: comparison of culture using different media supplemented with human platelet lysate or fetal bovine serum. *Stem Cell Res. Ther.* **2012**, *3*, 6, doi:10.1186/scrt97.
10. Dessels, C.; Potgieter, M.; Pepper, M.S. Making the switch: Alternatives to fetal bovine serum for adipose-derived stromal cell expansion. *Front. Cell Dev. Biol.* **2016**, *4*, 1–10, doi:10.3389/fcell.2016.00115.
11. Chen, C.-F.; Liao, H.-T. Platelet-rich plasma enhances adipose-derived stem cell-mediated angiogenesis in a mouse ischemic hindlimb model. *World J. Stem Cells* **2018**, *10*, 212–227, doi:10.4252/wjsc.v10.i12.212.
12. Chierigato, K.; Castegnaro, S.; Madeo, D.; Astori, G.; Pegoraro, M.; Rodeghiero, F. Epidermal growth factor, basic fibroblast growth factor and platelet-derived growth factor-bb can substitute for fetal bovine serum and compete with human platelet-rich plasma in the ex vivo expansion of mesenchymal stromal cells derived from adipose tis. *Cytotherapy* **2011**, *13*, 933–943, doi:10.3109/14653249.2011.583232.
13. Xu, Y.; Wang, X.; Liu, W.; Lu, W. Thrombin-activated platelet-rich plasma enhances osteogenic differentiation of human periodontal ligament stem cells by activating SIRT1-mediated autophagy. *Eur. J. Med. Res.* **2021**, *26*, 105, doi:10.1186/s40001-021-00575-x.
14. Tavakolinejad, S.; Khosravi, M.; Mashkani, B.; Ebrahimzadeh Bideskan, A.; Sanjar Mossavi, N.; Parizadeh, M.R.S.; Hamidi Alamdari, D. The effect of human platelet-rich plasma on adipose-derived stem cell proliferation and osteogenic differentiation. *Iran. Biomed. J.* **2014**, *18*, 151–157, doi:10.6091/ibj.1301.2014.
15. Arpornmaeklong, P.; Kochel, M.; Depprich, R.; Kübler, N.R.; Würzler, K.K. Influence of platelet-rich plasma (PRP) on osteogenic differentiation of rat bone marrow stromal cells. An in vitro study. *Int. J. Oral Maxillofac. Surg.* **2004**, *33*, 60–70, doi:https://doi.org/10.1054/ijom.2003.0492.
16. Kasten, P.; Vogel, J.; Beyen, I.; Weiss, S.; Niemyer, P.; Leo, A.; Luginbuhl, R. Effect of Platelet-rich Plasma on the in vitro Proliferation and Osteogenic Differentiation of Human Mesenchymal Stem Cells on Distinct Calcium Phosphate Scaffolds: The Specific Surface Area Makes a Difference. *J. Biomater. Appl.* **2008**, *23*, 169–188, doi:10.1177/0885328207088269.
17. Rubio-Azpeitia, E.; Andia, I. Partnership between platelet-rich plasma and mesenchymal stem cells: in vitro experience. *Muscles. Ligaments Tendons J.* **2014**, *4*, 52–62.
18. Iudicone, P.; Fioravanti, D.; Bonanno, G.; Miceli, M.; Lavorino, C.; Totta, P.; Frati, L.; Nuti, M.; Pierelli, L. Pathogen-free, plasma-poor platelet lysate and expansion of human mesenchymal stem cells. *J. Transl. Med.* **2014**, *12*, 28, doi:10.1186/1479-5876-12-28.
19. Oikonomopoulos, A.; van Deen, W.K.; Manansala, A.-R.; Lacey, P.N.; Tomakili, T.A.; Ziman, A.; Hommes, D.W. Optimization of human mesenchymal stem cell manufacturing: the effects of animal/xeno-free media. *Sci. Rep.* **2015**, *5*, 16570, doi:10.1038/srep16570.
20. Jafar, H.; Abuarqoub, D.; Ababneh, N.; Hasan, M.; Al-Sotari, S.; Aslam, N.; Kailani, M.; Ammouh, M.; Shraideh, Z.;

- Awidi, A. hPL promotes osteogenic differentiation of stem cells in 3D scaffolds. *PLoS One* **2019**, *14*, e0215667.
21. Shanbhag, S.; Mohamed-Ahmed, S.; Lunde, T.H.F.; Suliman, S.; Bolstad, A.I.; Hervig, T.; Mustafa, K. Influence of platelet storage time on human platelet lysates and platelet lysate-expanded mesenchymal stromal cells for bone tissue engineering. *Stem Cell Res. Ther.* **2020**, *11*, 351, doi:10.1186/s13287-020-01863-9.
  22. Karadjian, M.; Senger, A.-S.; Essers, C.; Wilkesmann, S.; Heller, R.; Fellenberg, J.; Simon, R.; Westhauser, F. Human Platelet Lysate Can Replace Fetal Calf Serum as a Protein Source to Promote Expansion and Osteogenic Differentiation of Human Bone-Marrow-Derived Mesenchymal Stromal Cells. *Cells* **2020**, *9*.
  23. Xia, W.; Li, H.; Wang, Z.; Xu, R.; Fu, Y.; Zhang, X.; Ye, X.; Huang, Y.; Xiang, A.P.; Yu, W. Human platelet lysate supports ex vivo expansion and enhances osteogenic differentiation of human bone marrow-derived mesenchymal stem cells. *Cell Biol. Int.* **2011**, *35*, 639–643, doi:https://doi.org/10.1042/CBI20100361.
  24. Chevallier, N.; Anagnostou, F.; Zilber, S.; Bodivit, G.; Maurin, S.; Barrault, A.; Bierling, P.; Hernigou, P.; Layrolle, P.; Rouard, H. Osteoblastic differentiation of human mesenchymal stem cells with platelet lysate. *Biomaterials* **2010**, *31*, 270–278, doi:https://doi.org/10.1016/j.biomaterials.2009.09.043.
  25. Nishimura, I.; Hisanaga, R.; Sato, T.; Arano, T.; Nomoto, S. Effect of osteogenic differentiation medium on proliferation and differentiation of human mesenchymal stem cells in three-dimensional culture with radial flow bioreactor. *Regen. Ther.* **2015**, *2*, 24–31, doi:10.1016/j.reth.2015.09.001.
  26. Prockop, D.J. Collagens: Molecular Biology, Diseases, and Potentials for Therapy. *Annu. Rev. Biochem.* **1995**, *64*, 403–434, doi:10.1146/annurev.biochem.64.1.403.
  27. Chung, C.H.; Golub, E.E.; Forbes, E.; Tokuoka, T.; Shapiro, I.M. Mechanism of action of beta-glycerophosphate on bone cell mineralization. *Calcif. Tissue Int.* **1992**, *51*, 305–311, doi:10.1007/BF00334492.
  28. Hamidouche, Z.; Haÿ, E.; Vaudin, P.; Charbord, P.; Schüle, R.; Marie, P.J.; Fromigüé, O. FHL2 mediates dexamethasone-induced mesenchymal cell differentiation into osteoblasts by activating Wnt/beta-catenin signaling-dependent Runx2 expression. *FASEB J. Off. Publ. Fed. Am. Soc. Exp. Biol.* **2008**, *22*, 3813–3822, doi:10.1096/fj.08-106302.
  29. Zuk, P.A.; Ph, D.; Zhu, M.I.N.; Mizuno, H.; Benhaim, P.; Lorenz, H.P. Multilineage Cells from Human Adipose Tissue : Implications for Cell-Based Therapies. *Tissue Eng.* **2001**, *7*, 211–228.
  30. Schallmoser, K.; Strunk, D. Generation of a pool of human platelet lysate and efficient use in cell culture. *Methods Mol. Biol.* **2013**, *946*, 349–362, doi:10.1007/978-1-62703-128-8\_22.
  31. Cates, N.C.; Oakley, D.J.; Onwuemene, O.A. Therapeutic white blood cell and platelet depletions using the spectra OPTIA system continuous mononuclear cell protocol. *J. Clin. Apher.* **2018**, *33*, 580–585, doi:10.1002/jca.21644.
  32. Mohamed-Ahmed, S.; Fristad, I.; Lie, S.A.; Suliman, S.; Mustafa, K.; Vindenes, H.; Idris, S.B. Adipose-derived and bone marrow mesenchymal stem cells: A donor-matched comparison. *Stem Cell Res. Ther.* **2018**, *9*, 1–15, doi:10.1186/s13287-018-0914-1.
  33. Dheda, K.; Huggett, J.F.; Bustin, S.A.; Johnson, M.A.; Rook, G.; Zumla, A. Validation of housekeeping genes for normalizing RNA expression in real-time PCR. *Biotechniques* **2004**, *37*, 112–119, doi:10.2144/04371RR03.
  34. Svec, D.; Tichopad, A.; Novosadova, V.; Pfaffl, M.W.; Kubista, M. How good is a PCR efficiency estimate: Recommendations for precise and robust qPCR efficiency assessments. *Biomol. Detect. Quantif.* **2015**, *3*, 9–16, doi:https://doi.org/10.1016/j.bdq.2015.01.005.
  35. Koellensperger, E.; Bollinger, N.; Dexheimer, V.; Gramley, F.; Germann, G.; Leimer, U. Choosing the right type of serum for different applications of human adipose tissue-derived stem cells: Influence on proliferation and differentiation abilities. *Cytotherapy* **2014**, *16*, 789–799, doi:10.1016/j.jcyt.2014.01.007.
  36. Gottipamula, S.; Muttigi, M.S.; Kolkundkar, U.; Seetharam, R.N. Serum-free media for the production of human mesenchymal stromal cells : a review. *Cell Prolif.* **2013**, *46*, 608–627, doi:10.1111/cpr.12063.
  37. Jayme, D.W.; Smith, S.R. Media formulation options and manufacturing process controls to safeguard against introduction of animal origin contaminants in animal cell culture. *Cytotechnology* **2000**, *36*, 27–36.
  38. Burnouf, T.; Strunk, D.; Koh, M.B.C.; Schallmoser, K. Human platelet lysate: Replacing fetal bovine serum as a gold standard for human cell propagation? *Biomaterials* **2016**, *76*, 371–387, doi:10.1016/j.biomaterials.2015.10.065.
  39. Bieback, K.; Hecker, A.; Kocaömer, A.; Lannert, H.; Schallmoser, K.; Strunk, D.; Klüter, H. Human alternatives to fetal bovine serum for the expansion of mesenchymal stromal cells from bone marrow. *Stem Cells* **2009**, *27*, 2331–2341, doi:10.1002/stem.139.
  40. Gstraunthaler, G.; Rauch, C.; Feifel; Lindl Preparation of Platelet Lysates for Mesenchymal Stem Cell Culture Media. *J Stem Cells Res, Rev Rep. J Stem Cells Res, Rev Rep* **2015**, *2*, 1021–1.
  41. Castegnaro, S.; Chierigato, K.; Maddalena, M.; Albiero, E.; Visco, C.; Madeo, D.; Pegoraro, M.; Rodeghiero, F. Effect of platelet lysate on the functional and molecular characteristics of mesenchymal stem cells isolated from adipose tissue. *Curr. Stem Cell Res. Ther.* **2011**, *6*, 105–114, doi:10.2174/157488811795495440.
  42. Camilleri, E.T.; Dudakovic, A.; Riester, S.M.; Galeano-Garces, C.; Paradise, C.R.; Bradley, E.W.; McGee-Lawrence, M.E.; Im, H.-J.; Karperien, M.; Krych, A.J.; et al. Loss of histone methyltransferase Ezh2 stimulates an osteogenic transcriptional program in chondrocytes but does not affect cartilage development. *J. Biol. Chem.* **2018**, *293*, 19001–19011, doi:10.1074/jbc.RA118.003909.
  43. Riis, S.; Zachar, V.; Boucher, S.; Vemuri, M.C.; Pennisi, C.P.; Fink, T. Critical steps in the isolation and expansion of adipose-derived stem cells for translational therapy. *Expert Rev. Mol. Med.* **2015**, *17*, e11, doi:10.1017/erm.2015.10.
  44. Panda, S.; Karanxha, L.; Goker, F.; Satpathy, A.; Taschieri, S.; Francetti, L.; Chandra Das, A.; Kumar, M.; Panda, S.;

- Del Fabbro, M. Autologous Platelet Concentrates in Treatment of Furcation Defects—A Systematic Review and Meta-Analysis. *Int. J. Mol. Sci.* 2019, *20*.
45. Metlerska, J.; Fagogeni, I.; Nowicka, A. Efficacy of Autologous Platelet Concentrates in Regenerative Endodontic Treatment: A Systematic Review of Human Studies. *J. Endod.* **2019**, *45*, 20-30.e1, doi:<https://doi.org/10.1016/j.joen.2018.09.003>.
  46. Mariani, E.; Pulsatelli, L. Platelet Concentrates in Musculoskeletal Medicine. *Int. J. Mol. Sci.* 2020, *21*.
  47. Fortunato, L.; Bennardo, F.; Buffone, C.; Giudice, A. Is the application of platelet concentrates effective in the prevention and treatment of medication-related osteonecrosis of the jaw? A systematic review. *J. Cranio-Maxillofacial Surg.* **2020**, *48*, 268–285, doi:<https://doi.org/10.1016/j.jcms.2020.01.014>.
  48. Astori, G.; Amati, E.; Bambi, F.; Bernardi, M.; Chierigato, K.; Schäfer, R.; Sella, S.; Rodeghiero, F. Platelet lysate as a substitute for animal serum for the ex-vivo expansion of mesenchymal stem/stromal cells: present and future. *Stem Cell Res. Ther.* **2016**, *7*, 93, doi:10.1186/s13287-016-0352-x.
  49. Scherer, S.S.; Tobalem, M.; Vigato, E.; Heit, Y.; Modarressi, A.; Hinz, B.; Pittet, B.; Pietramaggiore, G. Nonactivated versus thrombin-activated platelets on wound healing and fibroblast-to-myofibroblast differentiation in vivo and in vitro. *Plast. Reconstr. Surg.* **2012**, *129*, 46e-54e, doi:10.1097/PRS.0b013e3182362010.
  50. Maumus, M.; Peyrafitte, J.A.; D'Angelo, R.; Fournier-Wirth, C.; Bouloumié, A.; Casteilla, L.; Sengenès, C.; Bourin, P. Native human adipose stromal cells: Localization, morphology and phenotype. *Int. J. Obes.* **2011**, *35*, 1141–1153, doi:10.1038/ijo.2010.269.
  51. Patrikoski, M.; Juntunen, M.; Boucher, S.; Campbell, A.; Vemuri, M.C.; Mannerström, B.; Miettinen, S. Development of fully defined xeno-free culture system for the preparation and propagation of cell therapy-compliant human adipose stem cells. *Stem Cell Res. Ther.* **2013**, *4*, doi:10.1186/s13287-013-0175-7.
  52. Riis, S.; Nielsen, F.M.; Pennisi, C.P.; Zachar, V.; Fink, T. Comparative Analysis of Media and Supplements on Initiation and Expansion of Adipose-Derived Stem Cells. *Stem Cells Transl. Med.* **2016**, *5*, 314–324, doi:10.5966/sctm.2015-0148.
  53. Liao, H.T.; James, I.B.; Marra, K.G.; Rubin, J.P. The Effects of Platelet-Rich Plasma on Cell Proliferation and Adipogenic Potential of Adipose-Derived Stem Cells. *Tissue Eng. Part A* **2015**, *21*, 2714–2722, doi:10.1089/ten.tea.2015.0159.
  54. Haubner, F.; Muschter, D.; Schuster, N.; Pohl, F.; Ahrens, N.; Prantl, L.; Gassner, H.G. Platelet-rich plasma stimulates dermal microvascular endothelial cells and adipose derived stem cells after external radiation. *Clin. Hemorheol. Microcirc.* **2015**, *61*, 279–290, doi:10.3233/CH-151982.
  55. Bourin, P.; Bunnell, B.A.; Casteilla, L.; Dominici, M.; Katz, A.J.; March, K.L.; Redl, H.; Rubin, J.P. Stromal cells from the adipose tissue-derived stromal vascular fraction and culture expanded adipose tissue-derived stromal/stem cells: a joint statement of the International Federation for Adipose Therapeutics (IFATS) and Science and the International Society of Cytotherapy **2013**, *15*, 641–648, doi:10.1016/j.jcyt.2013.02.006.
  56. Januszyk, M.; Rennert, R.C.; Sorkin, M.; Maan, Z.N.; Wong, L.K.; Whittam, A.J.; Whitmore, A.; Duscher, D.; Gurtner, G.C. Evaluating the Effect of Cell Culture on Gene Expression in Primary Tissue Samples Using Microfluidic-Based Single Cell Transcriptional Analysis. **2015**, 540–550, doi:10.3390/microarrays4040540.
  57. Donnenberg, A.D.; Meyer, E.M.; Rubin, J.P.; Donnenberg, V.S. The cell-surface proteome of cultured adipose stromal cells. *Cytom. Part A* **2015**, *87*, 665–674, doi:10.1002/cyto.a.22682.
  58. Woodford-Thomas, T.; Thomas, M.L. The leukocyte common antigen, CD45 and other protein tyrosine phosphatases in hematopoietic cells. *Semin. Cell Biol.* **1993**, *4*, 409–418, doi:<https://doi.org/10.1006/scel.1993.1049>.
  59. Park, T.I.-H.; Feisst, V.; Brooks, A.E.S.; Rustenhoven, J.; Monzo, H.J.; Feng, S.X.; Mee, E.W.; Bergin, P.S.; Oldfield, R.; Graham, E.S.; et al. Cultured pericytes from human brain show phenotypic and functional differences associated with differential CD90 expression. *Sci. Rep.* **2016**, *6*, 26587, doi:10.1038/srep26587.
  60. Guo, J.; Nguyen, A.; Banyard, D.A.; Fadavi, D.; Toranto, J.D.; Wirth, G.A.; Paydar, K.Z.; Evans, G.R.D.; Widgerow, A.D. Stromal vascular fraction: A regenerative reality? Part 2: Mechanisms of regenerative action. *J. Plast. Reconstr. Aesthetic Surg.* **2016**, *69*, 180–188, doi:<https://doi.org/10.1016/j.bjps.2015.10.014>.
  61. Pierantozzi, E.; Badin, M.; Vezzani, B.; Curina, C.; Randazzo, D.; Petraglia, F.; Rossi, D.; Sorrentino, V. Human pericytes isolated from adipose tissue have better differentiation abilities than their mesenchymal stem cell counterparts. *Cell Tissue Res.* **2015**, *361*, 769–778, doi:10.1007/s00441-015-2166-z.
  62. Dubey, N.K.; Mishra, V.K.; Dubey, R.; Tsai, F.; Deng, W. Revisiting the Advances in Isolation, Characterization and Secretome of Adipose-Derived Stromal/Stem Cells. *Int. J. Mol. Sci.* **2018**, *19*, 1–23, doi:10.3390/ijms19082200.
  63. Bora, P.; Majumdar, A.S. Adipose tissue-derived stromal vascular fraction in regenerative medicine: a brief review on biology and translation. *Stem Cell Res. Ther.* **2017**, *8*, 145, doi:10.1186/s13287-017-0598-y.
  64. Skubis, A.; Gola, J.; Sikora, B.; Hybiak, J.; Paul-Samojedny, M.; Mazurek, U.; Łos, M.J. Impact of Antibiotics on the Proliferation and Differentiation of Human Adipose-Derived Mesenchymal Stem Cells. *Int. J. Mol. Sci.* **2017**, *18*, 2522, doi:10.3390/ijms18122522.
  65. Contentin, R.; Demoor, M.; Concari, M.; Desancé, M.; Audigié, F.; Branly, T.; Galéra, P. Comparison of the Chondrogenic Potential of Mesenchymal Stem Cells Derived from Bone Marrow and Umbilical Cord Blood Intended for Cartilage Tissue Engineering. *Stem Cell Rev. Reports* **2020**, *16*, 126–143, doi:10.1007/s12015-019-09914-2.
  66. Gupta, P.; Hall, G.N.; Geris, L.; Luyten, F.P.; Papantoniou, I. Human Platelet Lysate Improves Bone Forming

- Potential of Human Progenitor Cells Expanded in Microcarrier-Based Dynamic Culture. *Stem Cells Transl. Med.* **2019**, *8*, 810–821, doi:10.1002/sctm.18-0216.
67. Shanbhag, S.; Suliman, S.; Mohamed-Ahmed, S.; Kamplaitner, C.; Hassan, M.N.; Heimel, P.; Dobsak, T.; Tangl, S.; Bolstad, A.I.; Mustafa, K. Bone regeneration in rat calvarial defects using dissociated or spheroid mesenchymal stromal cells in scaffold-hydrogel constructs. *Stem Cell Res. Ther.* **2021**, *12*, 575, doi:10.1186/s13287-021-02642-w.
68. Qiu, G.; Wu, H.; Huang, M.; Ma, T.; Schneider, A.; Oates, T.W.; Weir, M.D.; Xu, H.H.K.; Zhao, L. Novel calcium phosphate cement with biofilm-inhibition and platelet lysate delivery to enhance osteogenesis of encapsulated human periodontal ligament stem cells. *Mater. Sci. Eng. C* **2021**, *128*, 112306, doi:https://doi.org/10.1016/j.msec.2021.112306.
69. Chignon-Sicard, B.; Kouidhi, M.; Yao, X.; Delerue-Audegond, A.; Villageois, P.; Peraldi, P.; Ferrari, P.; Rival, Y.; Piwnica, D.; Aubert, J.; et al. Platelet-rich plasma respectively reduces and promotes adipogenic and myofibroblastic differentiation of human adipose-derived stromal cells via the TGF $\beta$  signalling pathway. *Sci. Rep.* **2017**, *7*, 2954, doi:10.1038/s41598-017-03113-0.
70. Kang, S.; Bennett, C.N.; Gerin, I.; Rapp, L.A.; Hankenson, K.D.; Macdougald, O.A. Wnt Signaling Stimulates Osteoblastogenesis of Mesenchymal Precursors by Suppressing CCAAT / Enhancer-binding Protein  $\alpha$  and Peroxisome Proliferator-activated Receptor  $\alpha$ . *J. Biol. Chem.* **2007**, *282*, 14515–14524, doi:10.1074/jbc.M700030200.
71. Matta, C.; Szűcs-Somogyi, C.; Kon, E.; Robinson, D.; Neufeld, T.; Altschuler, N.; Berta, A.; Hangody, L.; Veréb, Z.; Zákány, R. Osteogenic differentiation of human bone marrow-derived mesenchymal stem cells is enhanced by an aragonite scaffold. *Differentiation.* **2019**, *107*, 24–34, doi:10.1016/j.diff.2019.05.002.
72. Puchtler, H.; Meloan, S.N.; Terry, M.S. On the History and Mechanisms of Alizarin and Alizarin Red S Stains for Calcium. *J. Histochem. Cytochem.* **1969**, *17*, 110–124.
73. Bruderer, M.; Richards, R.G.; Alini, M.; Stoddart, M.J. Role and regulation of RUNX2 in osteogenesis. *Eur. Cell. Mater.* **2014**, *28*, 269–286, doi:10.22203/ecm.v028a19.
74. Siffert, R.S. The role of alkaline phosphatase in osteogenesis. *J. Exp. Med.* **1951**, *93*, 415–426.
75. Zoch, M.L.; Clemens, T.L.; Riddle, R.C. New Insights into the Biology of Osteocalcin. *Bone* **2017**, *82*, 42–49, doi:10.1016/j.bone.2015.05.046.New.
76. Fink, T.; Zachar, V. Adipogenic differentiation of human mesenchymal stem cells. *Methods Mol. Biol.* **2011**, *698*, 243–251, doi:10.1007/978-1-60761-999-4\_19.
77. Bustin, S.A.; Benes, V.; Garson, J.A.; Hellemans, J.; Huggett, J.; Kubista, M.; Mueller, R.; Nolan, T.; Pfaffl, M.W.; Shipley, G.L.; et al. The MIQE Guidelines: Minimum Information for Publication of Quantitative Real-Time PCR Experiments. *Clin. Chem.* **2009**, *55*, 611–622, doi:10.1373/clinchem.2008.112797.

## Supplementary Information A: Cell counts, Immunophenotyping and Compensation Experiments



**E** Tube Name: A270620-01A P1F1  
Sample ID:  
Absolute Count: Beads Population=CAL, Beads Count=1007, Sample Volume=1 $\mu$ L

Population	Events	% Total	% Parent	Events/ $\mu$ L(B)
● All Events	10000	100,00%	100,00%	3581,08
● P1	3839	38,39%	99,33%	1374,78
● Viable	3865	38,65%	38,65%	1384,09
● Flow Count beads	2831	28,31%	28,31%	1013,80
● CAL	2812	28,12%	99,33%	####

Figure A1. Schematic representation of the flow cytometry protocol, including gating strategies used to determine absolute cell counts and cell viability.

A. Side-scatter versus 7-AAD visualised the viable cells. B. Forward scatter versus side-scatter gated on the viable cells created a P1 gate that was used to determine the cells/ul. C. An event count versus FITC identified the Flow-Count™ fluorospheres. D. FITC versus time gated on FlowCount beads identified the intact fluorospheres. E. The events/ul of P1 population was used to calculate the total cell count (Equation 2).

$$\text{Absolute cell count (Cells)} = \text{Absolute cell count} \left( \frac{\text{cells}}{\text{ul}} \right) \times \text{Volume of cells}$$

**Equation A1. Formula used to calculate absolute cell count (cells).**

**Table A1:** Monoclonal antibodies, fluorochromes, detector channels, lasers, filters and their respective manufacturers

Monoclonal antibodies	Fluorochromes	Fluorescent detector channel (FL)	Laser and band pass filters	Manufacturer
Mouse anti-human CD90	Fluorescein Isothiocyanate (FITC)	FL1	488 nm (525/40)	Beckman Coulter, Miami, USA
Mouse anti-human CD105	Phycoerythrin (PE)	FL2	488 nm (585/42)	Beckman Coulter, Miami, USA
Mouse anti-human CD34	Phycoerythrin-Cyanin 5 (PC5)	FL5	488 nm (690/50)	Beckman Coulter, Miami, USA
Mouse anti-human CD36	Allophycocyanine (APC)	FL6	635 nm (660/10)	Beckman Coulter, Miami, USA
Mouse anti-human CD44	Allophycocyanin: Cy-7 tandem conjugate (APC Cy7)	FL8	635 nm (780/60)	BioLegend, San Diego, USA
Mouse anti-human CD73	Brilliant Violet 421 (BV)	FL9	405 nm (450/45)	BD Biosciences, Franklin Lakes, New Jersey, USA
Mouse anti-human CD45	Krome Orange (KO)	FL10	405nm (525/40)	Beckman Coulter, Miami, USA

The ISCT guidelines recommended that ASCs should express certain pre-defined cell surface markers. We stained the ASCs with a panel of monoclonal antibodies consisting of CD34, CD36, CD44, CD45, CD73, CD90 and CD105.

The following tubes were prepared to generate a colour compensation matrix for the combination of fluorochromes used for phenotyping of the ASCs.

Tube 1: Unstained cells

Tube 2: Unstained VersaComp beads (as per manufacturer instructions)

Tubes 3-8: VersaComp beads stained with the individual monoclonal antibodies (as per manufacturer instructions).

Tube 9: Cells stained with CD90

Tube 10: Cells simultaneously stained with all 7 monoclonal antibodies (combination tube). This tube was used to verify the compensation matrix generated using the single colour staining tubes and to make final adjustment where needed (Table A2).

**Table A2.** Setup of experiment to calculate the ASC phenotype compensation matrix.

Flow tubes										
	Tube 1	Tube 2	Tube 3	Tube 4	Tube 5	Tube 6	Tube 7	Tube 8	Tube 9	Tube 10
Cells	x								*x	x
Beads (Positive and negative)		x	x	x	x	x	x	x		
Addition of monoclonal antibodies										
CD34			x							x
CD36				x						x
CD44					x					x
CD45						x				x
CD73							x			x
CD90								x		x
CD105									x	x

\* CD90 does not bind tightly to the beads, therefore cells are used.

The VersaComp Kit (B22804; Beckman Coulter) consist of two vials, a vial with positive beads and a vial with negative beads. Positive beads are coated with IgG binding agent, whereas the negative beads are not. Antibodies will bind to the positive beads, causing the beads to fluoresce, observed by the presence of a distinct positive population in the relevant channel (Figure A2). The positive population will be gated and used to detect the spectral spill

(Figure A1B) over in other channels. This setup is repeated for each monoclonal antibody in the panel.

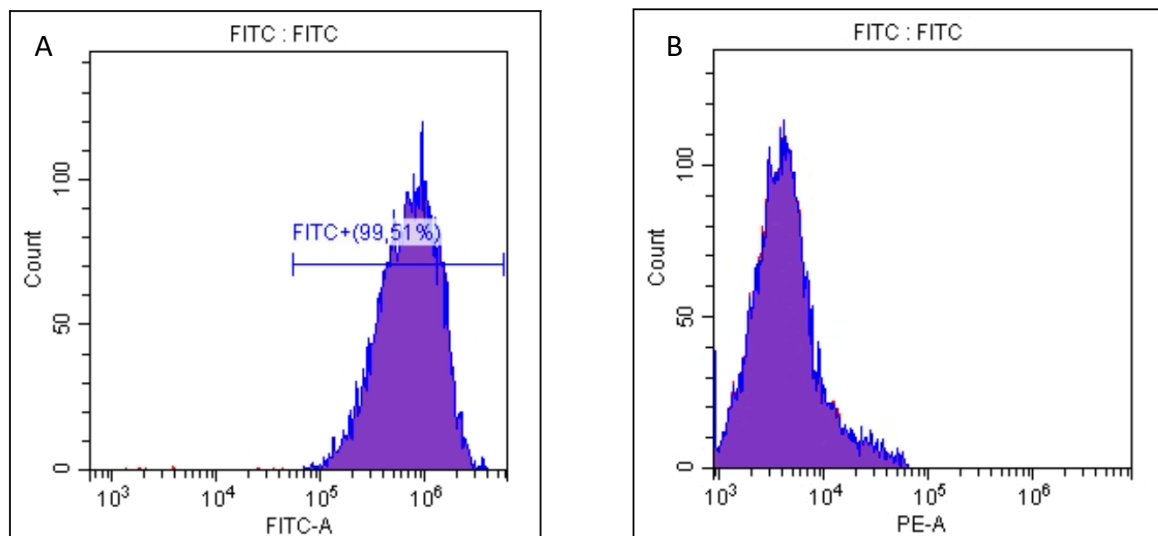


**Figure A2. Example of compensation experiment of FITC monoclonal antibody.**

A. Single stained FITC tube ran on the DxFLEX produces a positive FITC population that is used to gate other channels on to determine the amount of spill over to be removed from respective channels. B. Spill over of FITC fluorescence into PE channel that needs to be removed.

Positive and negative VersaComp beads were vortexed before use and one drop of each bead type (negative and positive) was added to the respective tubes (Tube 2-8) (Tube 9 contained a single stain of CD 90, however CD90 does not bind tightly to the beads and therefore cells were used instead of beads). Once all the antibodies were added to the respective tubes, the flow cytometry tubes were vortexed and incubated in the dark for 20 min. After incubation, the beads and cells were washed by adding 3 mL of PBS (2% pen/strep) to the tubes followed by centrifugation  $300 \times g$  for 10 min. The supernatant was aspirated and the cells or beads were resuspended in 400  $\mu$ l of PBS (2% pen/strep) before analysis on the CytoFLEX flow cytometer. Analyses was done on a minimum of 5 000 viable beads or ASCs.



The ASC population was visualised using a FSC-A vs. SSC-A two-parameter dot plot (Figure A2). A gate was drawn around the intact ASC population was gated to exclude any debris present in the samples. A histogram plot (Count vs. respective fluorescent channel) was created for each of the fluorochromes. All the histograms were gated on the intact ASC population. In the respective single colour positive tube (e.g Count vs FITC) a positive signal for that fluorochrome was observed. A region of interest was positioned over the positive population. If this fluoresce was picked up in any other channel it was subtracted from that channel and so a compensation matrix was setup to remove any spill-over that might occur during further immunophenotyping experiments (Figure A2). Compensation matrices generated from compensation experiments were applied to respective immunophenotyping experiments.

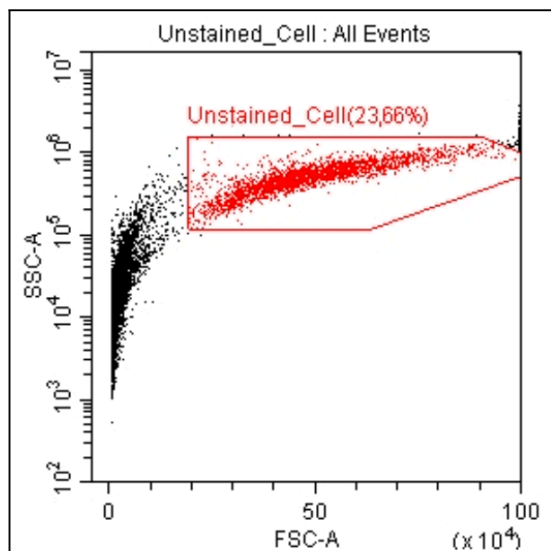
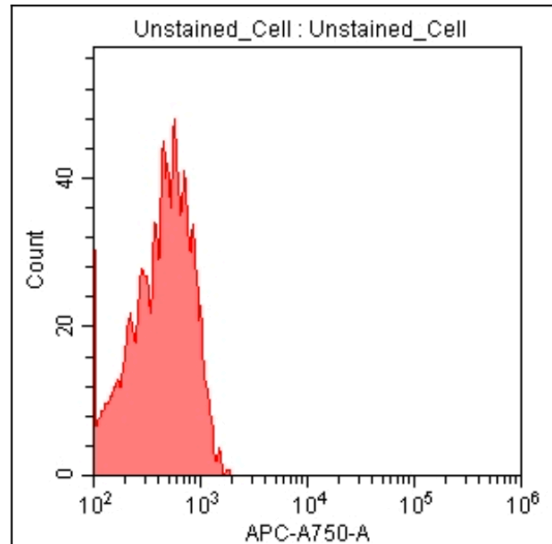
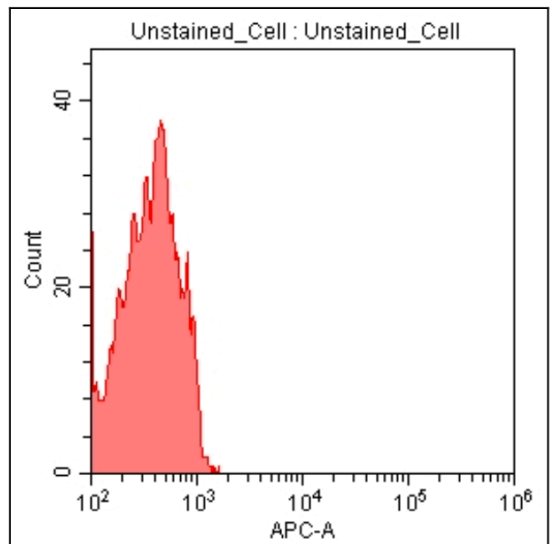
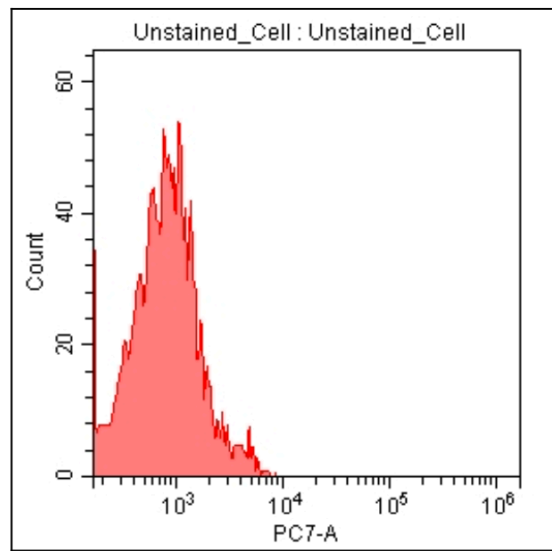
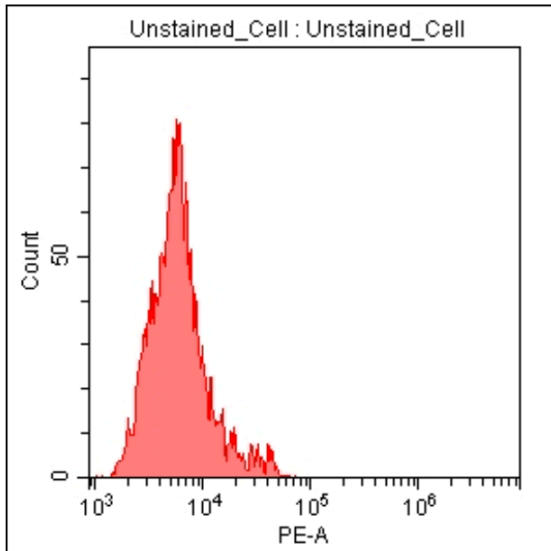
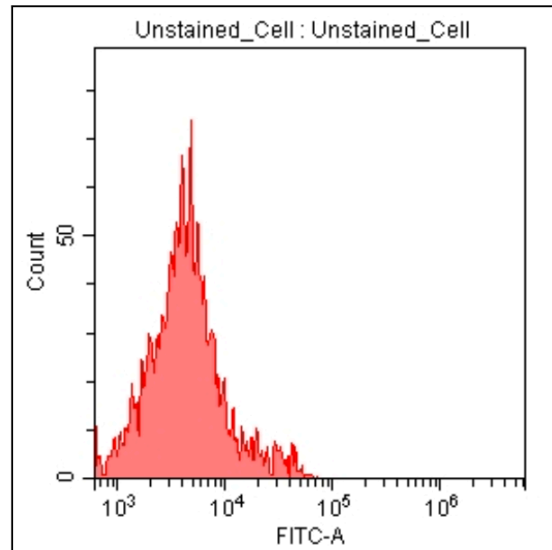
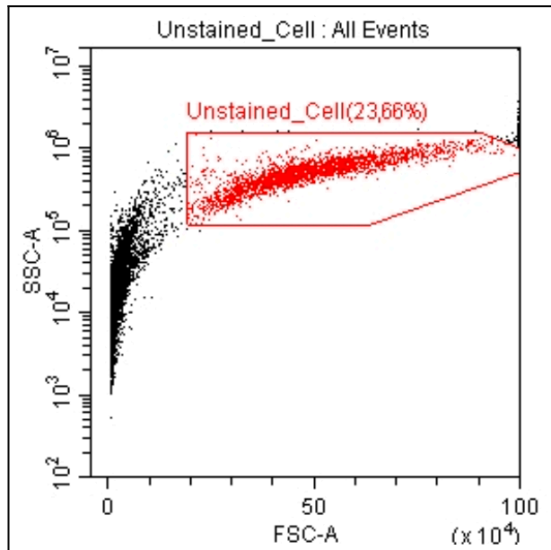
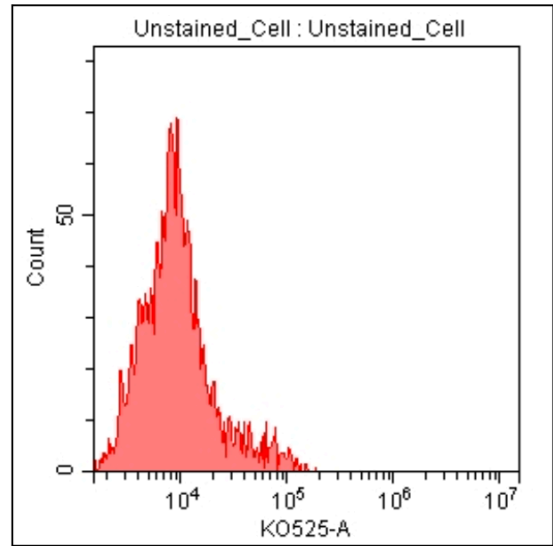
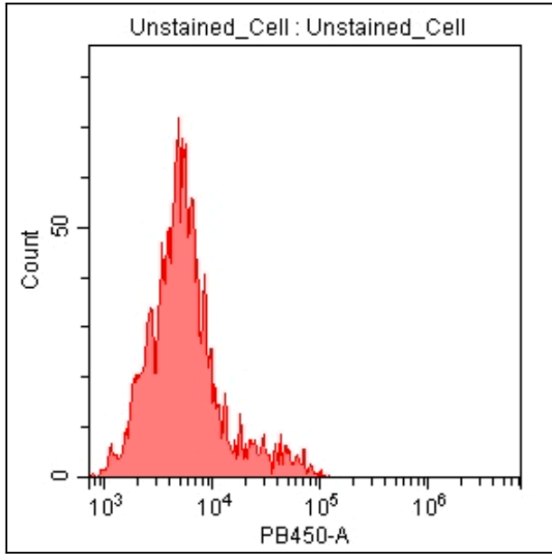


Figure A3. FSC-A vs. SSC-A two-parameter dot plot used to gate out debris.

### Unstained Cells

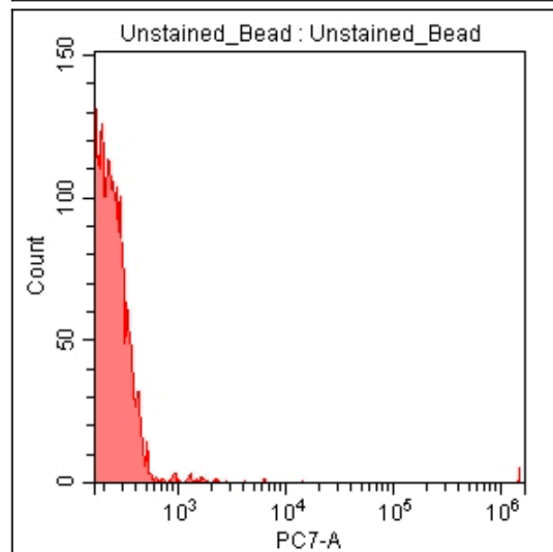
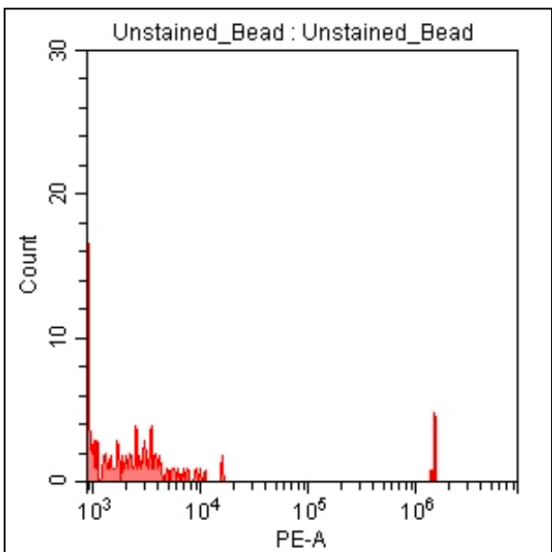
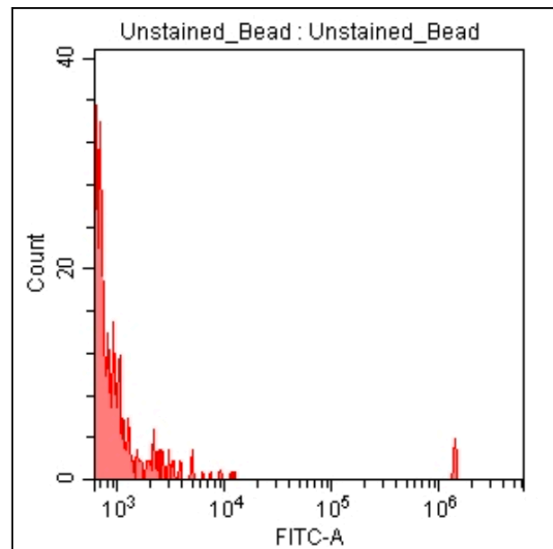
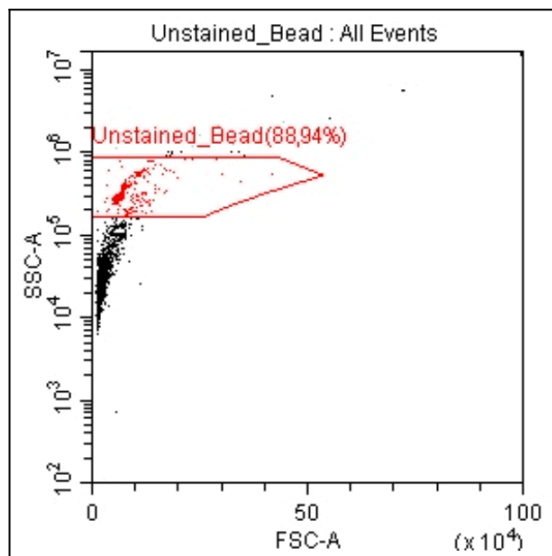
First control for autofluorescence

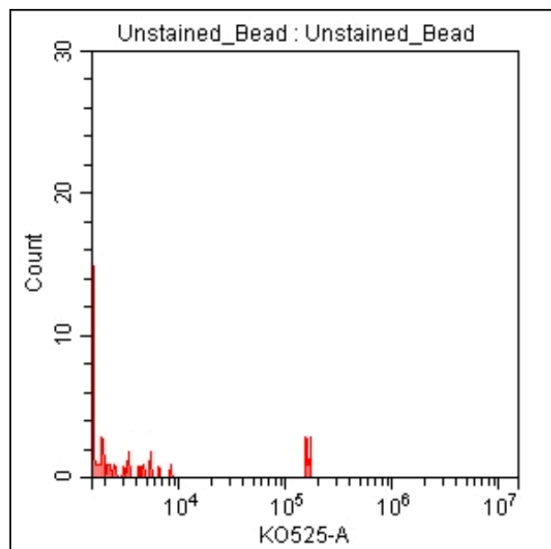
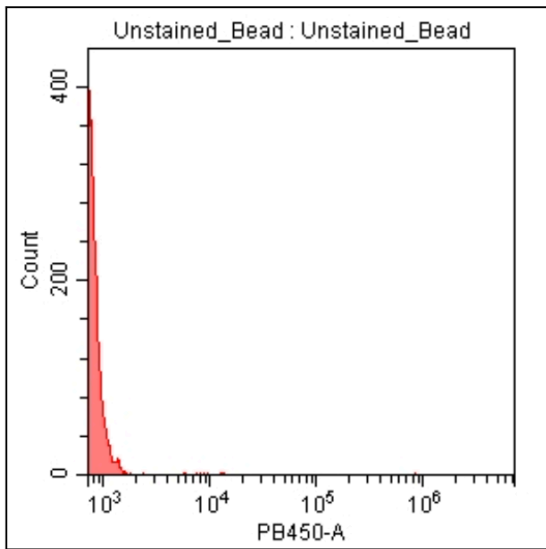
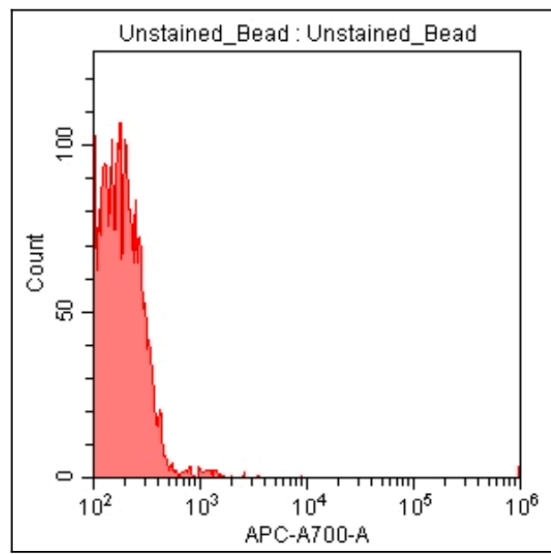
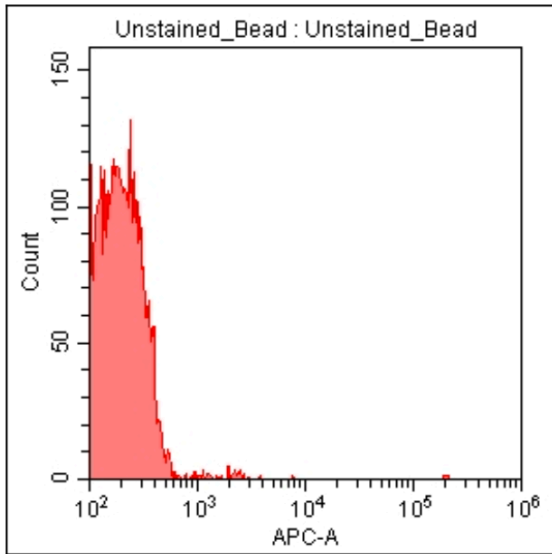




### Unstained Beads

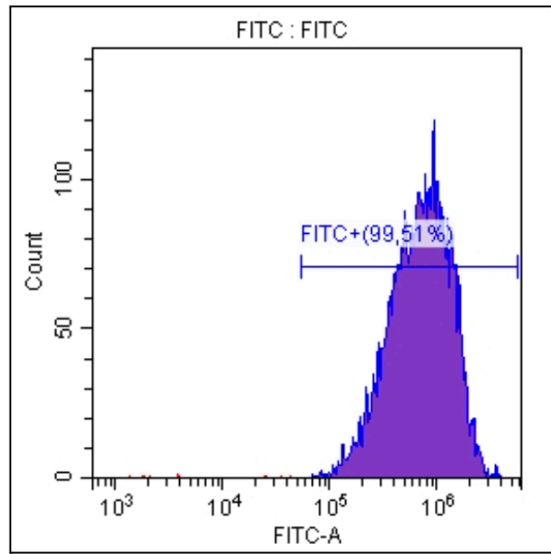
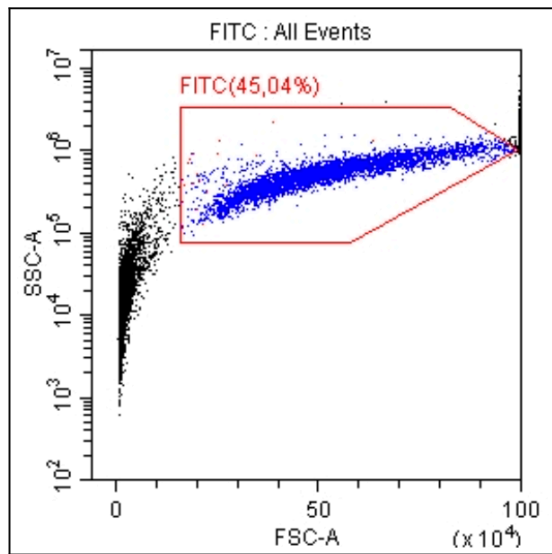
Second control for autofluorescence

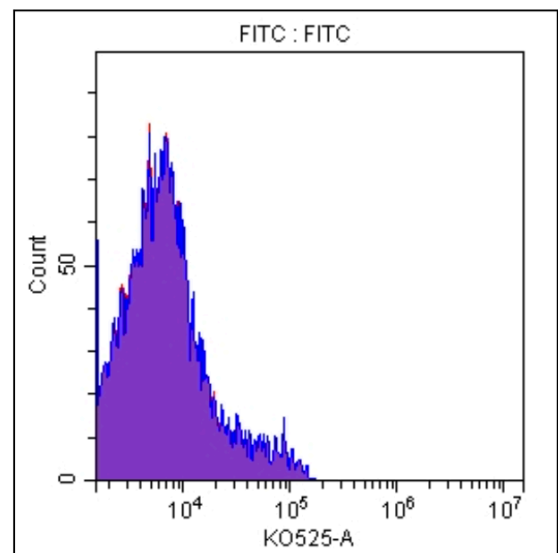
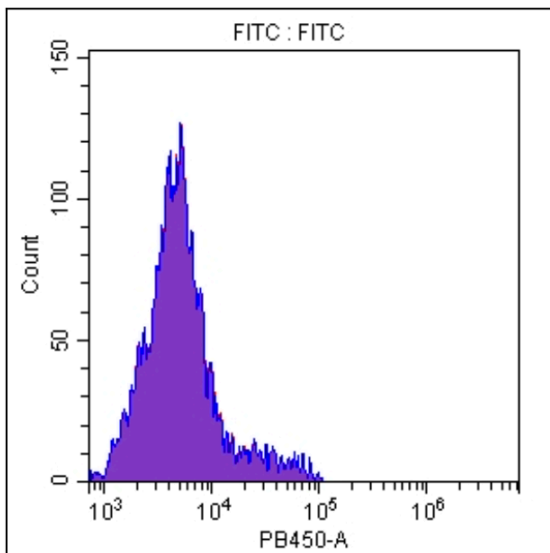
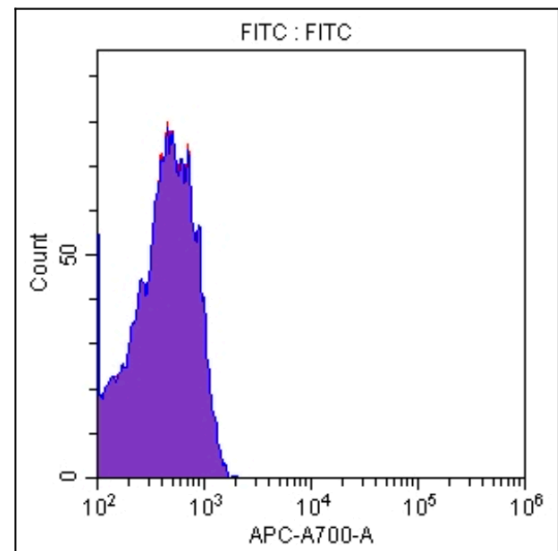
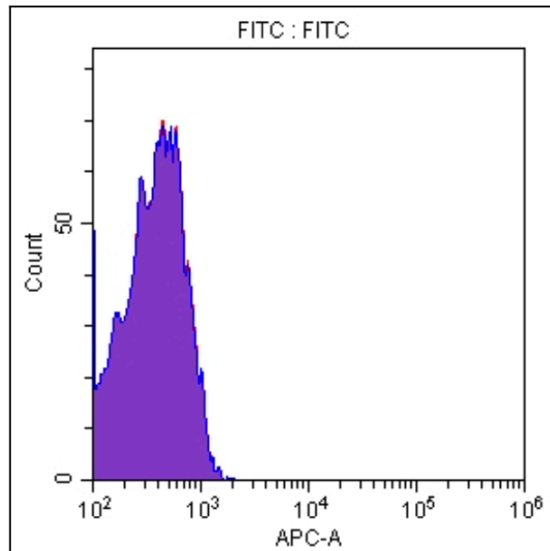
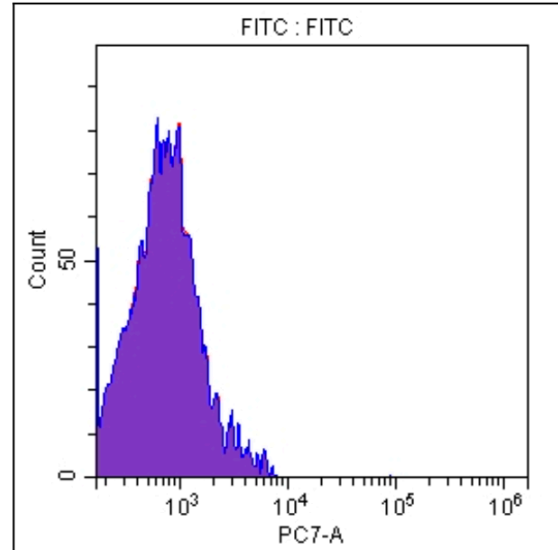
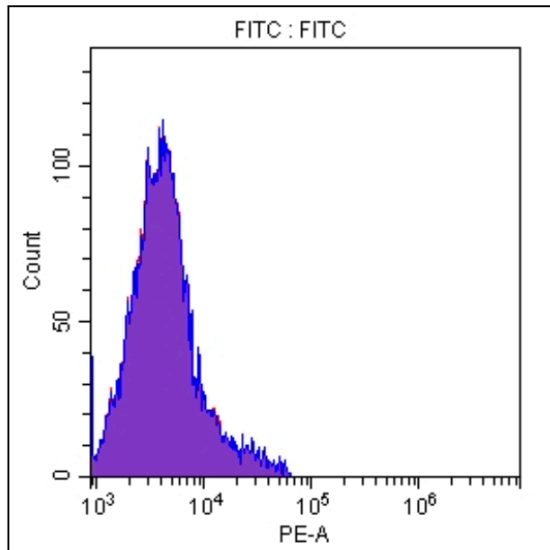




**FITC (FL1) channel:**

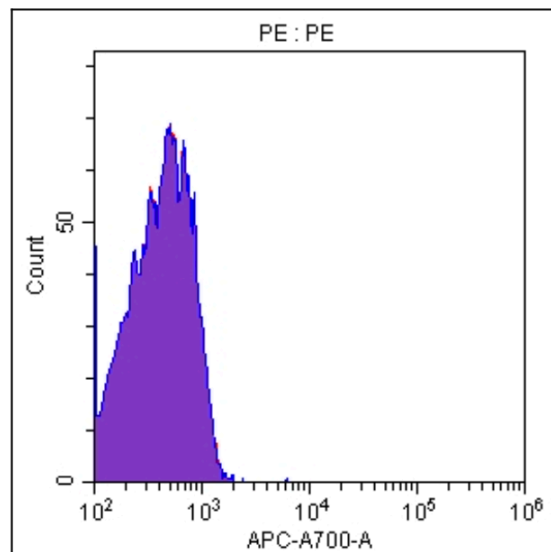
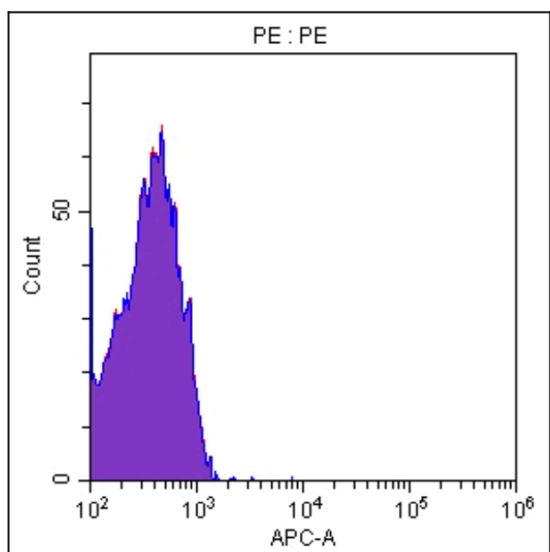
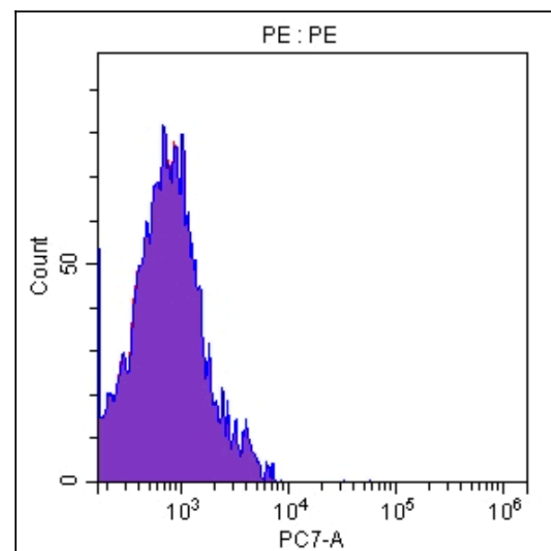
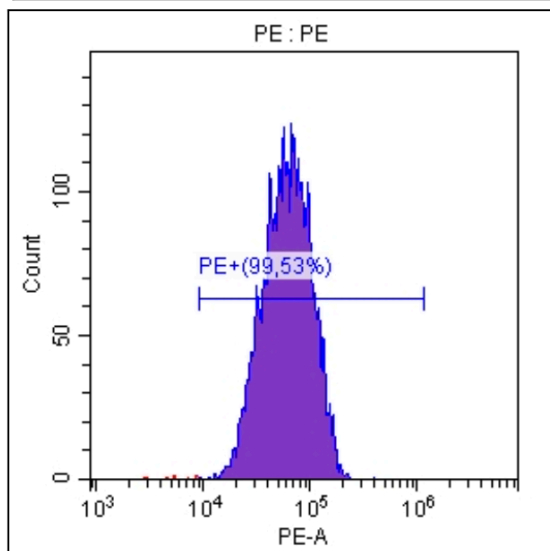
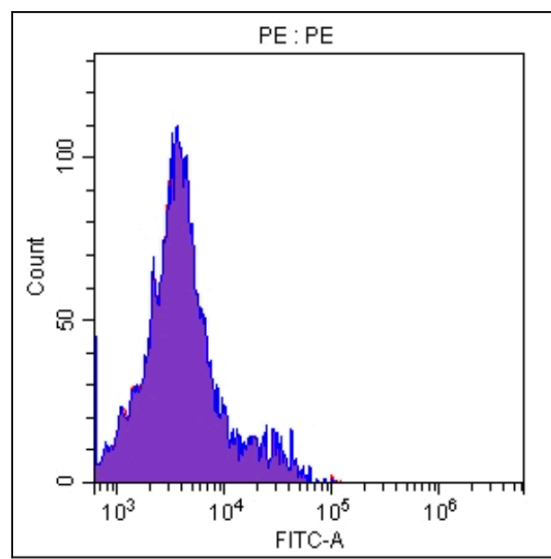
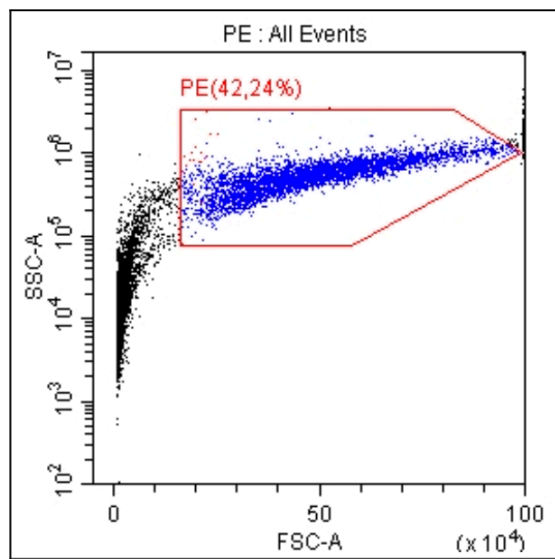
To determine the spillover of FITC (conjugate) into the other fluorescence channels

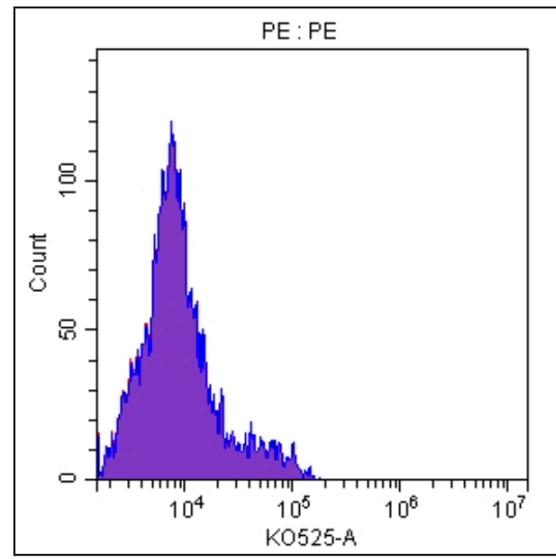
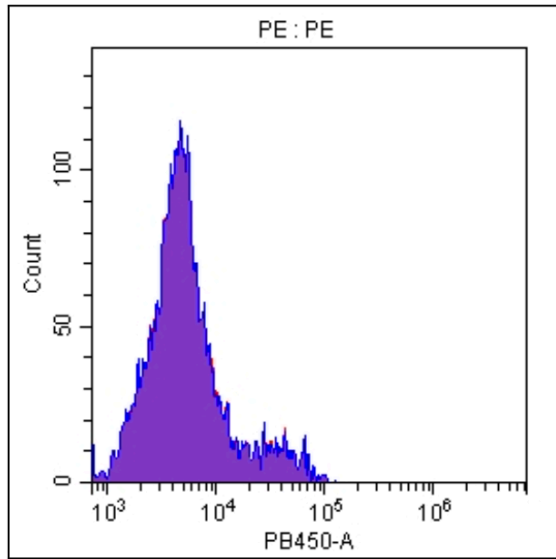




**PE (FL2 channel)**

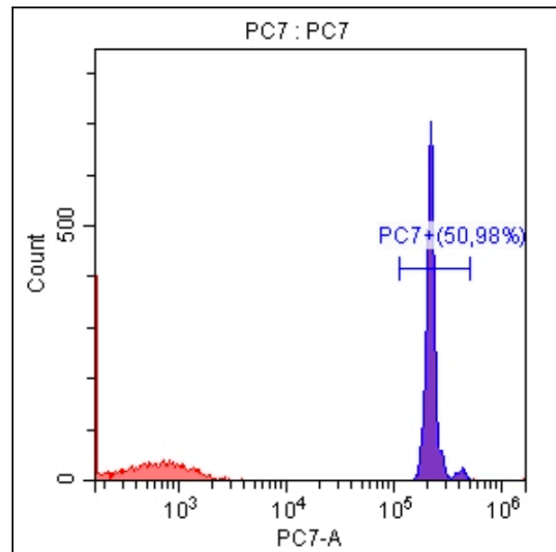
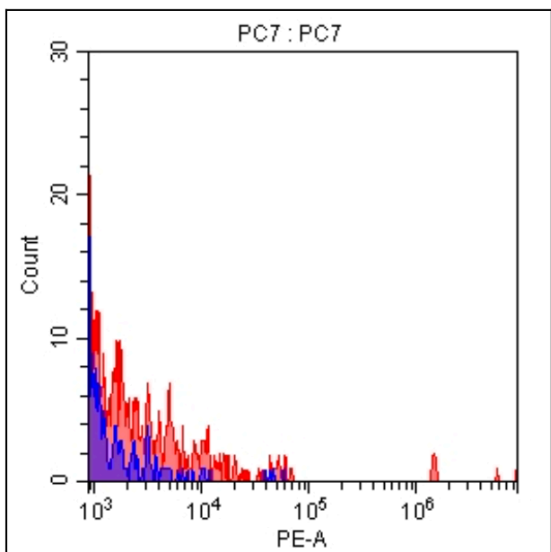
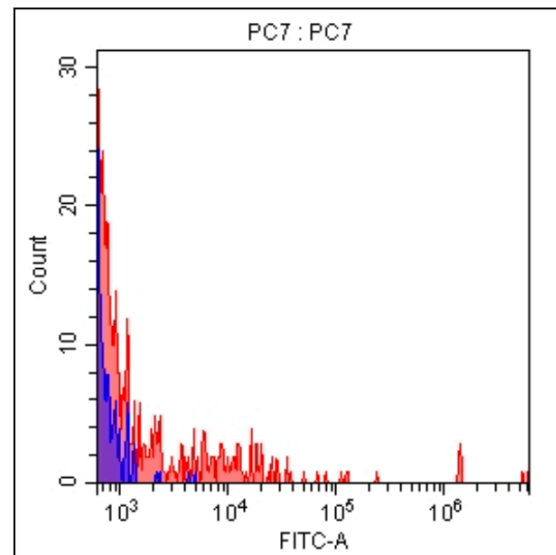
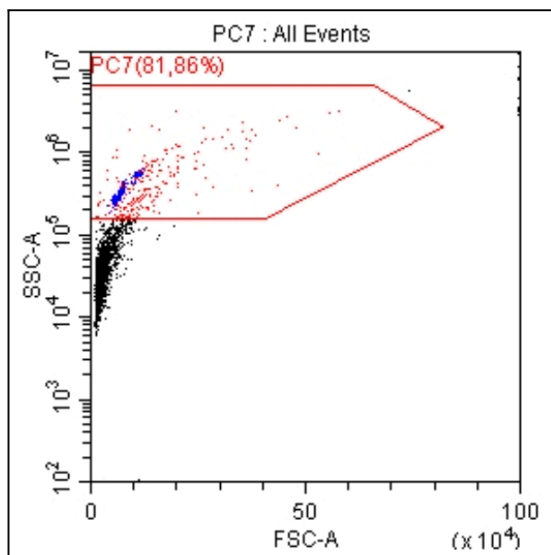
To determine the spillover of PE (conjugate) into the other fluorescence channels

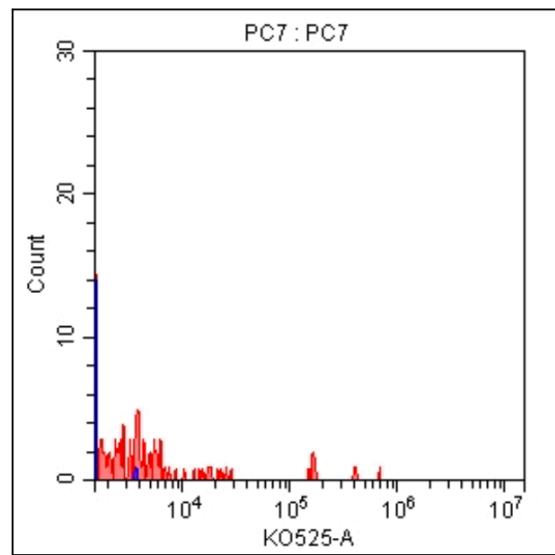
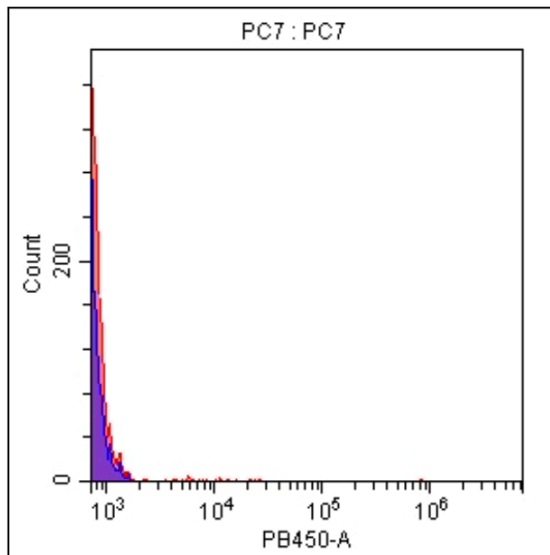
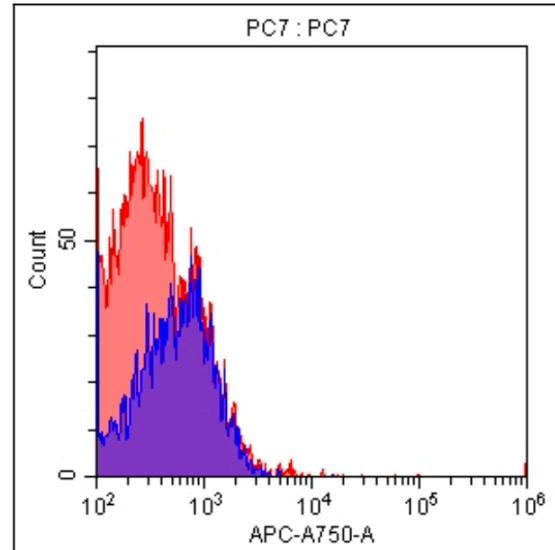
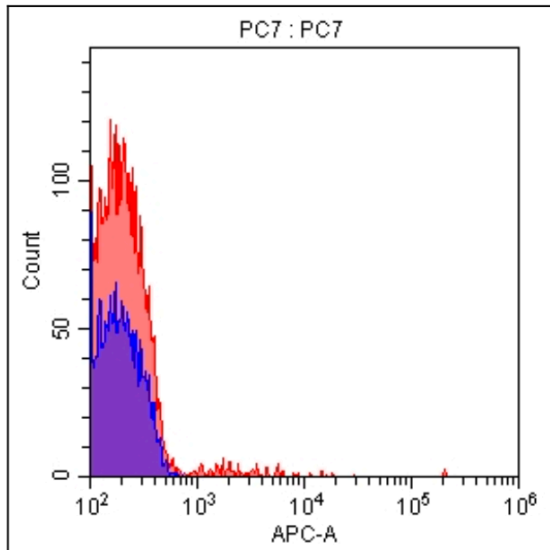




### PC7 (FL3 channel)

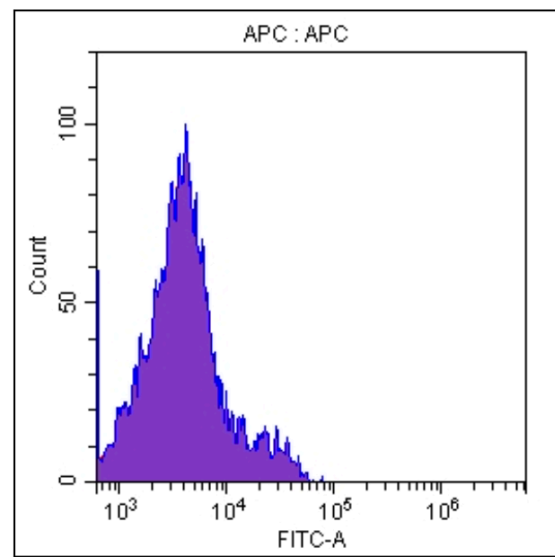
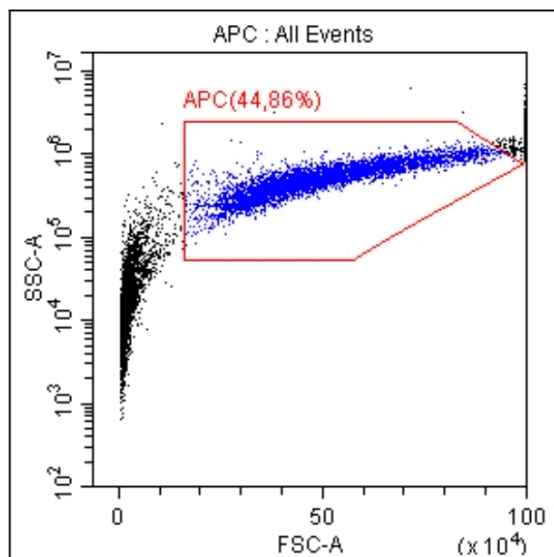
To determine the spillover of PC7 (conjugate) into the other fluorescence channels



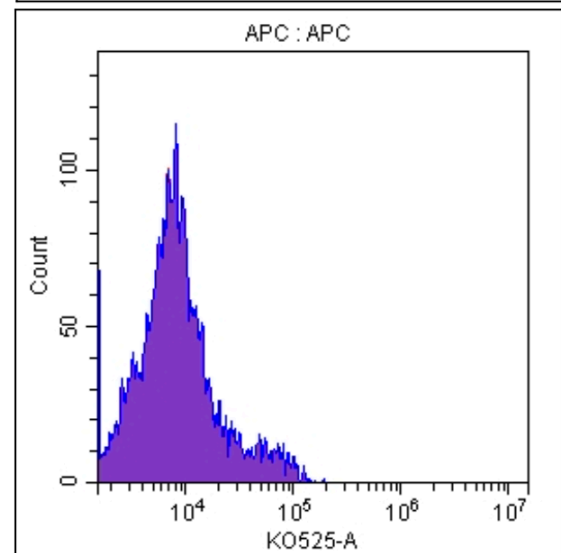
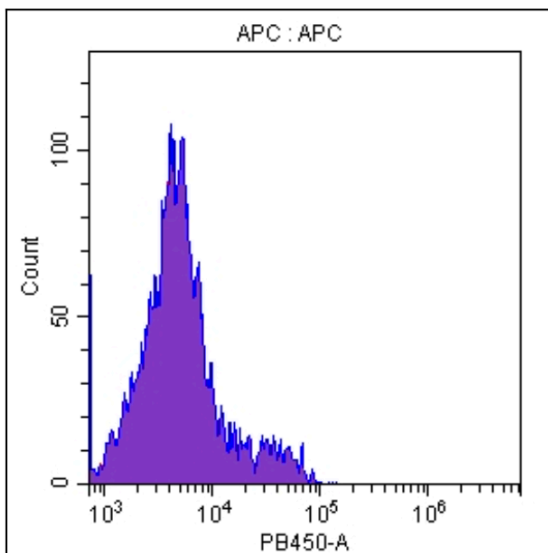
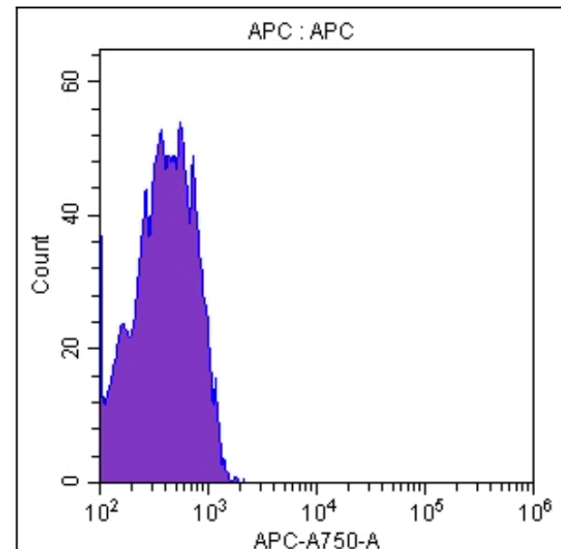
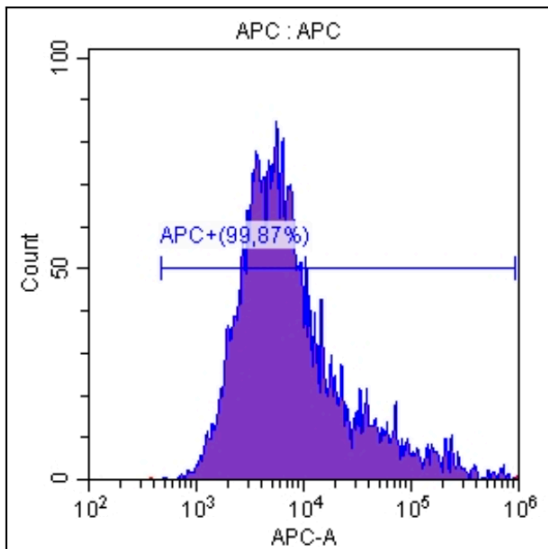
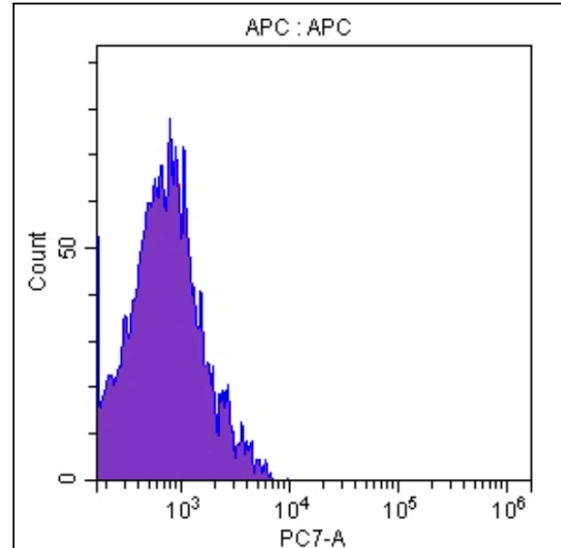
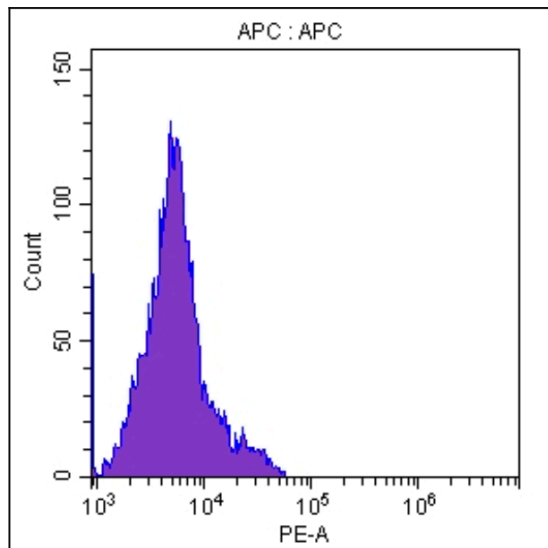


### APC (FL6 channel)

To determine the spillover of APC (conjugate) into the other fluorescence channels

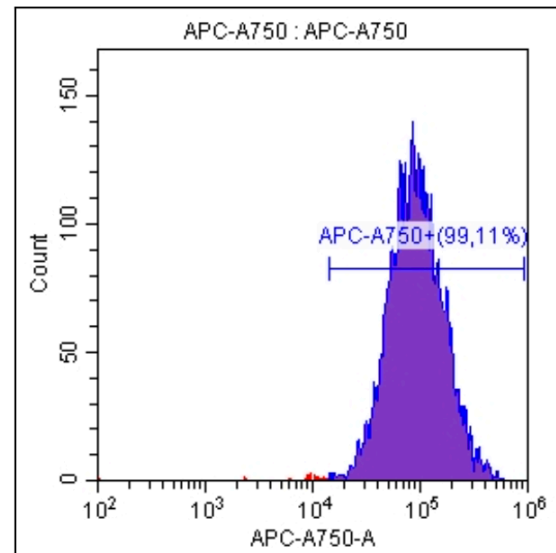
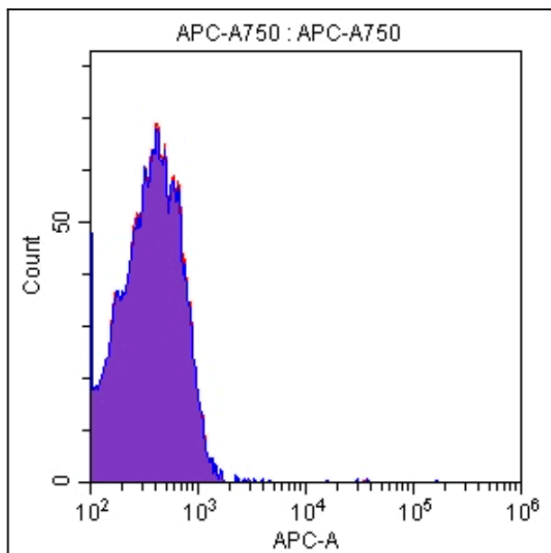
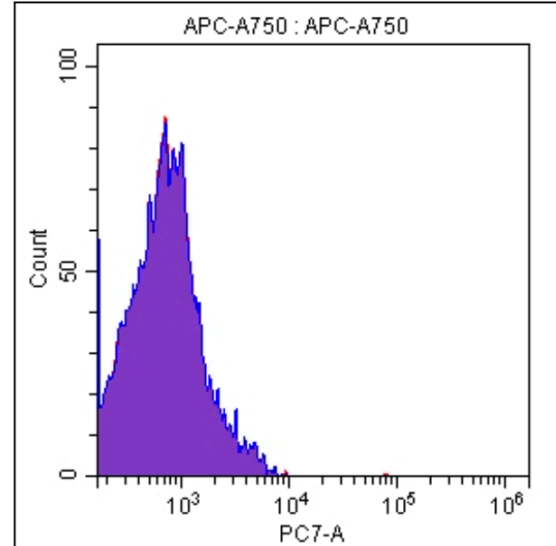
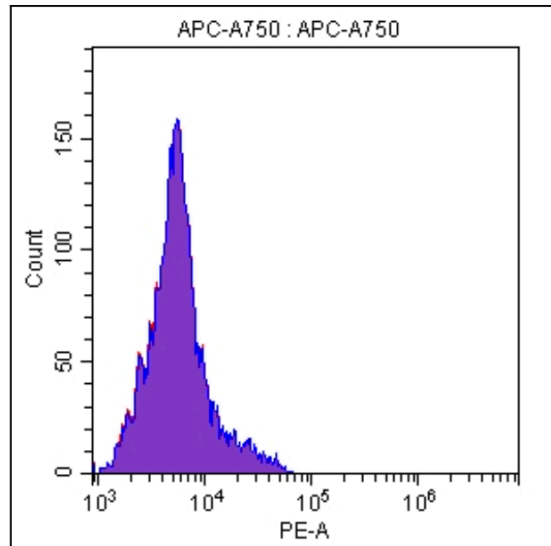
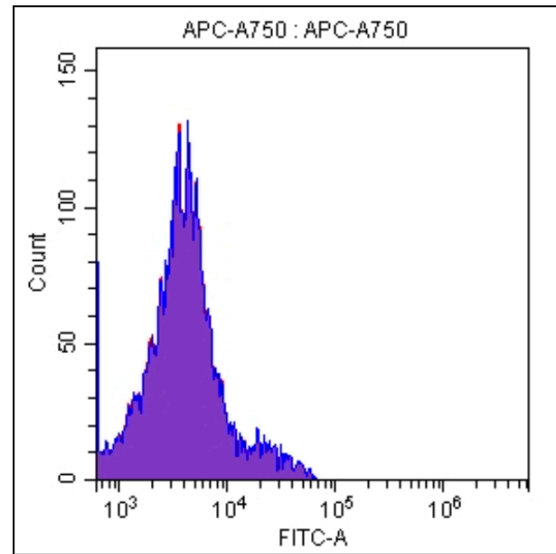
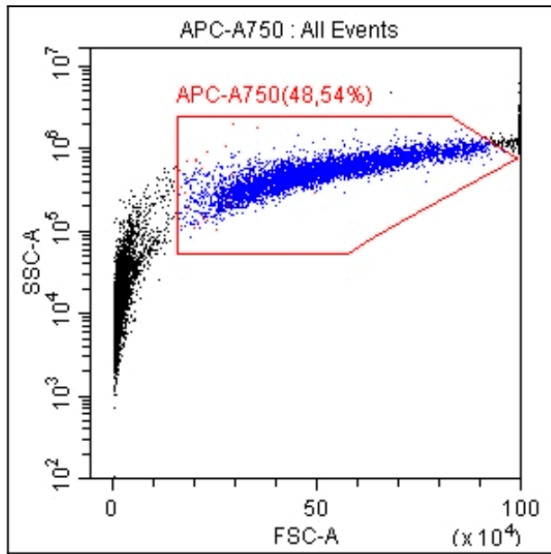


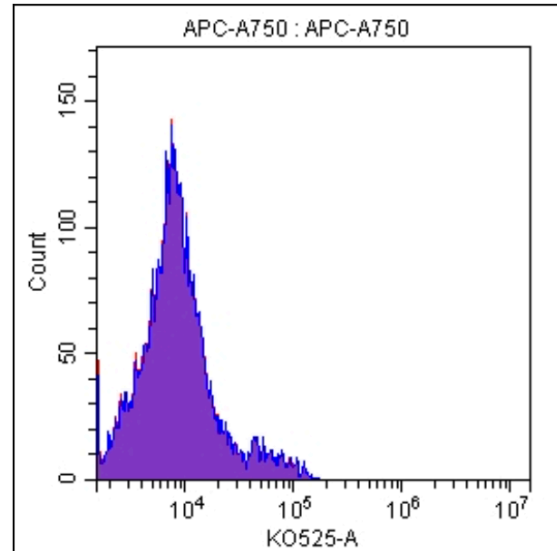
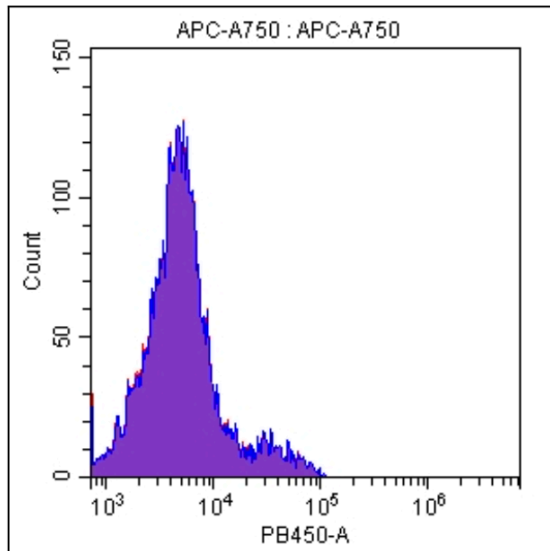




**APC-A750 (FL8 channel)**

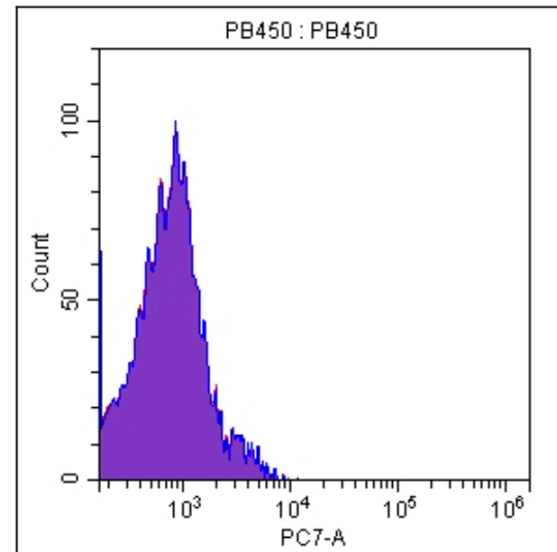
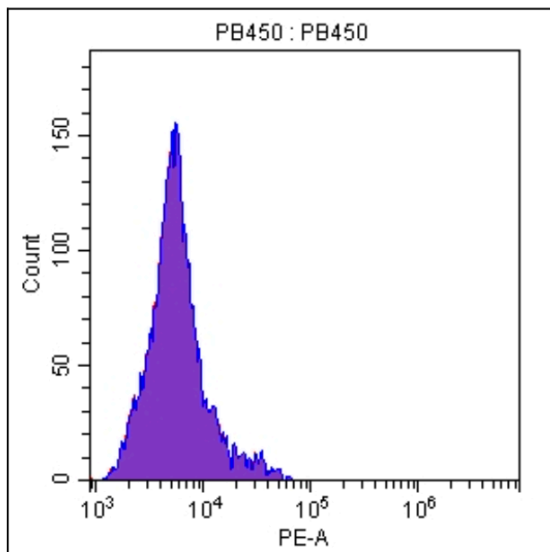
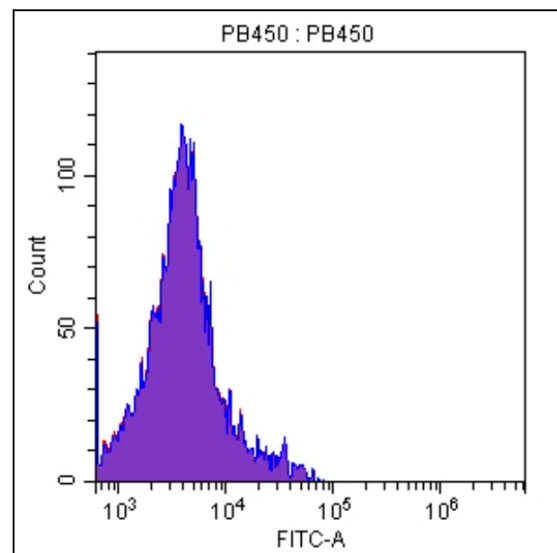
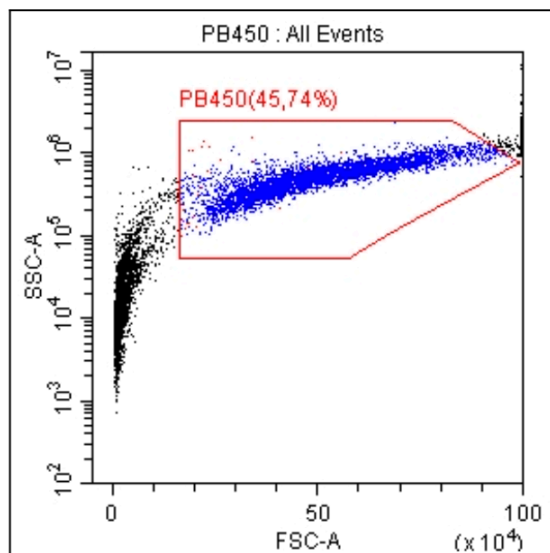
To determine the spillover of APC-A750 (conjugate) into the other fluorescence channels

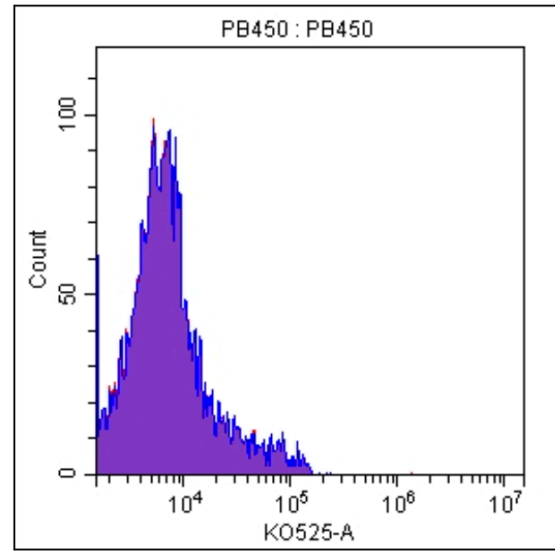
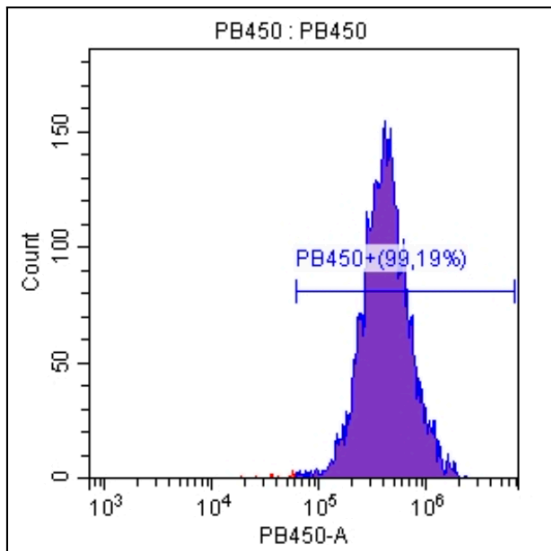
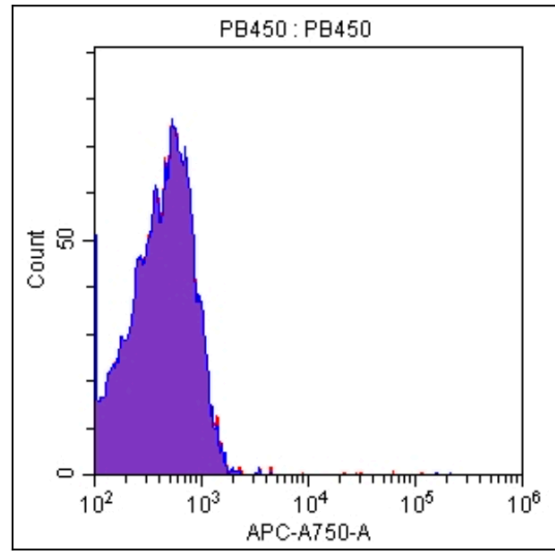
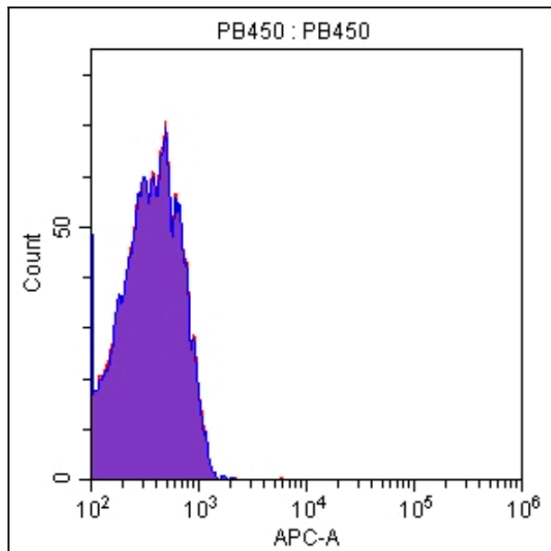




**PB450 (FL9 channel)**

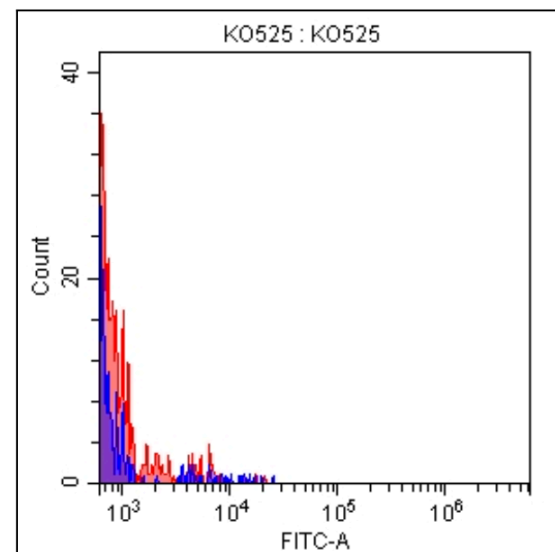
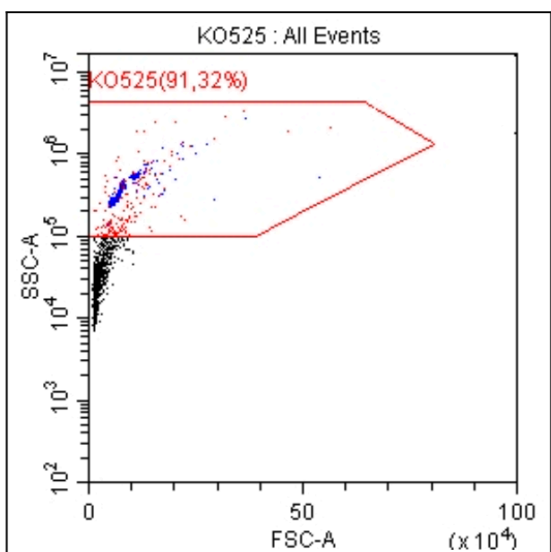
To determine the spillover of PB450 (conjugate) into the other fluorescence channels

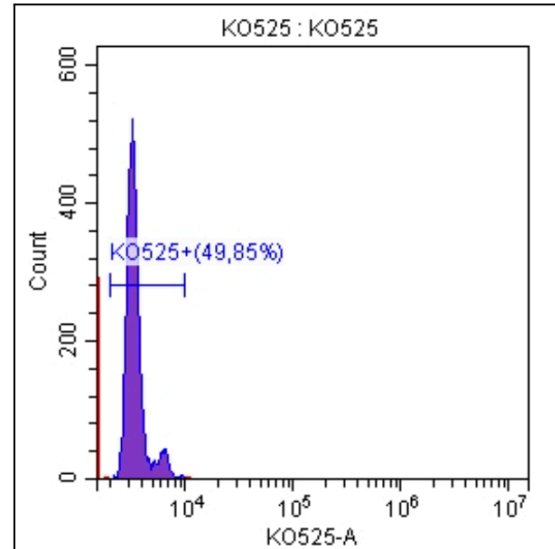
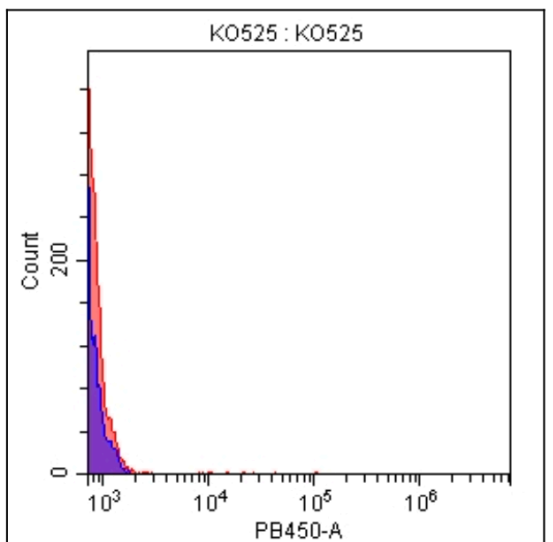
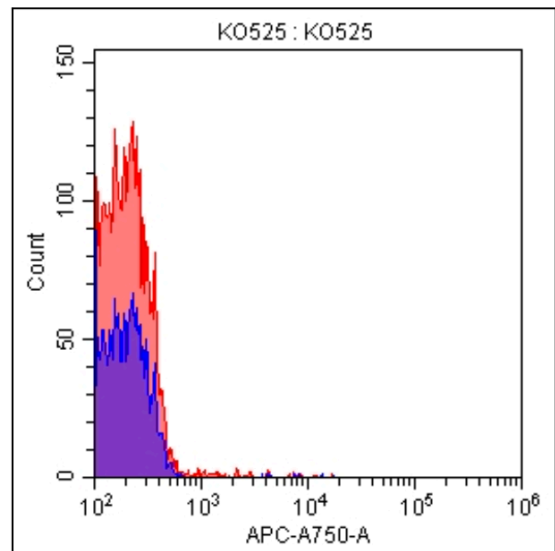
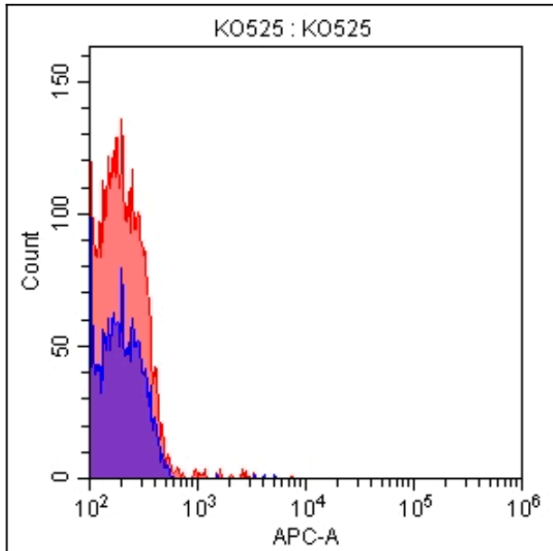
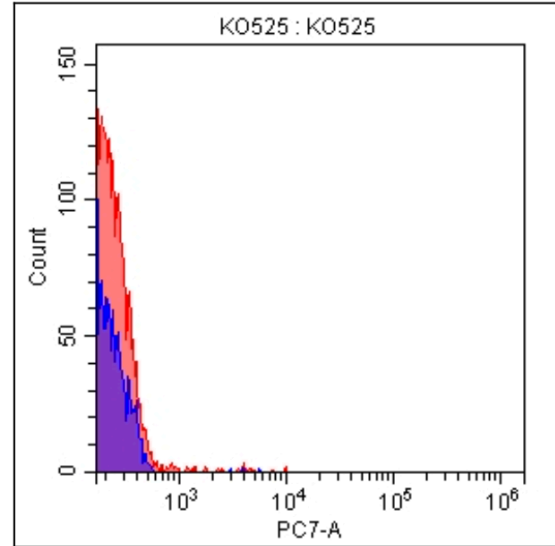
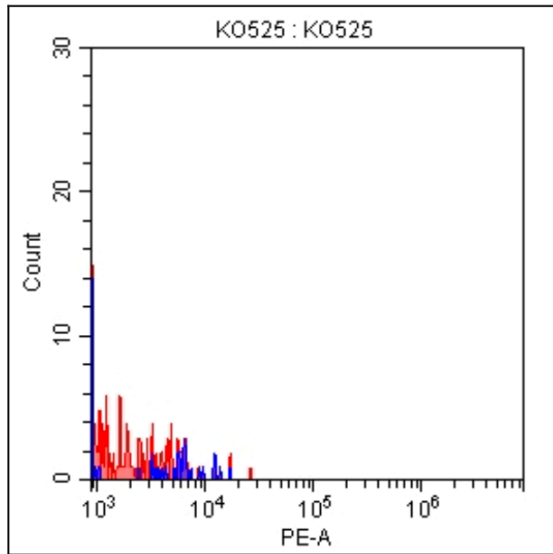




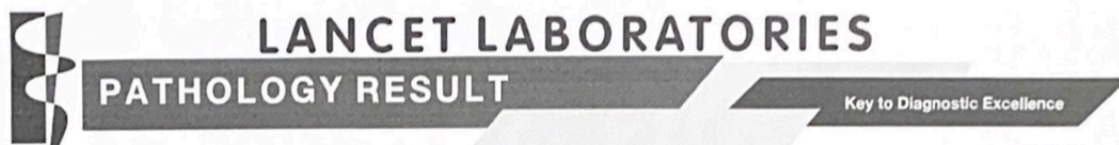
### KO(FL10 channel)

To determine the spillover of KO (conjugate) into the other fluorescence channels





## Supplementary Information B: Pre-donation Results and Post-donation Results



Page: 1/1

Patient Name :  
 Lab Ref : PRP240821  
 Age/Sex/DOB :  
 ID Num. :  
 Contact Nos :  
 Email :

Lab Name : Central  
 Dr. Ref No. : NOT AVAILABLE  
 Spec No. : 0823:HR05852R  
 Collection Date : 23/08/21 1700  
 Receive Date : 23/08/21 1703  
 Report Date : 24/08/21 1155

**Report for Doctor**  
 Sa National Blood Services  
 10 Eden Road  
 Pinetown - 3610

**Other Doctors**  
 Submit Dr : Sa National Blood Services

**Guarantor Information**  
 Name :  
 Contact Nos :  
 Email :  
 MedAid : CLIENT

**Tests:** CAL/P4 cor./MG, FBC

### Haematology

#### FULL BLOOD COUNT

ERYTHROCYTE COUNT		5.51 x10 <sup>12</sup> /L	4.5	-	6.5
HAEMOGLOBIN		16.1 g/dL	13.8	-	18.8
HAEMATOCRIT		0.46 L/L	0.40	-	0.56
MCV		83.7 fL	79	-	100
MCH		29.3 pg	27	-	35
MCHC		35.0 g/dL	32	-	36
RDW		13.3 %	11.0	-	16.0
LEUCOCYTE COUNT		7.15 x 10 <sup>9</sup> /L	4.0	-	12.0
Neutrophils	52.2%	3.73 x 10 <sup>9</sup> /L	2.0	-	7.5
Lymphocytes	37.9%	2.71 x 10 <sup>9</sup> /L	1.0	-	4.0
Monocytes	6.9%	0.49 x 10 <sup>9</sup> /L	0.2	-	1.0
Eosinophils	2.3%	0.16 x 10 <sup>9</sup> /L	0.0	-	0.5
Basophils	0.7%	0.05 x 10 <sup>9</sup> /L	0.0	-	0.3
NEUTRO/LYMPH RATIO(NLR)		1.38			
PLATELETS		254 x 10 <sup>9</sup> /L	150	-	450

**COMMENT:**  
 Normal red cell indices,  
 Absolute leucocyte values are normal,  
 Platelets are adequate.

For consultation by referring doctors only, please call:  
 Dr Prushini Moodley 031 3086519  
 Dr Nicole Holland +2711 358 0800

### Biochemistry

#### MINERAL AND BONE METABOLISM

S-CALCIUM Total	2.40 mmol/L	2.10	-	2.55
S-MAGNESIUM	0.85 mmol/L	0.66	-	1.07
S-PHOSPHATE inorganic	1.38 mmol/L	0.87	-	1.45

**COMMENT:**  
 Normal calcium and phosphate.

S-ALBUMIN	49 g/L	35	-	50
-----------	--------	----	---	----

For consultation by referring doctors only, please call:  
 Dr Kogie Reddi +2711 3580977  
 Dr Thavan Padayachi 031 3086547



## Pathology Report

24hr Contact No. 012 678 0700

Patient:

PRP260821

Age: 27 Sex: M  
H: None C: 0833898000  
dj.cloete05@gmail.com

Doctor:

Dr SANBS Spec. Doner Services  
Dr Neo Moleli  
Unitas lifestyle Suite 17  
Lyttelton 0157

Guarantor:

Mr Detlef J Cloete  
15 Murati Avenue  
9 Murati Corner  
Centurion 0157  
W: 0343121166 C: 0833898000  
Private Patient

### COPY REPORT

Req: 41074182

Ref By: Dr SANBS Spec. Doner Services  
Folio:

Specimen: 0825:AS08615R

Collected: 2021-08-25 14:32  
Received: 2021-08-25 14:47  
Printed: 2021-08-26 14:55  
Batch: PATIENT RESULTS STD

Ordered: Full Blood Count, Potassium, Calcium, Magnesium, Phosphate

Sample: E01 EDTA Haematology (1), S01 SST (1)

Test	ABN	Result	Reference Range	Unit
<b>Full Blood Count</b>				
Haemoglobin		15.1	14.3-18.3	g/dl
Red Cell Count		5.97	4.89-6.11	10 <sup>12</sup> /L
Haematocrit		46.7	43.0-55.0	%
MCV	L	78.2	79.1-98.9	fl
MCH	L	25.3	27.0-32.0	pg
MCHC		32.3	31.0-37.0	g/dl
RDW		13.9	10.0-16.3	%
White Cell Count		5.57	3.92-9.88	10 <sup>9</sup> /L
Neutrophils Abs		2.62	2.00-7.50	10 <sup>9</sup> /L
Lymphocytes Abs		2.30	1.00-4.00	10 <sup>9</sup> /L
Monocytes Abs		0.48	0.18-1.00	10 <sup>9</sup> /L
Eosinophils Abs		0.12	0.00-0.45	10 <sup>9</sup> /L
Basophils Abs		0.03	0.00-0.20	10 <sup>9</sup> /L
Immature Granulocytes Abs		0.02	0.00-0.10	10 <sup>9</sup> /L
Neut:Lymph ratio		1.00		
Platelet Count		301	150-450	10 <sup>9</sup> /L
Mean Platelet Volume		10.8	7.1-11.0	fl
FBC Comment		.		

The red cells appear hypochromic, microcytic with elliptocytes present.  
Suggest iron studies if clinically indicated.

Potassium	4.7	3.5-5.1	mmol/l
<b>Calcium</b>			
Calcium Corrected	2.44	2.15-2.50	mmol/l
Albumin	44	35-52	g/l
Magnesium	0.90	0.66-1.07	mmol/l
Phosphate	1.27	0.78-1.42	mmol/l

RUN DATE: 31/08/21  
 RUN TIME: 1419  
 RUN USER: LM4078

BBK/LAB SYSTEM  
 LAB SPECIMEN INTERNAL INQUIRY

PAGE 1

PATIENT: BB DONOR 04110797      ACCT #: Z83430220      LOC:      U #:  
 AGE/SX: 25/M      ROOM:      REG: 28/07/21  
 REG DR: Unkown,U      DOB:      BED:      DIS:  
 STATUS: BB DON      TLOC:

SPEC#: 0824:LB00322R      ORD FOR: 24/08/21-1202      STATUS: COMP      REQ #: 19149685  
 COLL: 24/08/21-1202      SUBM DR: Unkown,U  
 RECV: 24/08/21-1202      PT AGE AT COLL: 25

ENTERED: 24/08/21-1202      ENT BY: LM4078      OTHR DR:  
 COLL BY: LM4078  
 LAST RPTD: -      WKLD FN:  
 LAST ACT: 25/08/21-0705      BAR CD#: 441657.  
 ORDERED: FBC\_PRE  
 COL CATEG:  
 ORD SITE: GBT001      TRANSIT SITE:  
 RCV SITE: GBT001

(PRP240821) –  
 Pre-Collection

POINT OF TESTING  
PERFORM SITE      RCV DEPT      DATE-TIME      USR      AT SITE  
 GAL003 25/08/21-0704                          GAL003 25/08/21-0704

Test	Result	Flag	Reference
PLT	256.00 Ent:25/08-0704 autoins, Ver: 25/08-0705 MK9272 Method: Advia 2120		180-450 x10 <sup>3</sup> /ul Analyzer: GL3_ADV01
HGB	15.70 Ent:25/08-0704 autoins, Ver: 25/08-0705 MK9272 Method: Advia 2120		12.5-18.0 g/dl Analyzer: GL3_ADV01
HCT	46.90 Ent:25/08-0704 autoins, Ver: 25/08-0705 MK9272 Method: Advia 2120		38-54 % Analyzer: GL3_ADV01
RBC	5.73 Ent:25/08-0704 autoins, Ver: 25/08-0705 MK9272 Method: Advia 2120		4.2-6.1 x10 <sup>3</sup> /ul Analyzer: GL3_ADV01
WBC	6.88 Ent:25/08-0704 autoins, Ver: 25/08-0705 MK9272 Method: Advia 2120		4.0-12.6 x10 <sup>3</sup> /ul Analyzer: GL3_ADV01
MCV	81.90 Ent:25/08-0704 autoins, Ver: 25/08-0705 MK9272 Method: Advia 2120		80-99 fl Analyzer: GL3_ADV01
MCH	27.40 Ent:25/08-0704 autoins, Ver: 25/08-0705 MK9272 Method: Advia 2120		27-31 pg Analyzer: GL3_ADV01
MCHC	33.50 Ent:25/08-0704 autoins, Ver: 25/08-0705 MK9272 Method: Advia 2120		32-37 g/dl Analyzer: GL3_ADV01
COMMENTS	NP Ent:24/08-1202 AutoDft, Ver: 24/08-1202 AutoDft Method:		

\*\*\* End of Report \*\*\*



RUN DATE: 31/08/21  
 RUN TIME: 1419  
 RUN USER: LM4078

BBK/LAB SYSTEM  
 LAB SPECIMEN INTERNAL INQUIRY

PAGE 1

PATIENT: BB DONOR 04110797      ACCT #: Z83430220      LOC:      U #:  
 AGE/SX: 25/M      ROOM:      REG: 28/07/21  
 REG DR: Unkown,U      DOB:      BED:      DIS:  
 STATUS: BB DON      TLOC:

SPEC#: 0824:LB00324R      ORD FOR: 24/08/21-1203      STATUS: COMP      REQ #: 19149691  
 COLL: 24/08/21-1203      SUBM DR: Unkown,U  
 RECV: 24/08/21-1203      PT AGE AT COLL: 25

ENTERED: 24/08/21-1203      ENT BY: LM4078      OTHR DR:  
 COLL BY:      RCV BY: LM4078  
 LAST RPTD: -      WKLD FN:  
 LAST ACT: 25/08/21-0705      BAR CD#: 441658.  
 ORDERED: **FBC Post**  
 COL CATEG:  
 ORD SITE: GBT001      TRANSIT SITE:  
 RCV SITE: GBT001

(PRP240821) –  
 Post-Collection

POINT OF TESTING  
PERFORM SITE      RCV DEPT      DATE-TIME      USR      AT SITE  
 GAL003 25/08/21-0705                               GAL003 25/08/21-0705

Test	Result	Flag	Reference
PLT	195.00 Ent:25/08-0705 autoins, Ver: 25/08-0705 MK9272 Method: Advia 2120		180-450 x10 <sup>3</sup> /ul Analyzer: GL3_ADV01
HGB	16.00 Ent:25/08-0705 autoins, Ver: 25/08-0705 MK9272 Method: Advia 2120		12.5-18.0 g/dl Analyzer: GL3_ADV01
HCT	45.30 Ent:25/08-0705 autoins, Ver: 25/08-0705 MK9272 Method: Advia 2120		38-54 % Analyzer: GL3_ADV01
RBC	5.52 Ent:25/08-0705 autoins, Ver: 25/08-0705 MK9272 Method: Advia 2120		4.2-6.1 x10 <sup>3</sup> /ul Analyzer: GL3_ADV01
WBC	7.46 Ent:25/08-0705 autoins, Ver: 25/08-0705 MK9272 Method: Advia 2120		4.0-12.6 x10 <sup>3</sup> /ul Analyzer: GL3_ADV01
MCV	82.20 Ent:25/08-0705 autoins, Ver: 25/08-0705 MK9272 Method: Advia 2120		80-99 fl Analyzer: GL3_ADV01
MCH	28.90 Ent:25/08-0705 autoins, Ver: 25/08-0705 MK9272 Method: Advia 2120		27-31 pg Analyzer: GL3_ADV01
MCHC	35.20 Ent:25/08-0705 autoins, Ver: 25/08-0705 MK9272 Method: Advia 2120		32-37 g/dl Analyzer: GL3_ADV01
COMMENTS	NP Ent:24/08-1203 AutoDft, Ver: 24/08-1203 AutoDft Method:		

\*\*\* End of Report \*\*\*

RUN DATE: 31/08/21  
 RUN TIME: 1419  
 RUN USER: LM4078

BBK/LAB SYSTEM  
 LAB SPECIMEN INTERNAL INQUIRY

PAGE 1

PATIENT: RPPP #34861867 ACCT #: Z83828749 LOC: U #:  
 REG DR: Unkown,U AGE/SX: 25/M ROOM: REG: 24/08/21  
 DOB: BED: DIS:  
 STATUS: BB UNIT TLOC:

SPEC#: 0824:LB00387R ORD FOR: 24/08/21-1324 STATUS: COMP REQ #: 19150296  
 COLL: 24/08/21-1324 SUBM DR: Unkown,U  
 RECV: 24/08/21-1324 PT AGE AT COLL: 25

ENTERED: 24/08/21-1325 ENT BY: LM4078 OTHR DR:  
 COLL BY: RCV BY: LM4078  
 LAST RPTD: - WKLD FN:  
 LAST ACT: 25/08/21-1540 BAR CD#: 441765.  
 ORDERED: RPROD  
 COL CATEG:  
 ORD SITE: GBT001 TRANSIT SITE:  
 RCV SITE: GBT001

(PRP240821) -  
 Post-Collection  
 Analysis

POINT OF TESTING  
 PERFORM SITE RCV DEPT DATE-TIME USR AT SITE  
 GAL003 25/08/21-0930 GAL003 25/08/21-0930

Test	Result	Flag	Reference
WCC PRODUCT	0.00 Ent:25/08-1102 BT7888, Ver: 25/08-1102 BT7888 Method: Advia 2120		0-5 x10 <sup>6</sup>
PLT COUNT PROD	1386.00 Ent:25/08-0930 autoins, Ver: 25/08-0954 BT7888 Method: Advia 2120		1000-3000 x10 <sup>3</sup> /ul Analyzer: GL3_ADV01
PRODVOL	200 Ent:25/08-1102 BT7888, Ver: 25/08-1102 BT7888 Method: Manual		200-800 ML
STERILITY	NP Ent:24/08-1325 AutoDft, Ver: 24/08-1325 AutoDft Method:		
ANO2	NP Ent:24/08-1325 AutoDft, Ver: 24/08-1325 AutoDft Method:		Negative CFU
ANO2_BATCH	NP Ent:24/08-1325 AutoDft, Ver: 24/08-1325 AutoDft Method:		CFU
O2	NP Ent:24/08-1325 AutoDft, Ver: 24/08-1325 AutoDft Method:		Negative CFU
O2_Batch	NP Ent:24/08-1325 AutoDft, Ver: 24/08-1325 AutoDft Method:		CFU
PH	6.8 Ent:25/08-1540 BT7888, Ver: 25/08-1540 BT7888 Method: pH Meter		6.4-10.4 pH
COMMENTS	NP Ent:24/08-1325 AutoDft, Ver: 24/08-1325 AutoDft Method:		

Continued on next page ...

RUN DATE: 31/08/21  
 RUN TIME: 1357  
 RUN USER: LM4078

BBK/LAB SYSTEM  
 LAB SPECIMEN INTERNAL INQUIRY

PAGE 1

PATIENT: BB DONOR 02613663 ACCT #: Z30347381 LOC: U #:  
 REG DR: Unkown,U AGE/SX: 27/M ROOM: REG: 14/05/10  
 DOB: BED: DIS:  
 STATUS: BB DON TLOC:

SPEC#: 0826:LB00256R ORD FOR: 26/08/21-1455 STATUS: COMP REQ #: 19157545  
 COLL: 26/08/21-1455 SUBM DR: Unkown,U  
 RECV: 26/08/21-1455 PT AGE AT COLL: 27

ENTERED: 26/08/21-1455 ENT BY: LM4078 OTHR DR:  
 COLL BY: RCV BY: LM4078  
 LAST RPTD: - WKLD FN:  
 LAST ACT: 27/08/21-0740 BAR CD#: 442767.

(PRP260821) -  
 Pre-Collection

ORDERED: FBC\_PRE  
 COL CATEG:  
 ORD SITE: GBT001 TRANSIT SITE:  
 RCV SITE: GBT001

POINT OF TESTING  
 PERFORM SITE RCV DEPT DATE-TIME USR AT SITE  
 GAL003 27/08/21-0736 GAL003 27/08/21-0736

Test	Result	Flag	Reference
PLT	254.00		180-450 x10 <sup>3</sup> /ul
	Ent:27/08-0736 autoins, Ver: 27/08-0740 MK9272		
	Method: Advia 2120		Analyzer: GL3_ADV01
HGB	14.10		12.5-18.0 g/dl
	Ent:27/08-0736 autoins, Ver: 27/08-0740 MK9272		
	Method: Advia 2120		Analyzer: GL3_ADV01
HCT	44.70		38-54 %
	Ent:27/08-0736 autoins, Ver: 27/08-0740 MK9272		
	Method: Advia 2120		Analyzer: GL3_ADV01
RBC	5.49		4.2-6.1 x10 <sup>3</sup> /ul
	Ent:27/08-0736 autoins, Ver: 27/08-0740 MK9272		
	Method: Advia 2120		Analyzer: GL3_ADV01
WBC	5.50		4.0-12.6 x10 <sup>3</sup> /ul
	Ent:27/08-0736 autoins, Ver: 27/08-0740 MK9272		
	Method: Advia 2120		Analyzer: GL3_ADV01
MCV	81.40		80-99 fl
	Ent:27/08-0736 autoins, Ver: 27/08-0740 MK9272		
	Method: Advia 2120		Analyzer: GL3_ADV01
MCH	25.70	L	27-31 pg
	Ent:27/08-0740 MK9272, Ver: 27/08-0740 MK9272		
	Method: Advia 2120		
MCHC	31.50	L	32-37 g/dl
	Ent:27/08-0740 MK9272, Ver: 27/08-0740 MK9272		
	Method: Advia 2120		
COMMENTS	NP		
	Ent:26/08-1455 AutoDft, Ver: 26/08-1455 AutoDft		
	Method:		

\*\*\* End of Report \*\*\*

RUN DATE: 31/08/21  
 RUN TIME: 1357  
 RUN USER: LM4078

BBK/LAB SYSTEM  
 LAB SPECIMEN INTERNAL INQUIRY

PATIENT: BB DONOR 02613663	ACCT #: Z30347381	LOC:	U #:
REG DR: Unkown,U	AGE/SX: 27/M	ROOM:	REG: 14/05/10
	DOB:	BED:	DIS:
	STATUS: BB DON	TLOC:	

SPEC#: 0826:LB00257R	ORD FOR: 26/08/21-1456	STATUS: COMP	REQ #: 19157554
	COLL: 26/08/21-1456	SUBM DR: Unkown,U	
	RCV: 26/08/21-1456	PT AGE AT COLL: 27	

ENTERED: 26/08/21-1456	ENT BY: LM4078	OTHR DR:
COLL BY:	RCV BY: LM4078	
LAST RPTD: -	WKLD FN:	
LAST ACT: 27/08/21-0740	BAR CD#: 442775.	
ORDERED: FBC Post		
COL CATEG:		
ORD SITE: GBT001	TRANSIT SITE:	
RCV SITE: GBT001		

(PRP260821) –  
 Post-Collection

POINT OF TESTING	
PERFORM SITE	RCV DEPT DATE-TIME USR AT SITE
GAL003 27/08/21-0736	GAL003 27/08/21-0736

Test	Result	Flag	Reference
PLT	227.00 Ent:27/08-0736 autoins, Ver: 27/08-0740 MK9272 Method: Advia 2120		180-450 x10 <sup>3</sup> /ul Analyzer: GL3_ADV01
HGB	13.90 Ent:27/08-0736 autoins, Ver: 27/08-0740 MK9272 Method: Advia 2120		12.5-18.0 g/dl Analyzer: GL3_ADV01
HCT	46.30 Ent:27/08-0736 autoins, Ver: 27/08-0740 MK9272 Method: Advia 2120		38-54 % Analyzer: GL3_ADV01
RBC	5.67 Ent:27/08-0736 autoins, Ver: 27/08-0740 MK9272 Method: Advia 2120		4.2-6.1 x10 <sup>3</sup> /ul Analyzer: GL3_ADV01
WBC	7.41 Ent:27/08-0736 autoins, Ver: 27/08-0740 MK9272 Method: Advia 2120		4.0-12.6 x10 <sup>3</sup> /ul Analyzer: GL3_ADV01
MCV	81.60 Ent:27/08-0736 autoins, Ver: 27/08-0740 MK9272 Method: Advia 2120		80-99 fl Analyzer: GL3_ADV01
MCH	24.50 Ent:27/08-0740 MK9272, Ver: 27/08-0740 MK9272 Method: Advia 2120	L	27-31 pg
MCHC	30.00 Ent:27/08-0740 MK9272, Ver: 27/08-0740 MK9272 Method: Advia 2120	L	32-37 g/dl
COMMENTS	NP Ent:26/08-1456 AutoDft, Ver: 26/08-1456 AutoDft Method:		

\*\*\* End of Report \*\*\*

RUN DATE: 31/08/21  
 RUN TIME: 1358  
 RUN USER: LM4078

BBK/LAB SYSTEM  
 LAB SPECIMEN INTERNAL INQUIRY

PAGE 1

PATIENT: RPPP #34861744 ACCT #: Z83865057 LOC: U #:  
 AGE/SX: 27/M ROOM: REG: 26/08/21  
 REG DR: Unkown,U DOB: BED: DIS:  
 STATUS: BB UNIT TLOC:

SPEC#: 0826:LB00330R ORD FOR: 26/08/21-1730 STATUS: COMP REQ #: 19158536  
 COLL: 26/08/21-1730 SUBM DR: Unkown,U  
 RECV: 26/08/21-1730 PT AGE AT COLL: 27

ENTERED: 26/08/21-1730 ENT BY: LM4078 OTHR DR:  
 COLL BY: RCV BY: LM4078  
 LAST RPTD: - WKLD FN:  
 LAST ACT: 27/08/21-1306 BAR CD#: 442848.  
 ORDERED: RPROD  
 COL CATEG:  
 ORD SITE: GBT001 TRANSIT SITE:  
 RCV SITE: GBT001

(PRP260821) –  
 Post-Collection  
 Analysis

POINT OF TESTING  
 PERFORM SITE RCV DEPT DATE-TIME USR AT SITE  
 GAL003 27/08/21-0949 GAL003 27/08/21-0949

Test	Result	Flag	Reference
WCC PRODUCT	0.00 Ent:27/08-1306 BT7888, Ver: 27/08-1306 BT7888 Method: Advia 2120		0-5 x10 <sup>6</sup>
PLT COUNT PROD	1480.00 Ent:27/08-0949 autoins, Ver: 27/08-1022 BT7888 Method: Advia 2120 Analyzer: GL3_ADV01		1000-3000 x10 <sup>3</sup> /ul
PRODVOL	250 Ent:27/08-1306 BT7888, Ver: 27/08-1306 BT7888 Method: Manual		200-800 ML
STERILITY	NP Ent:26/08-1730 AutoDft, Ver: 26/08-1730 AutoDft Method:		
ANO2	NP Ent:26/08-1730 AutoDft, Ver: 26/08-1730 AutoDft Method:		Negative CFU
ANO2_BATCH	NP Ent:26/08-1730 AutoDft, Ver: 26/08-1730 AutoDft Method:		CFU
O2	NP Ent:26/08-1730 AutoDft, Ver: 26/08-1730 AutoDft Method:		Negative CFU
O2_Batch	NP Ent:26/08-1730 AutoDft, Ver: 26/08-1730 AutoDft Method:		CFU
PH	6.8 Ent:27/08-1306 BT7888, Ver: 27/08-1306 BT7888 Method: pH Meter		6.4-10.4 pH
COMMENTS	NP Ent:26/08-1730 AutoDft, Ver: 26/08-1730 AutoDft Method:		

Continued on next page ...

RUN DATE: 08/07/21  
 RUN TIME: 1615  
 RUN USER: CS4477

BBK/LAB SYSTEM  
 LAB SPECIMEN INTERNAL INQUIRY

PATIENT: BB DONOR 381287	ACCT #: Z23414586	LOC:	U #:
REG DR: Unkown,U	AGE/SX: 58/M	ROOM:	REG: 01/10/08
	DOB:	BED:	DIS:
	STATUS: BB DON	TLOC:	

SPEC#: 0707:LB00111R	ORD FOR: 07/07/21-1013	STATUS: COMP	REQ #: 19017779
	COLL: 07/07/21-1013	SUBM DR: Unkown,U	
	RCV: 07/07/21-1013	PT AGE AT COLL: 58	

ENTERED: 07/07/21-1014	ENT BY: LM4078	OTHR DR:
COLL BY:	RCV BY: LM4078	
LAST RPTD: -	WKLD FN:	
LAST ACT: 07/07/21-1522	BAR CD#: 423100.	
ORDERED: FBC_PRE		
COL CATEG:		
ORD SITE: GBT001		
RCV SITE: GBT001		

(PRP070721) –  
 Pre-Collection

TRANSIT SITE:

POINT OF TESTING

PERFORM SITE	RCV DEPT	DATE-TIME	USR	AT SITE
GAL003 07/07/21-1420				GAL003 07/07/21-1420

Test	Result	Flag	Reference
PLT	291.00 Ent: 07/07-1420 autoins, Ver: 07/07-1522 KM8060 Method: Advia 2120		180-450 x10 <sup>3</sup> /ul Analyzer: GL3_ADV01
HGB	12.60 Ent: 07/07-1420 autoins, Ver: 07/07-1522 KM8060 Method: Advia 2120		12.5-18.0 g/dl Analyzer: GL3_ADV01
HCT	39.20 Ent: 07/07-1420 autoins, Ver: 07/07-1522 KM8060 Method: Advia 2120		38-54 % Analyzer: GL3_ADV01
RBC	4.60 Ent: 07/07-1420 autoins, Ver: 07/07-1522 KM8060 Method: Advia 2120		4.2-6.1 x10 <sup>3</sup> /ul Analyzer: GL3_ADV01
WBC	4.63 Ent: 07/07-1420 autoins, Ver: 07/07-1522 KM8060 Method: Advia 2120		4.0-12.6 x10 <sup>3</sup> /ul Analyzer: GL3_ADV01
MCV	85.20 Ent: 07/07-1420 autoins, Ver: 07/07-1522 KM8060 Method: Advia 2120		80-99 fl Analyzer: GL3_ADV01
MCH	27.30 Ent: 07/07-1420 autoins, Ver: 07/07-1522 KM8060 Method: Advia 2120		27-31 pg Analyzer: GL3_ADV01
MCHC	32.00 Ent: 07/07-1420 autoins, Ver: 07/07-1522 KM8060 Method: Advia 2120		32-37 g/dl Analyzer: GL3_ADV01
COMMENTS	NP Ent: 07/07-1014 AutoDft, Ver: 07/07-1014 AutoDft Method:		

RUN DATE: 08/07/21  
RUN TIME: 1615  
RUN USER: CS4477

BBK/LAB SYSTEM  
LAB SPECIMEN INTERNAL INQUIRY

PAGE 1

PATIENT: BB DONOR 381287  
REG DR: Unkown,U

ACCT #: Z23414586  
AGE/SX: 58/M  
DOB:  
STATUS: BB DON

LOC:  
ROOM:  
BED:  
TLOC:

U #:  
REG: 01/10/08  
DIS:

SPEC#: 0707:LB00112R

ORD FOR: 07/07/21-1014 STATUS: COMP  
COLL: 07/07/21-1014 SUBM DR: Unkown,U  
RECV: 07/07/21-1014 PT AGE AT COLL: 58

REQ #: 19017781

ENTERED: 07/07/21-1015  
COLL BY:  
LAST RPTD: -  
LAST ACT: 07/07/21-1521  
ORDERED: FBC Post  
COL CATEG:  
ORD SITE: GBT001  
RCV SITE: GBT001

ENT BY: LM4078  
RCV BY: LM4078  
WKL D FN:  
BAR CD#: 423101.

OTHR DR:

(PRP070721) -  
Post-Collection

TRANSIT SITE:

PERFORM SITE  
GAL003 07/07/21-1420

POINT OF TESTING  
RCV DEPT DATE-TIME USR

AT SITE  
GAL003 07/07/21-1420

Test	Result	Flag	Reference
PLT	264.00 Ent: 07/07-1420 autoins, Ver: 07/07-1521 KM8060 Method: Advia 2120 Analyzer: GL3_ADV01		180-450 x10 <sup>3</sup> ul
HGB	13.00 Ent: 07/07-1420 autoins, Ver: 07/07-1521 KM8060 Method: Advia 2120 Analyzer: GL3_ADV01		12.5-18.0 g/dl
HCT	41.00 Ent: 07/07-1420 autoins, Ver: 07/07-1521 KM8060 Method: Advia 2120 Analyzer: GL3_ADV01		38-54 %
RBC	4.80 Ent: 07/07-1420 autoins, Ver: 07/07-1521 KM8060 Method: Advia 2120 Analyzer: GL3_ADV01		4.2-6.1 x10 <sup>3</sup> /ul
WBC	5.18 Ent: 07/07-1420 autoins, Ver: 07/07-1521 KM8060 Method: Advia 2120 Analyzer: GL3_ADV01		4.0-12.6 x10 <sup>3</sup> /ul
MCV	85.40 Ent: 07/07-1420 autoins, Ver: 07/07-1521 KM8060 Method: Advia 2120 Analyzer: GL3_ADV01		80-99 fl
MCH	27.10 Ent: 07/07-1420 autoins, Ver: 07/07-1521 KM8060 Method: Advia 2120 Analyzer: GL3_ADV01		27-31 pg
MCHC	31.70 Ent: 07/07-1521 KM8060, Ver: 07/07-1521 KM8060 Method: Advia 2120	L	32-37 g/dl
COMMENTS	NP Ent: 07/07-1015 AutoDft, Ver: 07/07-1015 AutoDft Method:		

\*\*\* End of Report \*\*\*

## Supplementary Information C: Osteogenic Experimental Design

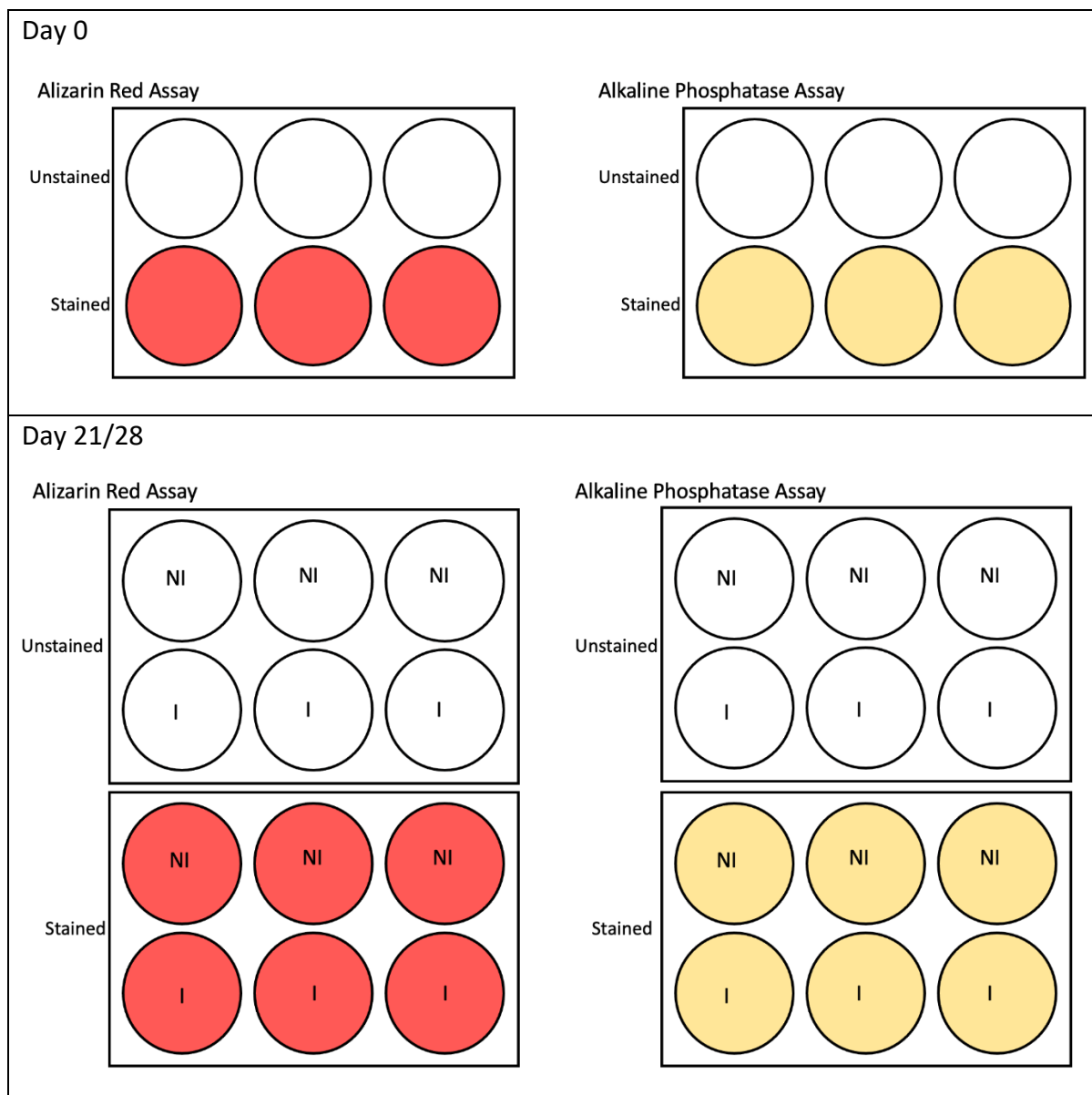


**Figure C1. Experimental culture plate setup for experimental days.**

ASCs were seeded into 6 well plates at 5000 cells/cm<sup>2</sup>. Day 0 represents non-induced samples on the day of osteogenic induction (rest of induced wells). An unstained control was included in each assay to determine the amount of background staining. For day 21/28 samples, a non-induced control as well as unstained controls were included for each of the assays. The same experimental procedure was followed to process both the unstained and stained wells, with the only exception being the exclusion of addition of Alizarin Red S or Alkaline phosphatase assay buffer in the respective unstained wells. PBS instead of the staining/buffer solution was added to the unstained controls wells.



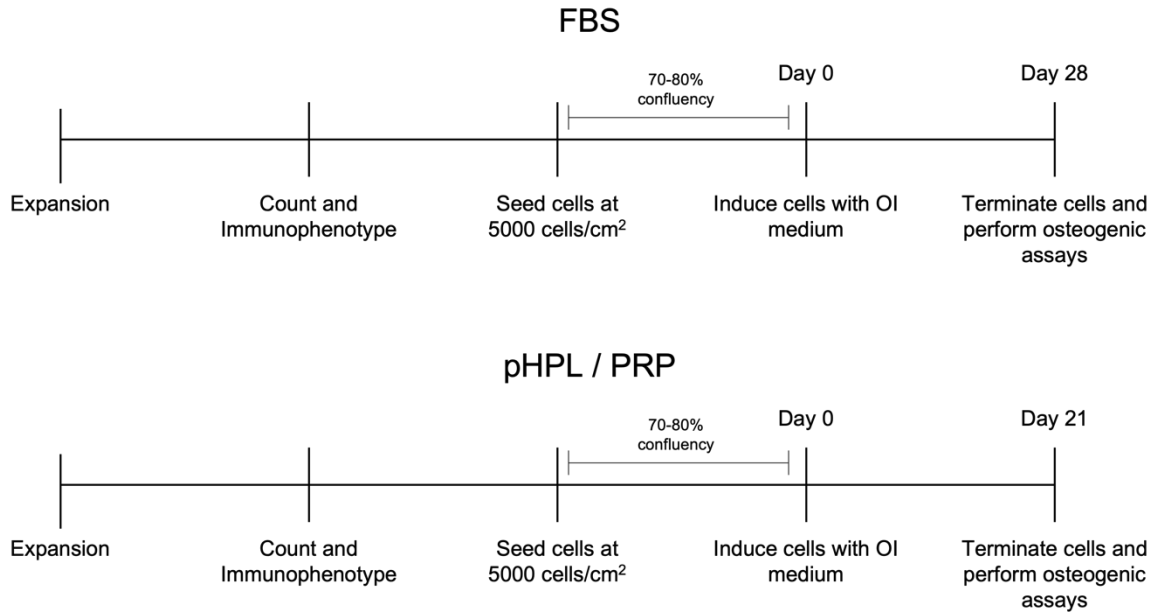


**Figure C2. Timeline of osteogenic induction.**

A basic illustration of the steps followed during osteogenic differentiation of the primary ASC cultures. Cells supplemented with FBS were investigated over a 28-day period while the pHPL and PRP supplemented cells were investigated over a 21-day period. OI; Osteogenic induction medium

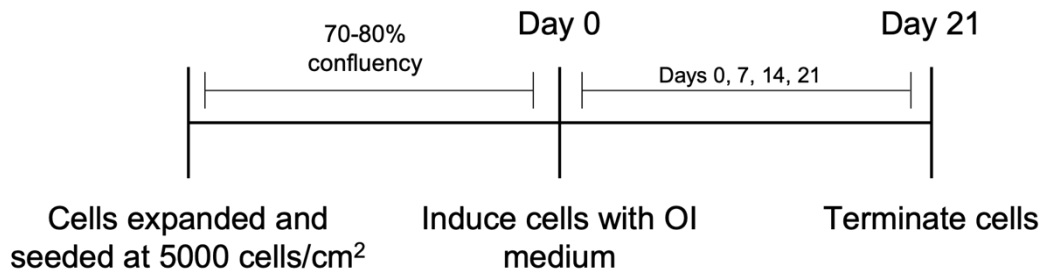


**Figure C3. RNA isolation strategy.**

Cells were expanded and seeded at 5000 cells/cm<sup>2</sup>. Once cells reached between 70 – 80% confluency they were induced with an osteogenic induction medium. Cells were terminated on days 0, 7, 14 and 21 for RNA extraction.

## Supplementary Information D: ARS Standard Curve

An ARS standard curve was used to convert OD readings into ARS concentrations (mM). The serial dilution ranged from 4 mM to 0.0625 mM ARS. The OD readings were read at 405 nm and 650nm (Reference wavelength used as an internal reference where no signal should be picked up). The average blank reading (reading of distilled water) was subtracted from all the other readings. The adjusted OD results were converted into a concentration using the formula  $y = 1.05119977x - 0.03407551$ ; where  $y$  is equal to the OD reading and  $x$  is the concentration of ARS Stain in mM. The linear correlation ( $R^2$ ) of the standard curve was 0.9997746 (Figure D1).

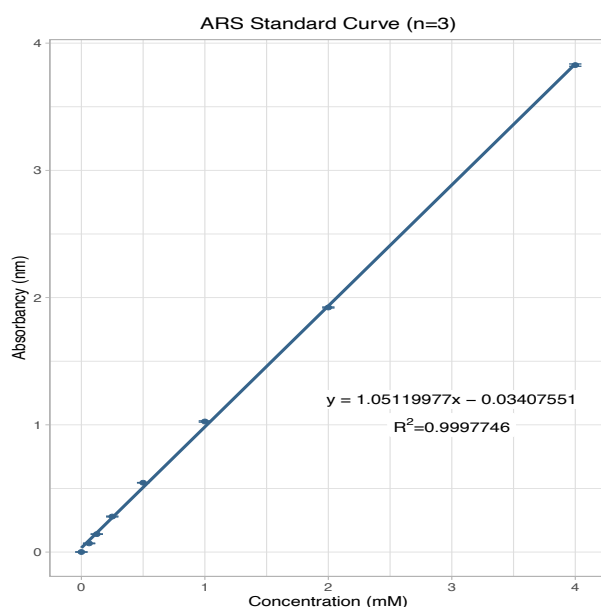


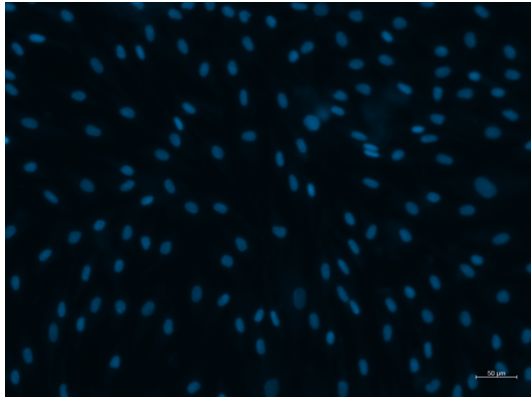
**Figure D1. ARS Standard Curve**

Standard curve displaying the equation  $y = 1.05119977x - 0.03407551$  used to calculate the concentration of ARS

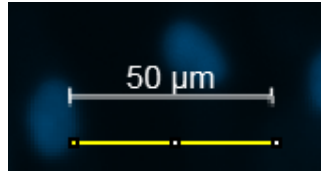
## Supplementary Information E: Protocol for obtaining cell counts with a well using ImageJ

Images captured on the fluorescent microscope were saved as a .tiff files and were opened and processed in ImageJ (Version 2.1.0/1.53c; Laboratory for Optical and Computational Instrumentation, University of Wisconsin, Wisconsin, USA). The brightness and contrast of the images was adjusted, but the images were not manipulated. The image was converted into an 8-bit image and the threshold was adjusted to Black and White ("B&W"). The image was converted into a mask using the binary option in ImageJ (Menu: Process > Binary > Convert to Mask). Watershed was then applied to the image (Menu: Process > Binary > Watershed) to separate out connected particles. The particles (individual nuclei) were then analysed using the count function under the Analyse menu (Menu: Analyse > Analyse particles). Everything less than 200-pixel units was excluded as this was seen as debris and not cells. The number of cells were displayed. Cells close to each other were sometimes identified (called) as a single cell. Therefore, images were also manually assessed to ensure that the correct calls were made by the software and the necessary adjustments were made when needed. The scale was calibrated by measuring the scale bar to determine the number of pixels (indicated as the yellow line) and setting the known distance given on the scale bar (e.g., 50 $\mu\text{m}$ ) and entering the correct units ( $\mu\text{m}$ ). The pixel aspect ratio is by default 1, meaning that the height and width of individual pixels are equal. The area of the field of vision is calculated using the formula  $A = \text{length} \times \text{breadth}$ . The length and breadth of the field of vision is given by the software once the distance in pixels, known distance and the correct units are entered e.g., 642.59 x 480.56  $\mu\text{m}$  (Figure D1).

A.



B.



**Set Scale**

Distance in pixels:

Known distance:

Pixel aspect ratio:

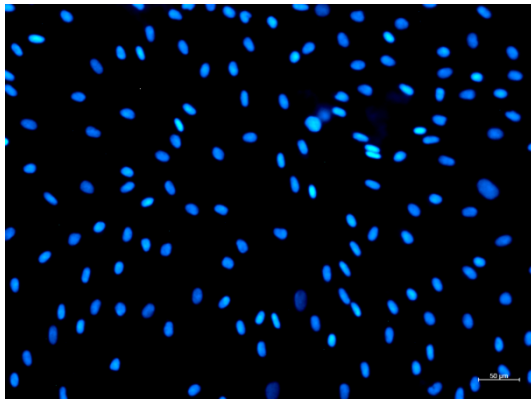
Unit of length:

Global

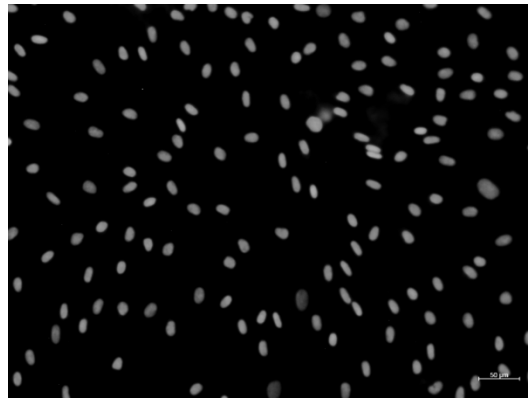
Scale: 2.16 pixels/um

642.59x480.56 μm

C.



D.



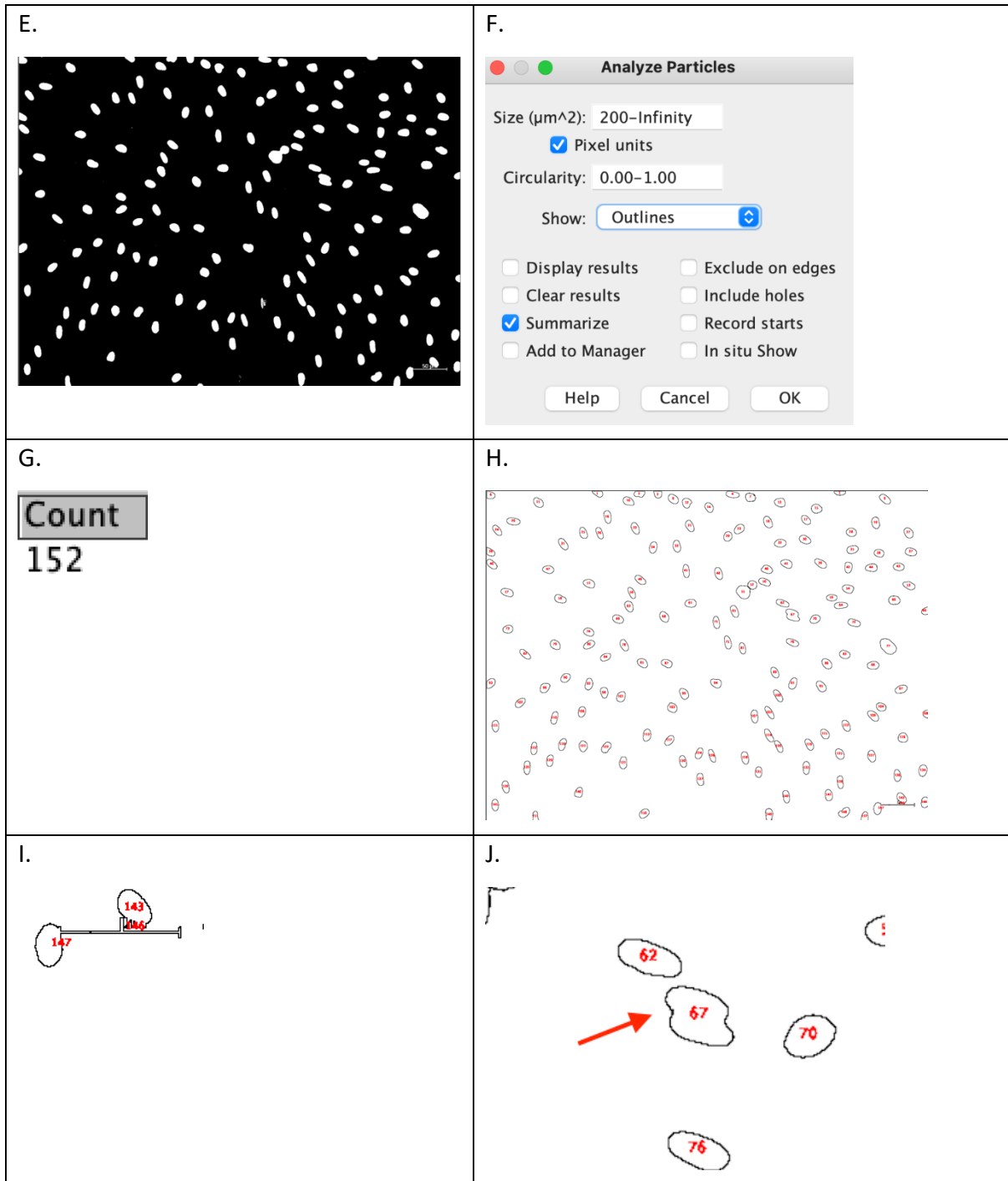


**Figure E1. A summary of the steps followed to obtain an approximate cell count per well using ImageJ software.**

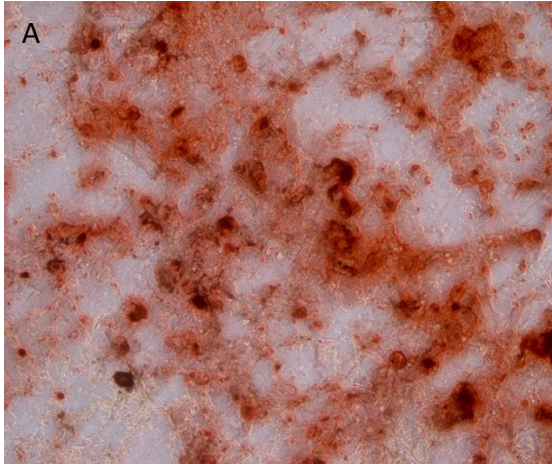
A. The original image captured. B. The scale was calibrated by measuring the scale bar to determine the number of pixels, setting the known distance and entering the correct units. These parameters were all used to calculate the area of the field of vision displayed by the software in the top left-hand corner e.g., 642.59 x 480.56  $\mu\text{m}$ . C. The brightness of the images was adjusted to improve the resolution of the nuclei. D. The image was converted to an 8-bit image. E. Threshold was adjusted to "B&N". F. The image was analysed to determine the number of nuclei per field of vision. G. The nuclei count as determined by the ImageJ software. I & J. Images were manually assessed and incorrect calling of events (nuclei), such as the scale bar counted as a nucleus (I) or nuclei in close proximity counted as a single event were corrected.

Supplementary Information F: Assessment of Osteogenic Differentiation

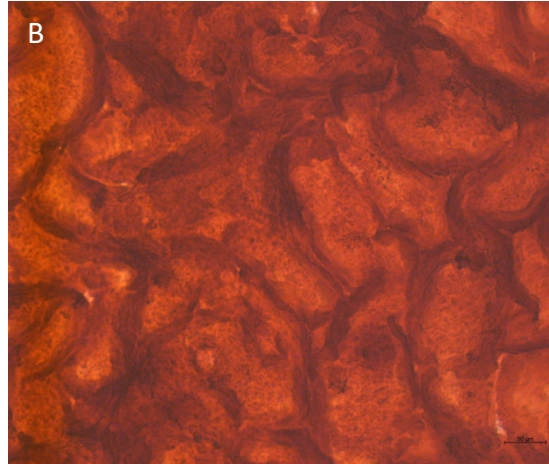
Culture

A311019  
-01A

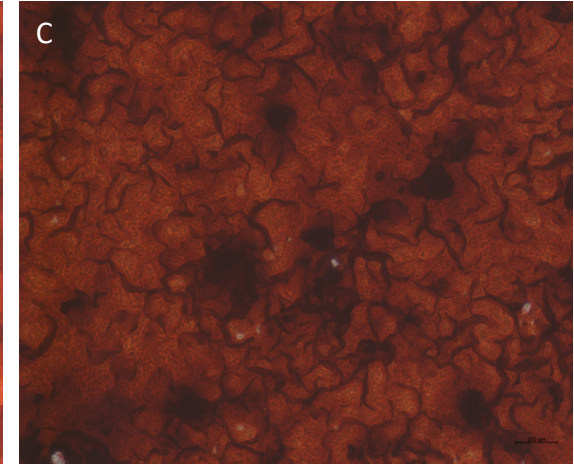
FBS (Day 28)



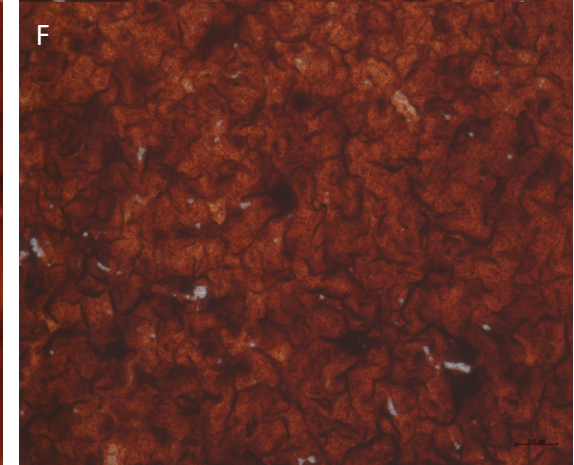
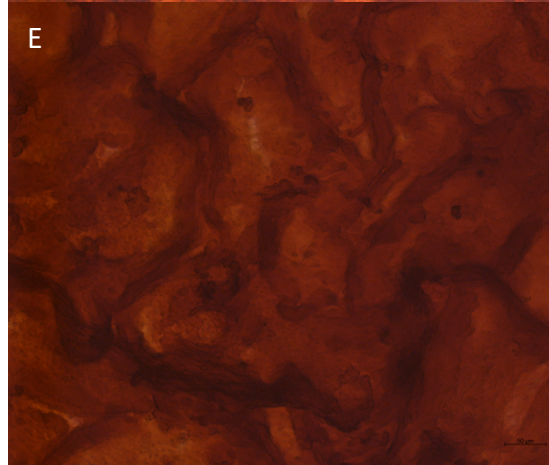
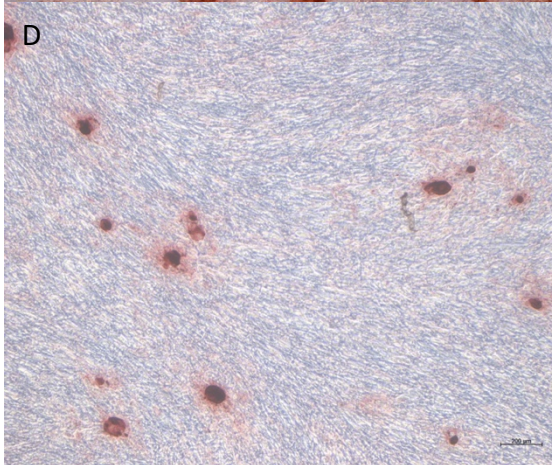
Condition  
pHPL (Day 21)



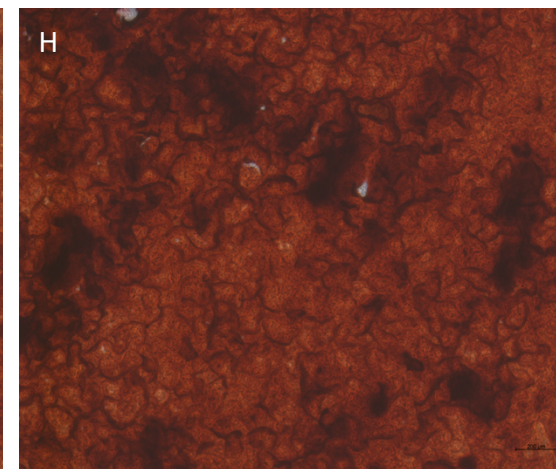
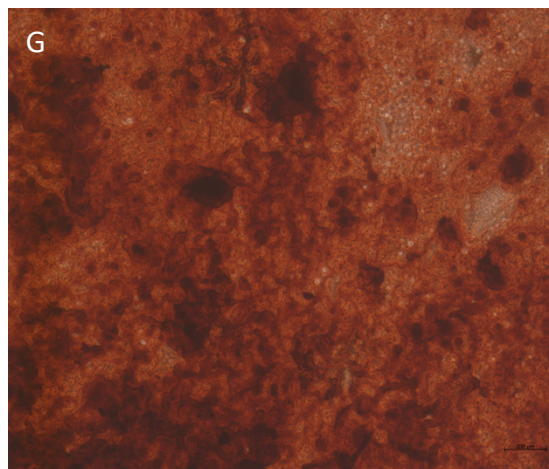
PRP (Day 21)



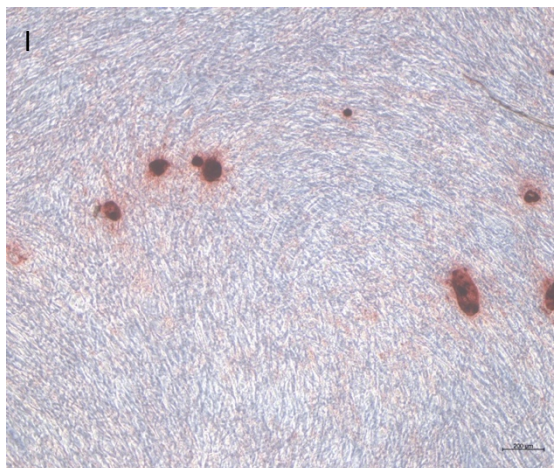
A311019  
-02T



A280621  
-01R



A150221  
-01A



A230221  
-01A

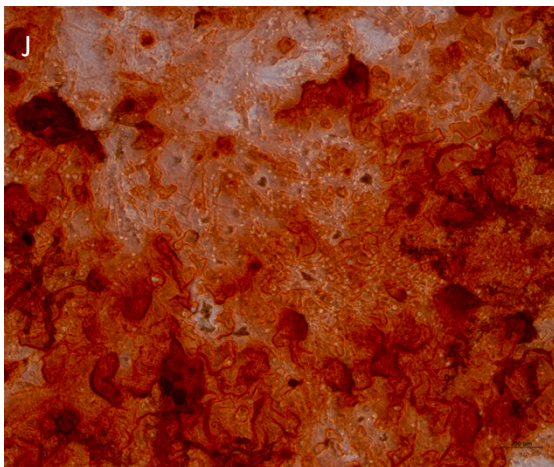


**Figure F1. Representative brightfield images of differentiated (induced) ASCs stained with Alizarin Red S.**

ASCs were induced to undergo osteogenic differentiation for 21 days (pHPL and PRP) or 28 days (FBS). After the differentiation period cells were fixed with paraformaldehyde and stained with ARS. Images taken at 5x magnification show a scale bar of 200  $\mu\text{m}$  and images taken at 20x magnification show a scale bar of 50  $\mu\text{m}$ . For FBS samples 4 biological repeats were used and for pHPL and PRP samples 3 biological repeats were used. Where possible the same ASC culture was used but was not possible for all cultures thus the reason for open spaces.



## Supplementary Information G: Minimum Information for Publication of Quantitative Real-Time PCR Experiments

Bustin et al. 2009 describe a set of guidelines that should be used for qPCR experiments [77]. When these guidelines are followed, data can be considered reliable. This study aimed to adhere to the MIQE guidelines as far as possible. All information labelled by the MIQE guidelines as 'essential' has been included in this document.

### Experimental Design

Please refer to section 2.7. – 2.10.

#### *Definition of control and experimental groups and the numbers in each group*

Three ASC biological replicates were used for each experimental group, and each replicate was run in triplicate for FBS and pHPL experiments. For PRP experiments, three ASC biological replicates and well as three donor PRP biological replicates were used, and each replicate was run in triplicate. For the controls, no induction medium was added, the cells were only maintained in the respective CGM. For experimental groups, cells were exposed to induction medium described in section 2.5.

### Sample

#### *Description*

RNA was isolated at the 4 timepoints (day 0, 7, 14, 21) throughout the differentiation process from both non-induced (control) and induced samples.

#### *Microdissection or macrodissection*

The samples were not subjected to micro- or macrodissection.

#### *Processing*

Please refer to section 2.8. – 2.11.

#### *If frozen -how and how quickly?*

Please refer to section 2.8.

*If fixed -how and how quickly?*

Samples for RT-qPCR were not fixed.

*Storage*

RNA extraction was performed immediately after trypsinisation (0.25% Trypsin/EDTA). The extracted RNA was then stored at -80°C until cDNA could be synthesised. cDNA was stored at -20°C until it was used for RT-qPCR.

**Nucleic Acid Extraction**

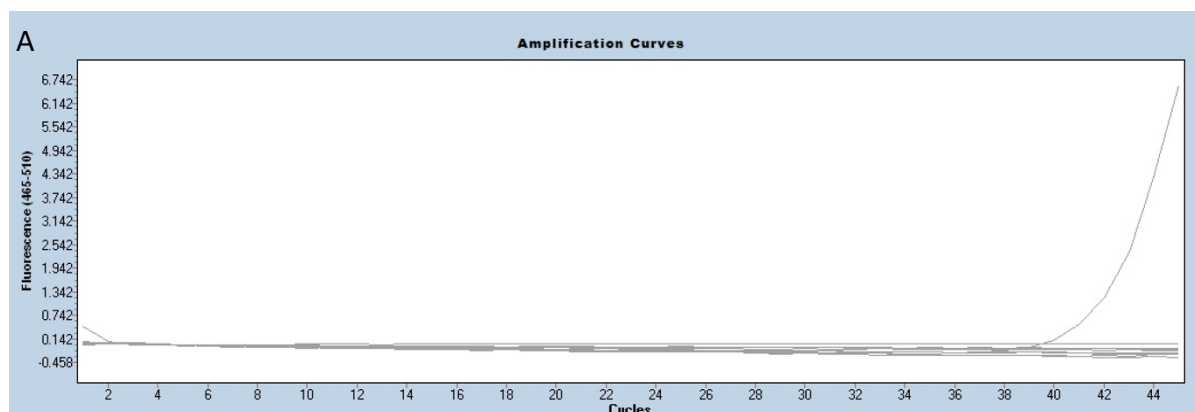
Total RNA was isolated from samples as described in section 2.8.

*DNase or RNase treatment*

Samples were not treated with DNase or RNase.

*Contamination assessment*

During the cDNA experiments, NRTs controls were generated. The reference gene TBP was used in the RT-qPCR reaction mix to determine if there was any genomic DNA (gDNA) contamination (Figure G1).



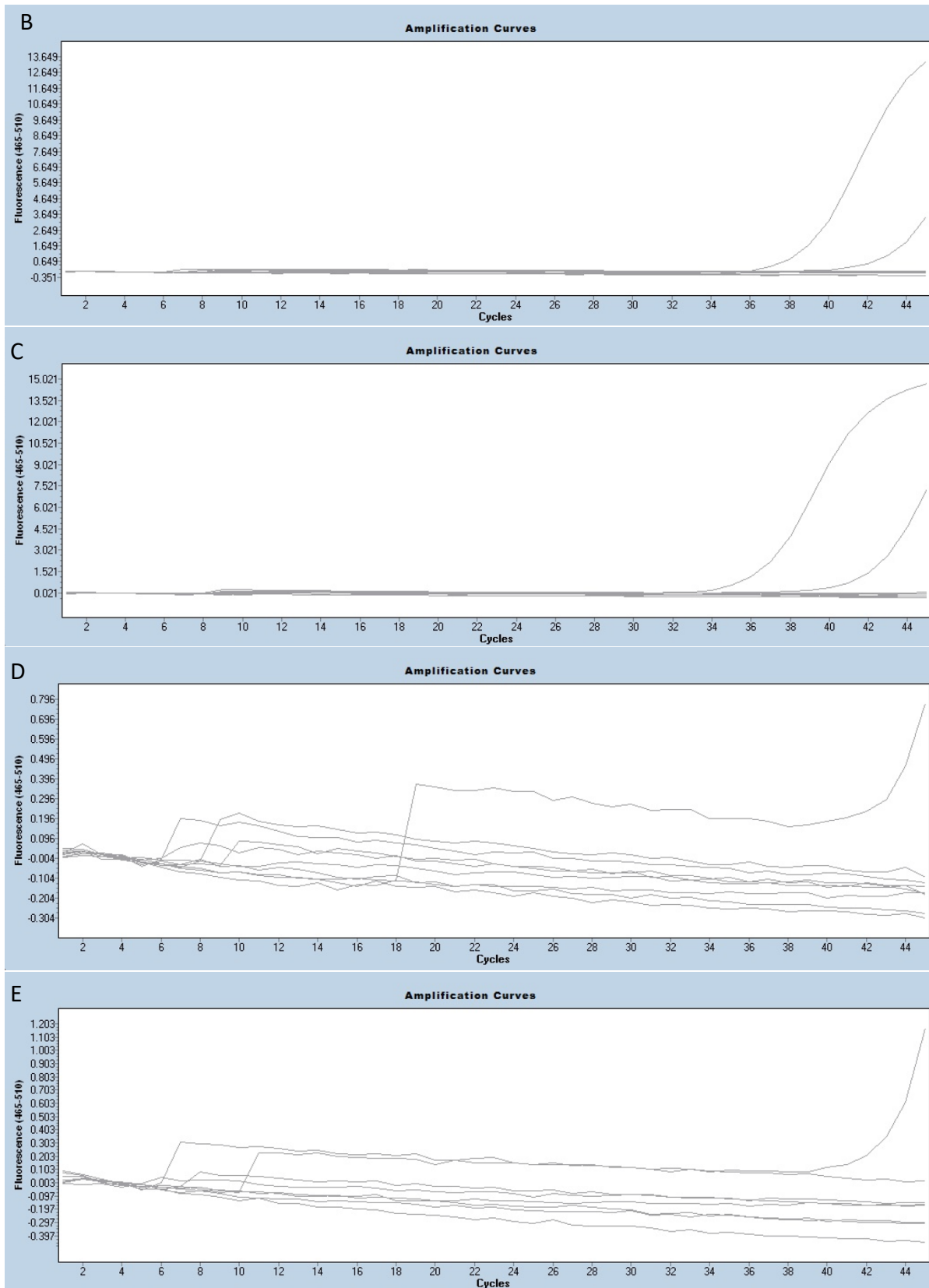


**Figure G1. Amplification Curves for respective NRT controls.**

A-E show FBS, pHPL, PRP070721, PRP240821 and PRP260821 respectively, amplification curves using the TBP gene to detect the presence of any gDNA using 2ng/ul of template. In some cases, there was amplification of NRT samples at 35 or more cycles indicating small to negligible amount of gDNA contamination.

Little to no gDNA contamination was seen in the samples. Some gDNA contamination was seen in FBS, pHPL and PRP070721 samples (Figure G1, B-C). In the instances where amplification was seen, it was only seen in one of the three technical repeats and not across all three repeats. The amplification of the gDNA in these samples occurred at a Ct of 35 or greater.

*Nucleic acid quantification, purity, and integrity*

Please see section 2.8.- 2.11 for sample preparation and instruments used to determine quantity, purity, and integrity of samples. Table G1 summarizes to concentrations, purity and integrity values for samples used in this study.

**Table G1. Total RNA concentration, purity and integrity values for samples used in this study.**

Culture	Timepoint	Non-induced(NI) /Induced(I)	NanoDrop® ND 1000 spectrophotometer			Tapestation ®2200		
			Concentration (ng/ul)	A260/280	A260/230	Concentration (ng/ul)	28S/18S (Area)	RINe
<b>FBS</b>								
A150221-01A	0		179.49	2.06	2.14	115	2.2	10
A311019-01A	0		107.71	2.04	2.1			
A311019-02T	0		50.47	2.05	1.54			
A150221-01A	7	NI	433.75	1.94	0.79	62.9	0.4	9.5
A150221-01A	7	I	336.54	1.86	0.73	151	0.2	9.5
A311019-01A	7	NI	534.53	1.63	0.28	26.6	0.3	9.3
A311019-01A	7	I	613.45	1.65	0.32	309	3.1	9.6
A311019-02T	7	NI	381.09	1.87	0.98	334	3	9.8
A311019-02T	7	I	571.4	1.7	0.35	355	3	9.6
A150221-01A	14	NI	68.96	2.06	1.59	100	2.6	9.9
A150221-01A	14	I	201.72	1.93	1.42	205	2.9	9.8
A311019-01A	14	NI	107.98	1.99	1.52			
A311019-01A	14	I	125.71	2	1.79			
A311019-02T	14	NI	134.97	2.04	2.04	171	3	9.9
A311019-02T	14	I	200.21	2.06	1.53			
A150221-01A	21	NI	138.78	2.04	1.95			
A150221-01A	21	I	213.68	2.06	2.15			
A311019-01A	21	NI	120.11	2.11	2.03	90.1	3.1	10
A311019-01A	21	I	172.68	2.05	2.17			
A311019-02T	21	NI	190.15	2.06	1.83			

A311019-02T	21	I	205.19	2.06	2.07	277	3.5	9.8
pHPL								
A311019-01A	0		72.46	2.15	2.21			
A311019-02T	0		35.44	2.16	1.51			
A280621-01R	0		176.73	2.08	1.91	277	3	10
A150221-01A	7	NI	40	2.17	2.11			
A150221-01A	7	I	95.07	2.1	2.23			
A311019-01A	7	NI	98.91	2.9	2.94	66.6	2.7	10
A311019-01A	7	I	11.29	2.11	0.45	16.8	2.1	9.6
A311019-02T	7	NI	64.25	2.12	2.15			
A311019-02T	7	I	14	2.51	0.03	44.5	2.1	9.4
A280621-01R	7	NI	65.8	2.02	2.14			
A280621-01R	7	I	239.02	2.06	2.1	449	1.9	9.6
A150221-01A	14	NI	64.6	2.05	1.81			
A150221-01A	14	I	34.69	1.97	1.88			
A311019-01A	14	NI	12.11	1.74	1.58	35.4	2	9.4
A311019-01A	14	I	1.41	3.34	0.07	8.28		3.7*
A311019-02T	14	NI	18.89	1.65	0.82	36.5	2.1	9.9
A311019-02T	14	I	8.73	1.75	0.47	6.45		8
A280621-01R	14	NI	119.78	2.03	1.97	150	2.5	9.8
A280621-01R	14	I	476.59	2.02	1.84	342	3.2	9.8
A150221-01A	21	NI	33.04	1.95	0.36			
A150221-01A	21	I	253.83	2.06	1.11			
A311019-01A	21	NI	65.68	2.09	1.23			
A311019-01A	21	I	35.9	2.09	0.65	4.5		2.7*
A311019-02T	21	NI	47.95	2.05	1.41	50.5	2.3	9.8

A311019-02T	21	I	22.37	1.79	1.2	5.52	1.5	6.1*
A280621-01R	21	NI	136.55	2.1	2.18			
A280621-01R	21	I	147.1	2.1	2.12			
<b>PRP070721</b>								
A280621-01R	0		103,95	0.75	1.13	117	3.2	10
A311019-01A	0		63.1	2.09	1.62			
A311019-02T	0		43.49	0.07	1.61	22	2.4	10
A280621-01R	7	NI	224.78	2.07	2.17			
A280621-01R	7	I	519.2	2.07	2.18			
A311019-01A	7	NI	303.15	2.04	1.62	181	2.9	9.7
A311019-01A	7	I	312.89	2.05	1.89			
A311019-02T	7	NI	227.26	2.06	1.93			
A311019-02T	7	I	294.45	2.05	2.15	269	3.2	9.9
A280621-01R	14	NI	189.39	2	1.81			
A280621-01R	14	I	267.52	2.07	1.99			
A311019-01A	14	NI	205.69	2.07	2.11	419	3.3	9.8
A311019-01A	14	I	313.81	2.05	2.2	402	3	9.4
A311019-02T	14	NI	159.56	2.06	1.87			
A311019-02T	14	I	146.93	2.05	1.86			
A280621-01R	21	NI	174.47	2.1	2.16			
A280621-01R	21	I	525.98	2.06	2.16			
A311019-01A	21	NI	294.82	2.07	2.17			
A311019-01A	21	I	179.51	2.08	2.13			
A311019-02T	21	NI	106.29	2.08	1.43	64.9	2.1	9.5
A311019-02T	21	I	147.38	2.12	1.95	168	2.9	9.5
<b>PRP240821</b>								

A280621-01R	0		263.7	2.01	0.8	574	3.4	10
A311019-01A	0		214.02	1.98	0.79	277	4	10
A311019-02T	0		136.46	1.99	0.72	71	3.3	10
A280621-01R	7	NI	200.7	2.06	2.11			
A280621-01R	7	I	432.55	2.03	2.28	743	3.7	9.7
A311019-01A	7	NI	236.86	2.08	2.3	247	2.7	9.6
A311019-01A	7	I	286.53	2.07	2.38			
A311019-02T	7	NI	214.13	2.11	2.33			
A311019-02T	7	I	141.58	2.07	2.05			
A280621-01R	14	NI	549.06	2.1	2.27	676	2.8	9.2
A280621-01R	14	I	167.14	2.11	2.24			
A311019-01A	14	NI	251.32	2.05	2.21			
A311019-01A	14	I	14.12	3.51	1.31			
A311019-02T	14	NI	173.15	2.09	2.08			
A311019-02T	14	I	336.46	2.05	2.23	382	3.3	9.7
A280621-01R	21	NI	904.31	2.11	2.27	309	2.7	9.6
A280621-01R	21	I	401.28	2.04	2			
A311019-01A	21	NI	296.97	2.09	1.54			
A311019-01A	21	I	161	2.09	1.62	79.6	2.8	9.4
A311019-02T	21	NI	84.48	2.12	1.83			
A311019-02T	21	I	52.2	1.9	1.23			
<b>PRP260821</b>								
A280621-01R	0		276.86	1.79	0.6	13.2	2.3	10
A311019-01A	0		141.82	1.72	0.33	7.76	2.3	10
A311019-02T	0		97.49	1.7	0.27	6.64	1.9	10
A280621-01R	7	NI	73.51	2.07	2.38	63.4	2.4	10



A280621-01R	7	I	182.11	2.11	2.42			
A311019-01A	7	NI	96.45	2.1	2.03			
A311019-01A	7	I	231.96	2.08	2.26	258	2.8	9.9
A311019-02T	7	NI	66.24	2.17	2.23			
A311019-02T	7	I	196.17	2.08	2.18			
A280621-01R	14	NI	167.33	2.12	2.28	161	2.2	9.3
A280621-01R	14	I	56.08	2.09	2.14			
A311019-01A	14	NI	51.69	2.24	2.12			
A311019-01A	14	I	23.98	2.25	1.24	37.4	2.3	9.4
A311019-02T	14	NI	64.4	2.2	2.09			
A311019-02T	14	I	141.17	2.09	2			
A280621-01R	21	NI	224.16	2.08	2.02			
A280621-01R	21	I	229.64	2.08	2.04	121	3	9.5
A311019-01A	21	NI	52.65	1.92	0.82	25.4	2.1	9.8
A311019-01A	21	I	97.04	2.08	1.62			
A311019-02T	21	NI	121.48	2.04	1.91	28.4	2.4	9.8
A311019-02T	21	I	157.83	2.04	1.92			

\*Any sample with a RIN value lower than 6.5, together with its counterpart (e.g. pHPL sample A311019-01A Day 14 I had a RIN<sup>e</sup> value of 3.7 therefore this sample together with sample A311019-01A Day 14 NI was excluded from downstream experiments).

### *Inhibition testing*

No inhibition testing was performed.

## Reverse Transcription

Please see section 2.9 for details regarding the synthesis of cDNA. To convert mRNA isolated from cells to cDNA the SensiFast™ cDNA synthesis kit (Bioline, London, England) was used. Information provided by the kit: *“one unit catalyses the incorporation of 1 nmol of dTTP into acid- soluble material in 10 min at 37°C in 50mM Tris-HCl, pH8.6, 40mM KCl, 1mM MnSO<sub>4</sub>, 1 mM DTT, and 0.5 mM [3H]TTP, using 200 μM oligo(dT)<sub>12-18</sub>- primed poly(A)<sub>n</sub> as template.”*

### *cDNA quantification and purity*

Please see sections 5.2.8, 5.2.9 and 5.2.10 regarding the synthesis of cDNA and the determination of purity and integrity. The NanoDrop® ND 1000 spectrophotometer was used to determine the concentration(ng/ul), A260/A280 ratio and A260/230 for cDNA.

### *Quantitation cycle (Cq) values with and without reverse transcriptase (RT)*

NRTs were produced for 10% of samples. These samples were selected for at random. The reference gene TBP was used for the detection of gDNA contamination using a template concentration of 2ng/ul. The results obtained is summarised in Table G2, while the results are visually represented in Figure G1.

**Table G2. Cq values of NRT control sample.**

Medium Supplementation	Culture	Timepoint	Non-induced(NI) /Induced(I)	Cq (Average of three technical repeats)
FBS	A150221-01A	0		40
	A311019-02T	0		ND
	A311019-02T	21	I	ND
pHPL	A311019-01A	0		ND
	A311019-01A	7	NI	40
	A280621-01R	7	I	38.4
PRP070721	A280621-01R	0		36.01
	A311019-01A	7	NI	ND
	A280621-01R	14	NI	40

<b>PRP240821</b>	A311019-02T	7	NI	ND
	A311019-02T	7	I	ND
	A280621-01R	14	NI	ND
<b>PRP260821</b>	A280621-01R	7	I	40
	A280621-01R	14	I	ND
	A311019-02T	14	I	ND

Cq=Ct=Crossing point; ND= Not detected.

### *cDNA Storage*

Once the mRNA was converted to cDNA, the cDNA was stored at -20°C until used in RT-qPCR experiments.

### qPCR target information

Please see section 2.10, Table 2 for the forward and reverse primer sequences for each gene of interest.

### *In silico specificity screen and primer locations*

The NCBI Primer BLAST® tool was used to determine the specificity of the primers. Results from NCBI Primer BLAST® tool are displayed in Figure G2.

<b>RUNX2</b>	<b>Forward primer</b>	<b>Sequence (5'-&gt;3')</b>	<b>Length</b>	<b>Tm</b>	<b>GC%</b>	<b>Self complementarity</b>	<b>Self 3' com</b>	
		ACCCATATCAGAGTTCCAG	19	53.15	47.37	4.00	1.00	
	<b>Reverse primer</b>	GACCGTCTAAAGAGCAAAC	19	53.78	47.37	5.00	0.00	
	<b>Products on target templates</b>							
	>NM_001015051.4 Homo sapiens RUNX family transcription factor 2 (RUNX2), transcript variant 2, mRNA							
	product length = 117							
	Forward primer	1	ACCCATATCAGAGTTCCAG	19				
	Template	4615	.....	4633				
	Reverse primer	1	GACCGTCTAAAGAGCAAAC	19				
	Template	4731	.....	4713				
<b>ALP</b>	<b>Forward primer</b>	<b>Sequence (5'-&gt;3')</b>	<b>Length</b>	<b>Tm</b>	<b>GC%</b>	<b>Self complementarity</b>	<b>Self 3' com</b>	
		GCAACTCTATCTTTGGTCTG	20	53.73	45.00	3.00	1.00	
	<b>Reverse primer</b>	GGTAGTTGTTGTGAGCATAG	20	53.75	45.00	2.00	0.00	
	<b>Products on target templates</b>							
	>XM_017000903.2 PREDICTED: Homo sapiens alkaline phosphatase, biomineralization associated (ALPL), transcript variant X1, mRNA							
	product length = 150							
	Forward primer	1	GCAACTCTATCTTTGGTCTG	20				
	Template	1019	.....	1038				
	Reverse primer	1	GGTAGTTGTTGTGAGCATAG	20				
	Template	1168	.....	1149				

OCN	Forward primer	Sequence (5'->3')	Length	Tm	GC%	Self complementarity	Self 3' com
	Reverse primer	ACCTTCTTCTCTTCC	18	52.88	50.00	1.00	0.00
		CCCACAGATTCTTCT	18	52.67	50.00	3.00	0.00
	<b>Products on target templates</b>						
	>NM_001199662.1 Homo sapiens PMF1-BGLAP readthrough (PMF1-BGLAP), transcript variant 2, mRNA						
	product length = 111						
	Forward primer	1 ACCCTTCTTCTCTTCC	18				
	Template	884 .....	901				
	Reverse primer	1 CCCACAGATTCTTCT	18				
	Template	994 .....	977				
PPARY	Forward primer	Sequence (5'->3')	Length	Tm	GC%	Self complementarity	Self 3' com
	Reverse primer	CGTGGATCTCTCCGTAAT	18	53.11	50.00	4.00	2.00
		TGGATCTGTTCTGTGAATG	20	53.21	40.00	4.00	0.00
	<b>Products on target templates</b>						
	>NM_001354666.3 Homo sapiens peroxisome proliferator activated receptor gamma (PPARG), transcript variant 6, mRNA						
	product length = 124						
	Forward primer	1 CGTGGATCTCTCCGTAAT	18				
	Template	441 .....	458				
	Reverse primer	1 TGGATCTGTTCTGTGAATG	20				
	Template	564 .....	545				
FABP4	Forward primer	Sequence (5'->3')	Length	Tm	GC%	Self complementarity	Self 3' com
	Reverse primer	ATCAACCACCATAAAGAGAAA	21	52.71	33.33	2.00	0.00
		ACCTTCAGTCCAGGTCAA	18	54.82	50.00	5.00	0.00
	<b>Products on target templates</b>						
	>NM_001442.3 Homo sapiens fatty acid binding protein 4 (FABP4), mRNA						
	product length = 126						
	Forward primer	1 ATCAACCACCATAAAGAGAAA	21				
	Template	369 .....	389				
	Reverse primer	1 ACCTTCAGTCCAGGTCAA	18				
	Template	494 .A.....	477				
TBP	Forward primer	Sequence (5'->3')	Length	Tm	GC%	Self complementarity	Self 3' com
	Reverse primer	CCGAAACGCCGAATATAA	18	52.62	44.44	4.00	2.00
		GGACTGTTCTTCACTCTTG	19	52.94	47.37	3.00	0.00
	<b>Products on target templates</b>						
	>NM_001172085.2 Homo sapiens TATA-box binding protein (TBP), transcript variant 2, mRNA						
	product length = 130						
	Forward primer	1 CCGAAACGCCGAATATAA	18				
	Template	602 .....	619				
	Reverse primer	1 GGACTGTTCTTCACTCTTG	19				
	Template	731 .....	713				
GUSB	Forward primer	Sequence (5'->3')	Length	Tm	GC%	Self complementarity	Self 3' com
	Reverse primer	GATCGCTCACACCAAATC	18	53.57	50.00	4.00	0.00
		TCGTGATACCAAGAGTAGTAG	21	53.71	42.86	6.00	1.00
	<b>Products on target templates</b>						
	>XM_047420289.1 PREDICTED: Homo sapiens glucuronidase beta (GUSB), transcript variant X6, mRNA						
	product length = 132						
	Forward primer	1 GATCGCTCACACCAAATC	18				
	Template	707 .....	724				
	Reverse primer	1 TCGTGATACCAAGAGTAGTAG	21				
	Template	838 .....	818				
YWHAZ	Forward primer	Sequence (5'->3')	Length	Tm	GC%	Self complementarity	Self 3' com
	Reverse primer	TGACATTGGGTAGCATTAAC	20	53.27	40.00	4.00	2.00
		GCACCTGACAAATAGAAAGA	20	53.22	40.00	3.00	0.00
	<b>Products on target templates</b>						
	>XM_017013811.2 PREDICTED: Homo sapiens tyrosine 3-monooxygenase/tryptophan 5-monooxygenase activation protein zeta (YWHAZ), transcript variant X4, mRNA						
	product length = 126						
	Forward primer	1 TGACATTGGGTAGCATTAAC	20				
	Template	2613 .....	2632				
	Reverse primer	1 GCACCTGACAAATAGAAAGA	20				
	Template	2738 .....	2719				

Figure G2. *In silico* primer BLAST results.

The binding specificity of each primer was assessed using the NCBI Primer BLAST® tool.

### Splice variants targeted

No splice variants were targeted.

### Additional primer analysis

#### ALP

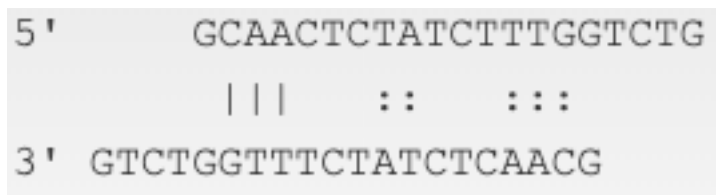
Table G3. Primer analysis of ALP primer used in the study.

Parameter	Optimal criteria for primer design for SYBR Green assay	Forward primer	Reverse primer	Accepted
Primer length	18 – 25 bases	20	20	Yes
PCR product size	100 – 150 bp	150		Yes
Melting temperature*	55°C - 60°C >5°C difference between forward and reverse primer	50.7	50.7	No
GC content	40% - 60%	45	45	Yes
GC clamp	More than 3 G's or C's should be avoided in the last 5 bases at the 3' end of the primer	3	2	Yes
Hairpin formation	3' end hairpin > -2kcal.mol <sup>-1</sup> Internal hairpin > -3kcal.mol <sup>-1</sup>	0.33	0.71	Yes
Internal annealing bases	< 4 bases	3	3	Yes
Self dimer	3' end hairpin > -5kcal.mol <sup>-1</sup> Internal hairpin > -6kcal.mol <sup>-1</sup>	-3.9	-3.14	Yes
Cross dimer/ Hetro-dimer	3' end hairpin > -5kcal.mol <sup>-1</sup> Internal hairpin > -6kcal.mol <sup>-1</sup>	-6.84		No
3' end sequence	3' end terminate with G or C	Yes	Yes	Yes
Cross homology	Specifically binds to target of interest	Yes	Yes	Yes

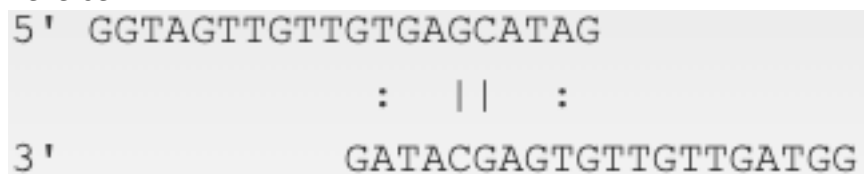
Table adapted from DNAbiotec® (Pty) Ltd Essential qPCR™ Short Course notes (2019). Calculations were done using OligoAnalyzer available on <https://eu.idtdna.com/calc/analyzer>.

Self-dimer:

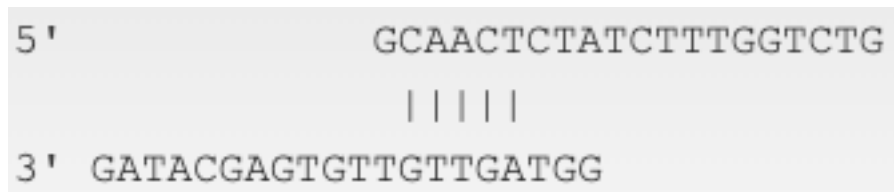
Forward:



Reverse:



Cross dimer:



*Osteocalcin (OCN)*

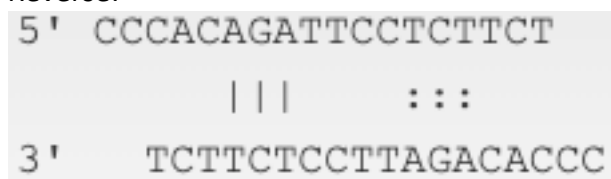
**Table G4. Primer analysis of OCN primer used in the study.**

Parameter	Optimal criteria for primer design for SYBR Green assay	Forward primer	Reverse primer	Accepted
Primer length	18 – 25 bases	18	18	Yes
PCR product size	100 – 150 bp	111		Yes
Melting temperature	55°C - 60°C >5°C difference between forward and reverse primer	51.1	50.8	No
GC content	40% - 60%	50	50	Yes
GC clamp	More than 3 G's or C's should be avoided in the last 5 bases at the 3' end of the primer	3	2	Yes
Hairpin formation	3' end hairpin > -2kcal.mol <sup>-1</sup> Internal hairpin > -3kcal.mol <sup>-1</sup>	-	0.44	Yes
Internal annealing bases	< 4 bases	-	3	Yes
Self dimer	3' end hairpin > -5kcal.mol <sup>-1</sup> Internal hairpin > -6kcal.mol <sup>-1</sup>	-	-3.17	Yes
Cross dimer/ Hetro-dimer	3' end hairpin > -5kcal.mol <sup>-1</sup> Internal hairpin > -6kcal.mol <sup>-1</sup>	-3.17		Yes
3' end sequence	3' end terminate with G or C	Yes	No	No
Cross homology	Specifically binds to target of interest	Yes	Yes	Yes

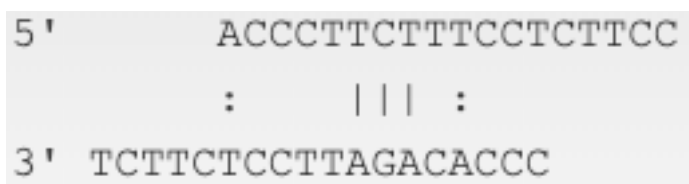
Table adapted from DNAbiotec® (Pty) Ltd Essential qPCR™ Short Course notes (2019). Calculations were done using OligoAnalyzer available on <https://eu.idtdna.com/calc/analyzer>.

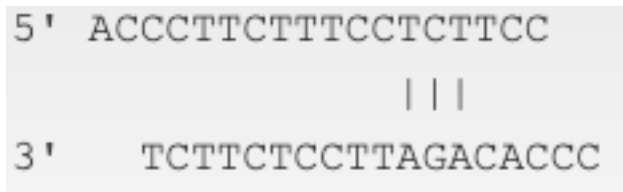
Self-dimer:

Reverse:



Cross dimer:





## RUNX2

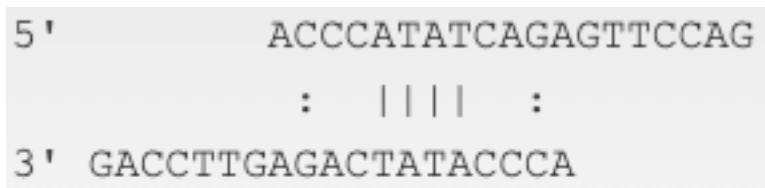
Table G5. Primer analysis of RUNX2 primer used in the study.

Parameter	Optimal criteria for primer design for SYBR Green assay	Forward primer	Reverse primer	Accepted
Primer length	18 – 25 bases	19	19	Yes
PCR product size	100 – 150 bp	117		Yes
Melting temperature	55°C - 60°C >5°C difference between forward and reverse primer	50.9	50.9	No
GC content	40% - 60%	47.4	47.4	Yes
GC clamp	More than 3 G's or C's should be avoided in the last 5 bases at the 3' end of the primer	3	2	Yes
Hairpin formation	3' end hairpin > -2kcal.mol <sup>-1</sup> Internal hairpin > -3kcal.mol <sup>-1</sup>	1.93	0.82	Yes
Internal annealing bases	< 4 bases	1	2	Yes
Self dimer	3' end hairpin > -5kcal.mol <sup>-1</sup> Internal hairpin > -6kcal.mol <sup>-1</sup>	-3.91	-3.61	Yes
Cross dimer/ Hetro-dimer	3' end hairpin > -5kcal.mol <sup>-1</sup> Internal hairpin > -6kcal.mol <sup>-1</sup>	-3.29		Yes
3' end sequence	3' end terminate with G or C	Yes	Yes	Yes
Cross homology	Specifically binds to target of interest	Yes	Yes	Yes

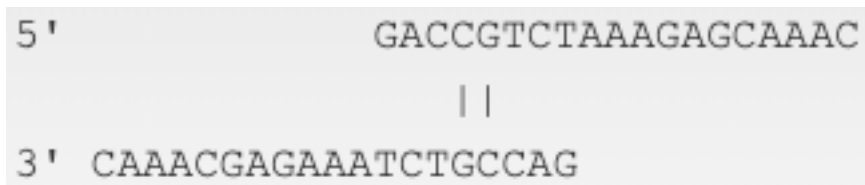
Table adapted from DNAbiotec® (Pty) Ltd Essential qPCR™ Short Course notes (2019). Calculations were done using OligoAnalyzer available on <https://eu.idtdna.com/calc/analyzer>.

Self-dimer:

Forward:



Reverse:



Cross dimer:

```

5' ACCCATATCAGAGTTCCAG
      |||
3' CAAACGAGAAATCTGCCAG

```

### PPAR $\gamma$

Table G6. Primer analysis of PPAR $\gamma$  primer used in the study.

Parameter	Optimal criteria for primer design for SYBR Green assay	Forward primer	Reverse primer	Accepted
Primer length	18 – 25 bases	18	20	Yes
PCR product size	100 – 150 bp	124		Yes
Melting temperature	55°C - 60°C >5°C difference between forward and reverse primer	50.9	50.1	No
GC content	40% - 60%	50	40	Yes
GC clamp	More than 3 G's or C's should be avoided in the last 5 bases at the 3' end of the primer	1	2	Yes
Hairpin formation	3' end hairpin > -2kcal.mol <sup>-1</sup> Internal hairpin > -3kcal.mol <sup>-1</sup>	-0.63	0.25	Yes
Internal annealing bases	< 4 bases	4	3	Yes
Self dimer	3' end hairpin > -5kcal.mol <sup>-1</sup> Internal hairpin > -6kcal.mol <sup>-1</sup>	-4.64	-4.62	Yes
Cross dimer/ Hetro-dimer	3' end hairpin > -5kcal.mol <sup>-1</sup> Internal hairpin > -6kcal.mol <sup>-1</sup>	-4.64		Yes
3' end sequence	3' end terminate with G or C	No	Yes	No
Cross homology	Specifically binds to target of interest	Yes	Yes	Yes

Table adapted from DNAbiotech® (Pty) Ltd Essential qPCR™ Short Course notes (2019). Calculations were done using OligoAnalyzer available on <https://eu.idtdna.com/calc/analyzer>.

### Self-dimer:

#### Forward:

```

5' CGTGGATCTCTCCGTAAT
      |||   :::
3' TAATGCCTCTCTAGGTGC

```

#### Reverse:

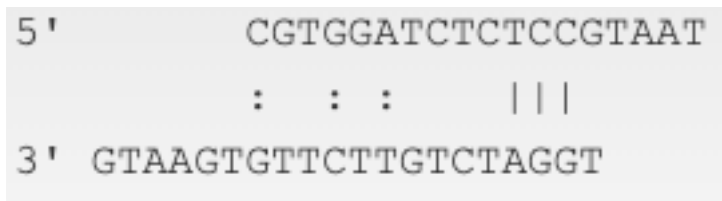
```

5' TGGATCTGTTCTTGTGAATG
      ||||
3' GTAAGTGTCTTGTCTAGGT

```



Cross dimer:



*FABP4*

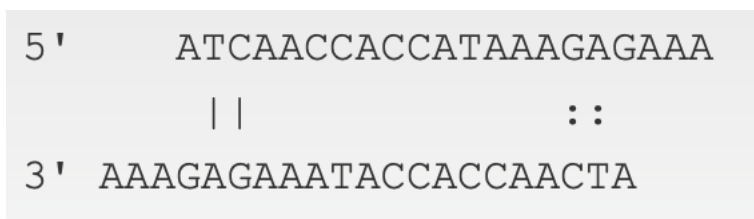
Table G7. Primer analysis of *FABP4* primer used in the study.

Parameter	Optimal criteria for primer design for SYBR Green assay	Forward primer	Reverse primer	Accepted
Primer length	18 – 25 bases	21	18	Yes
PCR product size	100 – 150 bp	126		Yes
Melting temperature	55°C - 60°C >5°C difference between forward and reverse primer	49.4	53	No
GC content	40% - 60%	33.3	50	No
GC clamp	More than 3 G's or C's should be avoided in the last 5 bases at the 3' end of the primer	1	2	Yes
Hairpin formation	3' end hairpin > -2kcal.mol <sup>-1</sup> Internal hairpin > -3kcal.mol <sup>-1</sup>	-15.8	-0.51	Yes
Internal annealing bases	< 4 bases	2	3	Yes
Self dimer	3' end hairpin > -5kcal.mol <sup>-1</sup> Internal hairpin > -6kcal.mol <sup>-1</sup>	-1.57	-6.01	Yes
Cross dimer/ Hetro-dimer	3' end hairpin > -5kcal.mol <sup>-1</sup> Internal hairpin > -6kcal.mol <sup>-1</sup>	-4.41		Yes
3' end sequence	3' end terminate with G or C	No	No	No
Cross homology	Specifically binds to target of interest	Yes	Yes	Yes

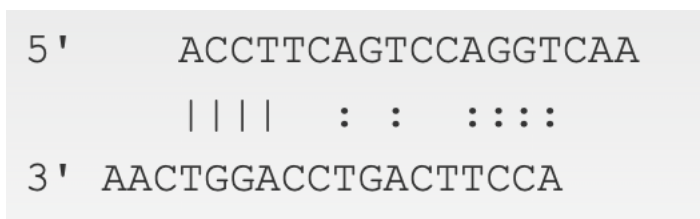
Table adapted from DNAbiotec® (Pty) Ltd Essential qPCR™ Short Course notes (2019). Calculations were done using OligoAnalyzer available on <https://eu.idtdna.com/calc/analyzer>.

Self-dimer:

Forward:



Reverse:



Cross dimer:

```

5' ATCAACCACCATAAAGAGAAA
   : ||| : : :
3' AACTGGACCTGACTTCCA
  
```

TBP

Table G8. Primer analysis of TBP primer used in the study.

Parameter	Optimal criteria for primer design for SYBR Green assay	Forward primer	Reverse primer	Accepted
Primer length	18 – 25 bases	18	19	Yes
PCR product size	100 – 150 bp	130		Yes
Melting temperature	55°C - 60°C >5°C difference between forward and reverse primer	49.8	50.2	No
GC content	40% - 60%	44.4	47.4	Yes
GC clamp	More than 3 G's or C's should be avoided in the last 5 bases at the 3' end of the primer	0	2	Yes
Hairpin formation	3' end hairpin > -2kcal.mol <sup>-1</sup> Internal hairpin > -3kcal.mol <sup>-1</sup>	-0.46	0.3	Yes
Internal annealing bases	< 4 bases	2	2	Yes
Self dimer	3' end hairpin > -5kcal.mol <sup>-1</sup> Internal hairpin > -6kcal.mol <sup>-1</sup>	-3.91	-1.95	Yes
Cross dimer/ Hetro-dimer	3' end hairpin > -5kcal.mol <sup>-1</sup> Internal hairpin > -6kcal.mol <sup>-1</sup>	-3.52		Yes
3' end sequence	3' end terminate with G or C	No	Yes	No
Cross homology	Specifically binds to target of interest	Yes	Yes	Yes

Table adapted from DNAbiotec® (Pty) Ltd Essential qPCR™ Short Course notes (2019). Calculations were done using OligoAnalyzer available on <https://eu.idtdna.com/calc/analyzer>.

Self-dimer:

Forward:

```

5' CCGAAACGCCGAATATAA
   ||||
3'           AATATAAGCCGCAAAGCC
  
```

Reverse:

```

5'   GGACTGTTCTTCACTCTTG
   :: || :: ::
3' GTTCTCACTTCTTGTCAGG
  
```

Cross dimer:

```

5'          CCGAAACGCCGAATATAA
           |||  :  :
3'  GTTCTCACTTCTTGTCAGG
  
```

*GUSB*

Table G9. Primer analysis of *GUSB* primer used in the study.

Parameter	Optimal criteria for primer design for SYBR Green assay	Forward primer	Reverse primer	Accepted
Primer length	18 – 25 bases	18	21	Yes
PCR product size	100 – 150 bp	132		Yes
Melting temperature	55°C - 60°C >5°C difference between forward and reverse primer	51	50.5	No
GC content	40% - 60%	50	42.9	Yes
GC clamp	More than 3 G's or C's should be avoided in the last 5 bases at the 3' end of the primer	1	2	Yes
Hairpin formation	3' end hairpin > -2kcal.mol <sup>-1</sup> Internal hairpin > -3kcal.mol <sup>-1</sup>	0.88	-0.05	Yes
Internal annealing bases	< 4 bases	2	3	Yes
Self dimer	3' end hairpin > -5kcal.mol <sup>-1</sup> Internal hairpin > -6kcal.mol <sup>-1</sup>	-4.62	-3.61	Yes
Cross dimer/ Hetro-dimer	3' end hairpin > -5kcal.mol <sup>-1</sup> Internal hairpin > -6kcal.mol <sup>-1</sup>	-4.87		Yes
3' end sequence	3' end terminate with G or C	Yes	Yes	Yes
Cross homology	Specifically binds to target of interest	Yes	Yes	Yes

Table adapted from DNAbiotec® (Pty) Ltd Essential qPCR™ Short Course notes (2019). Calculations were done using OligoAnalyzer available on <https://eu.idtdna.com/calc/analyzer>.

Self-dimer:

Forward:

```

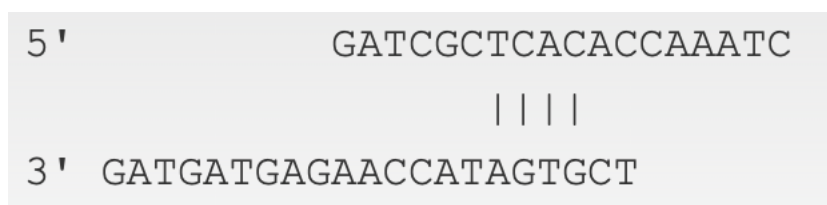
5'          GATCGCTCACACCAAATC
           ||||
3'  CTAAACCACACTCGCTAG
  
```

Reverse:

```

5'          TCGTGATACCAAGAGTAGTAG
           ||
3'  GATGATGAGAACCATAGTGCT
  
```

Cross dimer:



YWHAZ

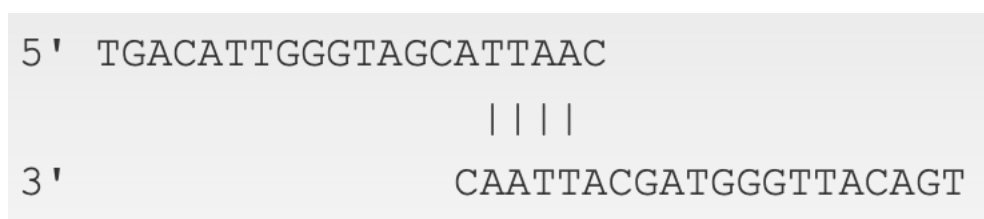
Table G10. Primer analysis of YWHAZ primer used in the study.

Parameter	Optimal criteria for primer design for SYBR Green assay	Forward primer	Reverse primer	Accepted
Primer length	18 – 25 bases	20	20	Yes
PCR product size	100 – 150 bp			Yes
Melting temperature	55°C - 60°C >5°C difference between forward and reverse primer	50.2	50.1	No
GC content	40% - 60%	40	40	Yes
GC clamp	More than 3 G's or C's should be avoided in the last 5 bases at the 3' end of the primer	1	1	Yes
Hairpin formation	3' end hairpin > -2kcal.mol <sup>-1</sup> Internal hairpin > -3kcal.mol <sup>-1</sup>	0.14	0.92	Yes
Internal annealing bases	< 4 bases	2	3	Yes
Self dimer	3' end hairpin > -5kcal.mol <sup>-1</sup> Internal hairpin > -6kcal.mol <sup>-1</sup>	-4.85	-3.14	Yes
Cross dimer/ Hetro-dimer	3' end hairpin > -5kcal.mol <sup>-1</sup> Internal hairpin > -6kcal.mol <sup>-1</sup>		-4.41	Yes
3' end sequence	3' end terminate with G or C	Yes	Yes	Yes
Cross homology	Specifically binds to target of interest	Yes	Yes	Yes

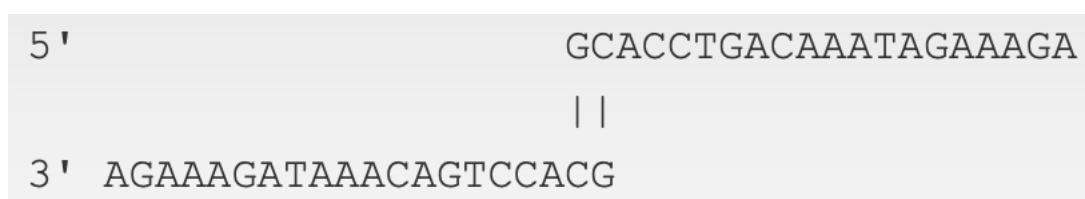
Table adapted from DNAbiotec® (Pty) Ltd Essential qPCR™ Short Course notes (2019). Calculations were done using OligoAnalyzer available on <https://eu.idtdna.com/calc/analyzer>.

Self-dimer:

Forward:



Reverse:



Cross dimer:

```
5'          TGACATTGGGTAGCATTAAC
           :   |||
3' AGAAAGATAAACAGTCCACG
```

qPCR Oligonucleotides

Primer sequences used in this study have been summarised in section 2.10, Table 2.

*Location and identity of any locations*

There were no modifications.

*Manufacture of oligonucleotides*

Integrated DNA Technologies (IDT; Coralville, IA, USA) manufactured all oligonucleotides used in this study.

RT-qPCR protocol

The protocol used in this study is described in section 2.10.

*Polymerase identity and concentration*

The LightCycler® 480 SYBR Green I Master Mix was used in this study. The polymerase in the master mix is FastStart™ Taq DNA polymerase (Roche, Basel, Switzerland), and the concentration was not indicated.

*Buffer/kit identity and manufacturer*

The LightCycler® 480 SYBR Green I Master Mix (Roche, Basel, Switzerland; Catalogue number: 04887352001) was used.

*Additives*

No additives were used.

### *Manufacture of plates/tubes and catalogue numbers*

LightCycler® 480 Multiwell Plate 96 white plates (Roche, Basel, Switzerland; Catalogue 17 number: 04729692001) were used.

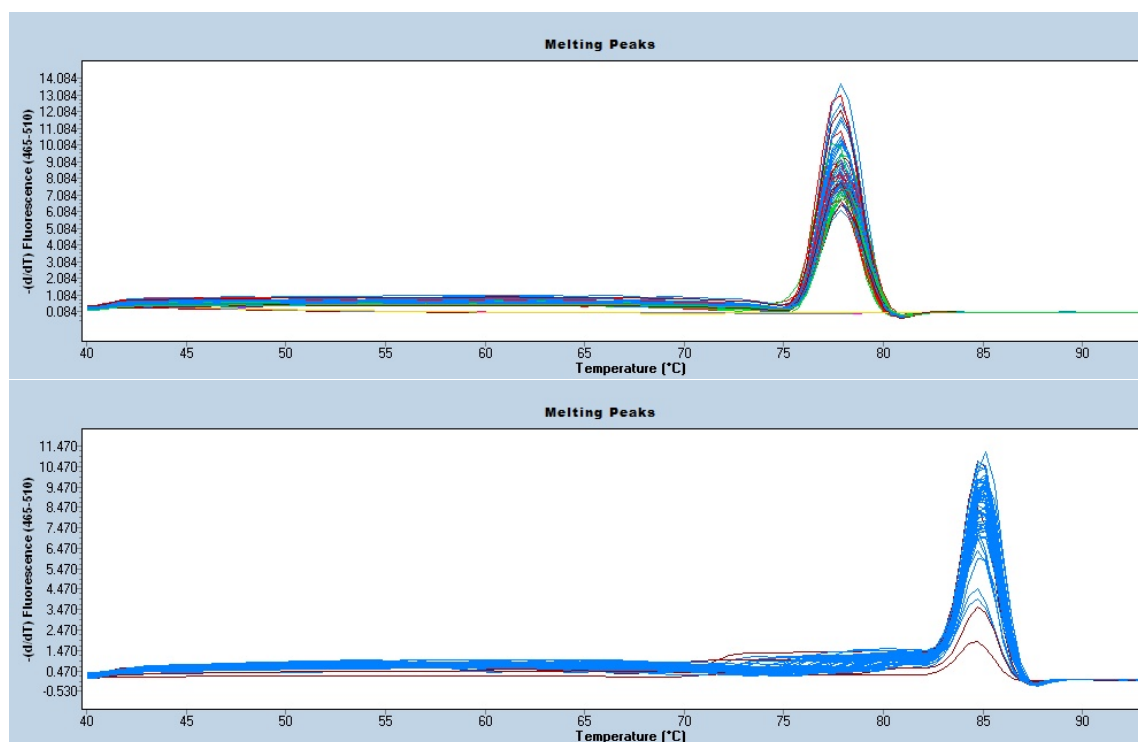
### *Manufacturer of qPCR instrument*

The LightCycler® 480 II instrument was manufactured by Roche (Basel, Switzerland).

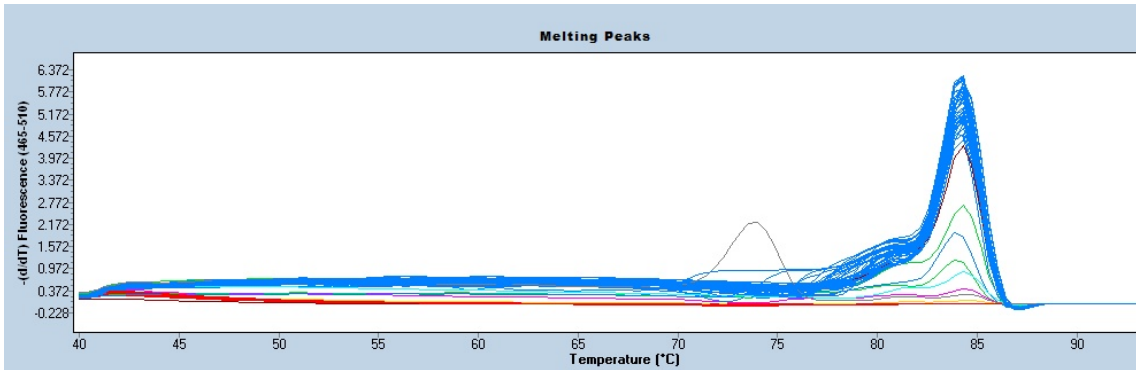
### qPCR Validation

#### *Specificity*

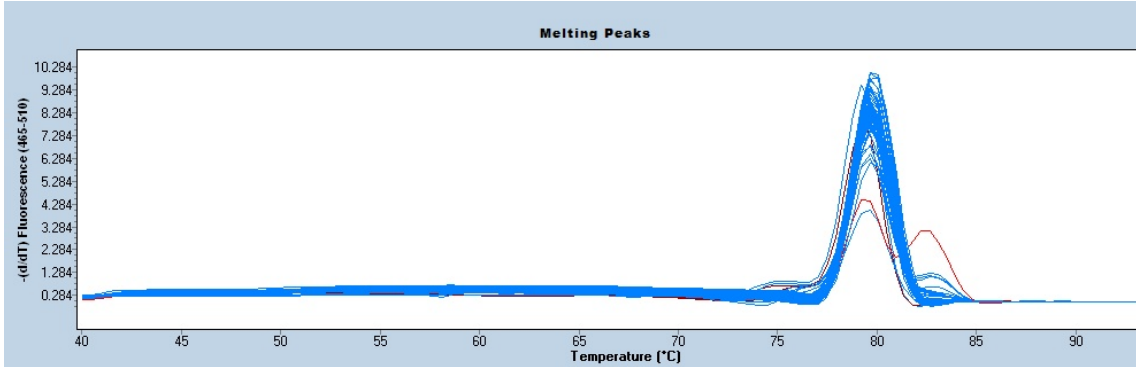
The specificity of the primer binding to their targets was tested through the generation of melt curves. Melt curves can be visualised in Figure G3.



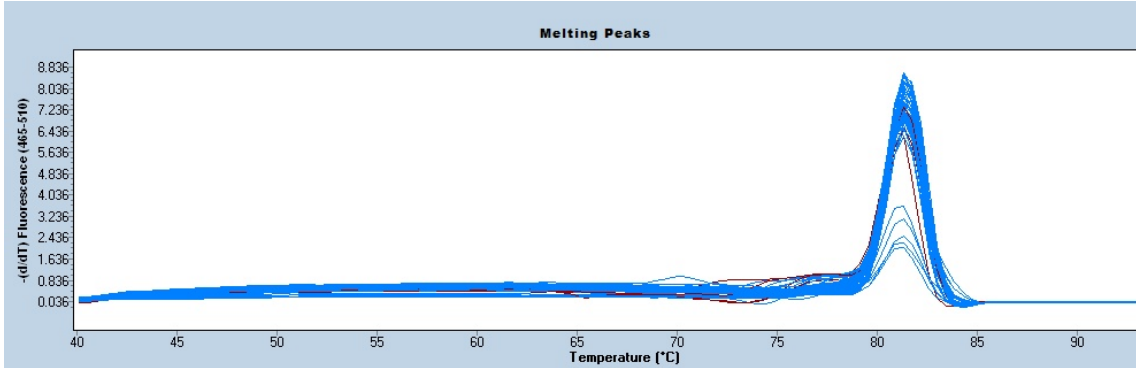
OCN



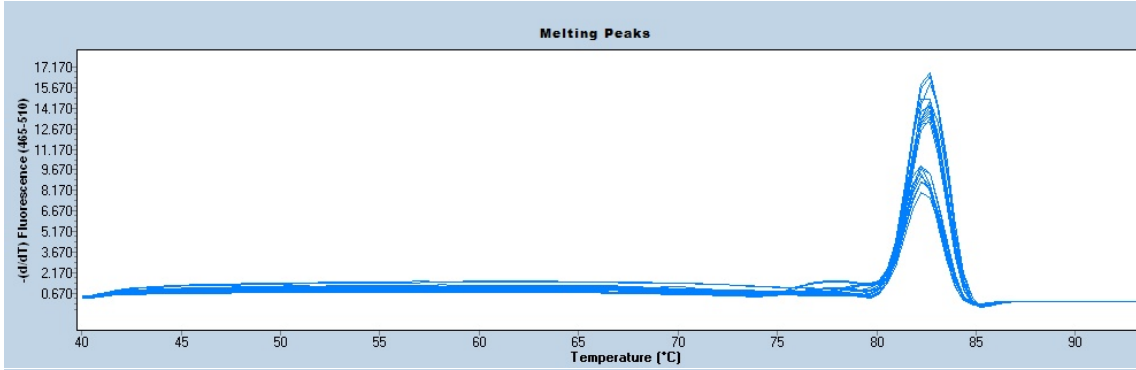
PPARY



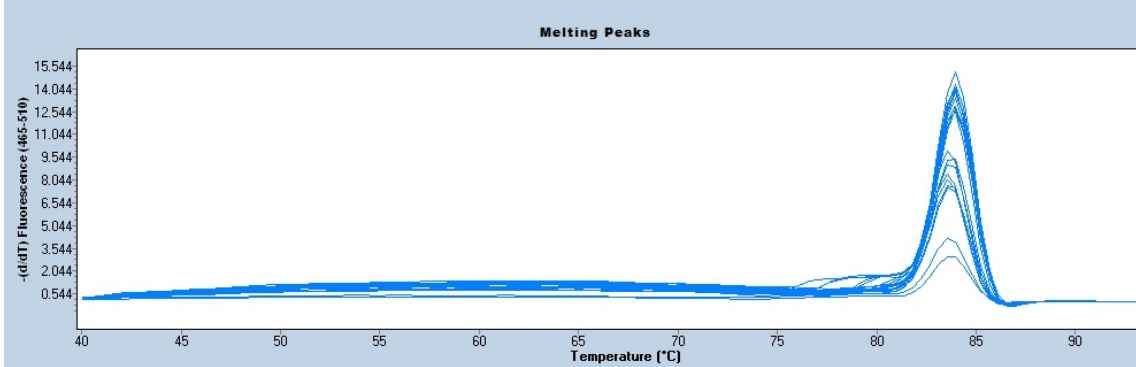
FABP4



TBP



GUSB



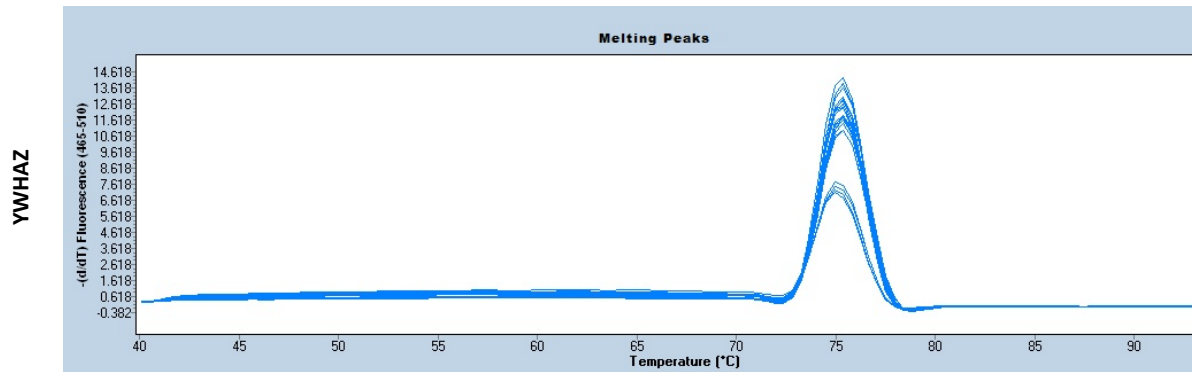


**Figure G3. Melt curves of primers used in the study.**  
Melt curves were used to analyse the specificity of each primer binding to their binding target sites.

*No template controls*

No template controls were included on every plate for every target- and reference gene used in the study (Figure G4).

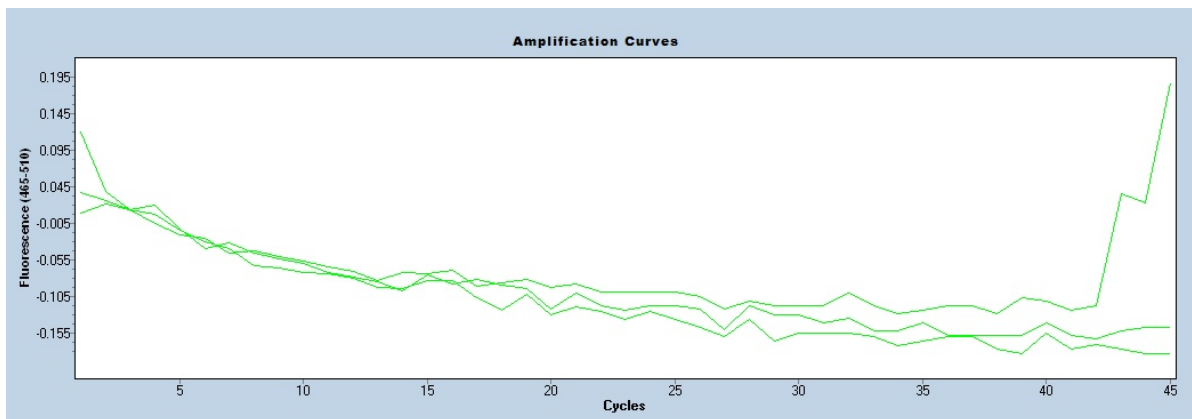


**Figure G4. Representative Amplification Curves for No Template Control.**  
No template controls were included on every plate and were run in triplicate.

If amplification was detected in more than two of the three technical repeats, the plate was repeated.

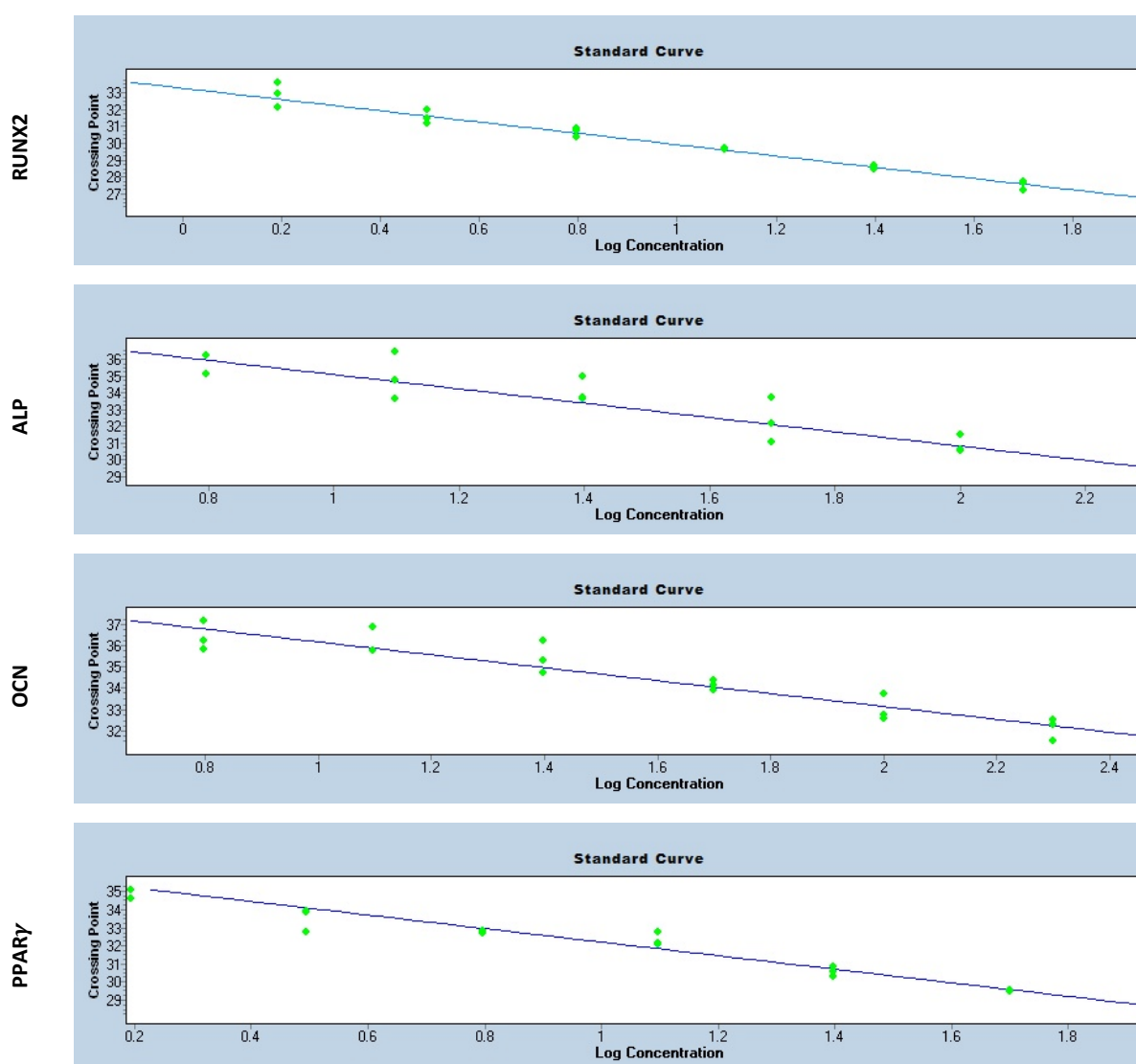
*Standard curves*

Standard curves were run for all genes in the study to determine the efficiency of each primer pair by subjecting samples to at least 5, 2-fold dilutions (in triplicate)(Table G11). The efficiency was then used to calculate relative gene expression. Figure G6 depicts the standard curves run in this study. Standards from standard curves was included on every plate and those standards had to fall on the standard curve graphs for the plate to be acceptable (Figure G7).



Table G11. Description of the serial dilutions made for the standard curves.

100ng	100ng	100ng
50ng	50ng	50ng
25ng	25ng	25ng
12.5ng	12.5ng	12.5ng
6.25ng	6.25ng	6.25ng
NTC	NTC	NTC



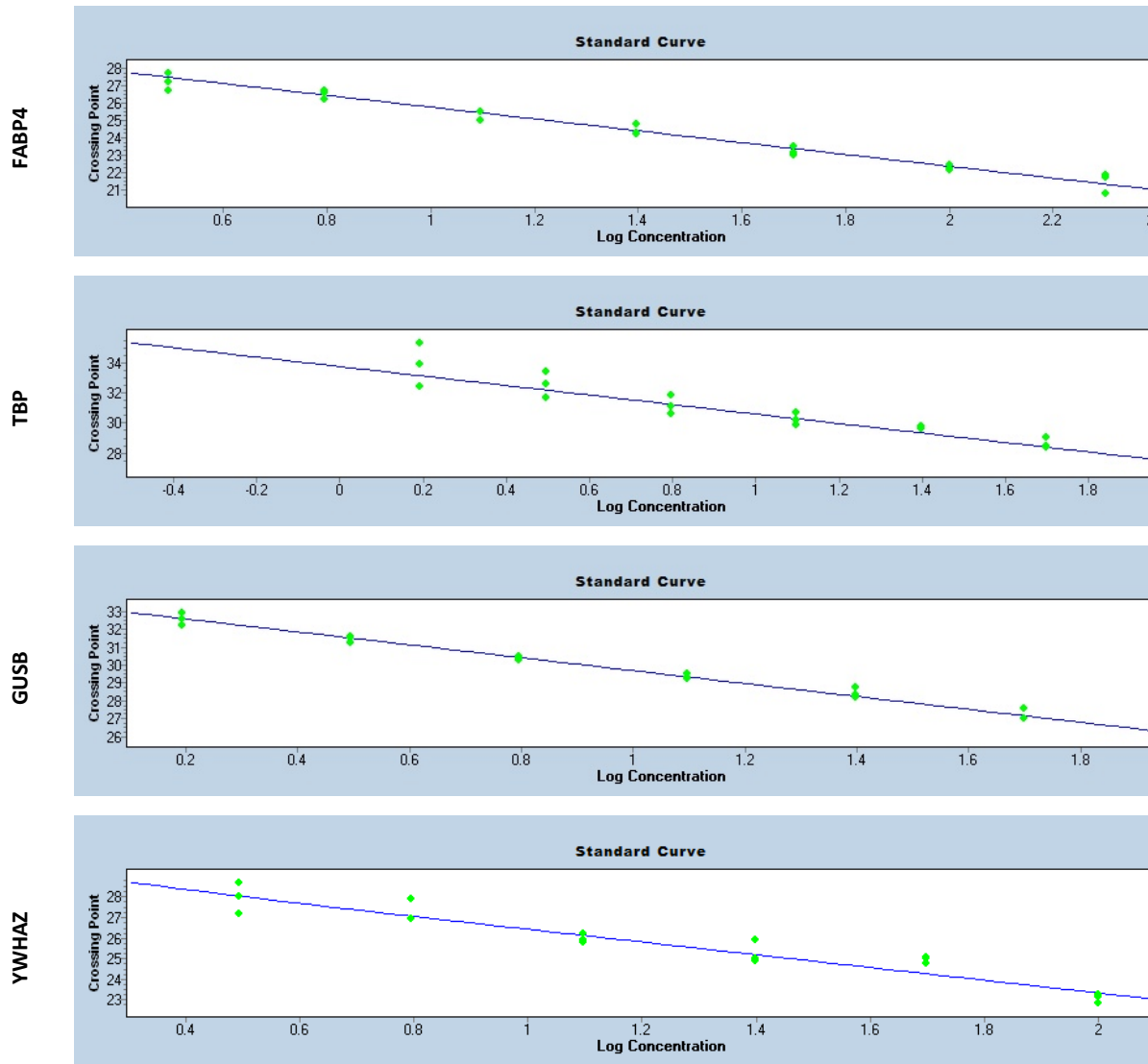
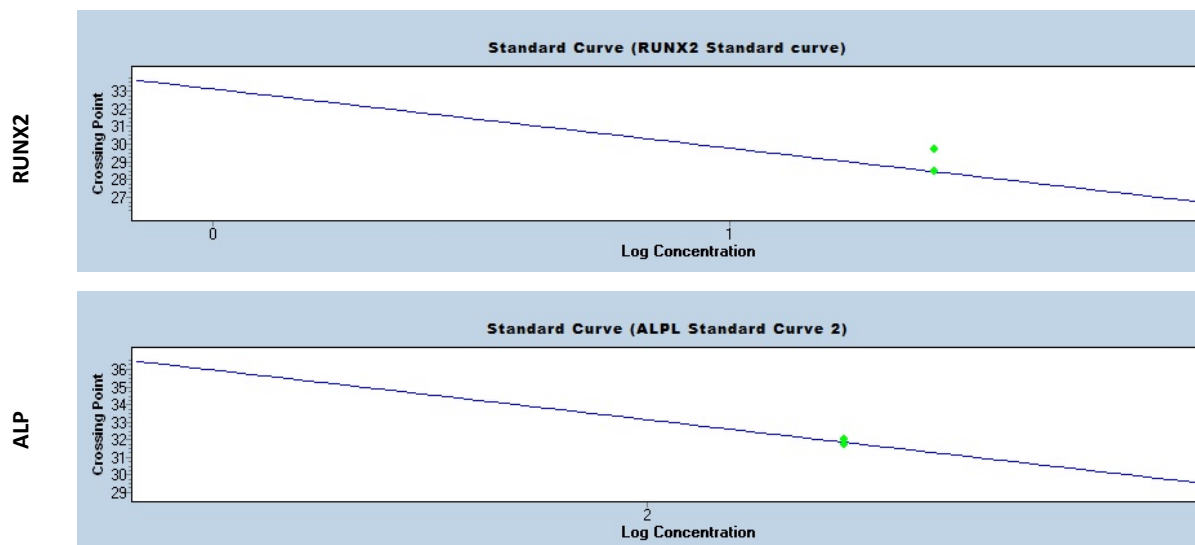
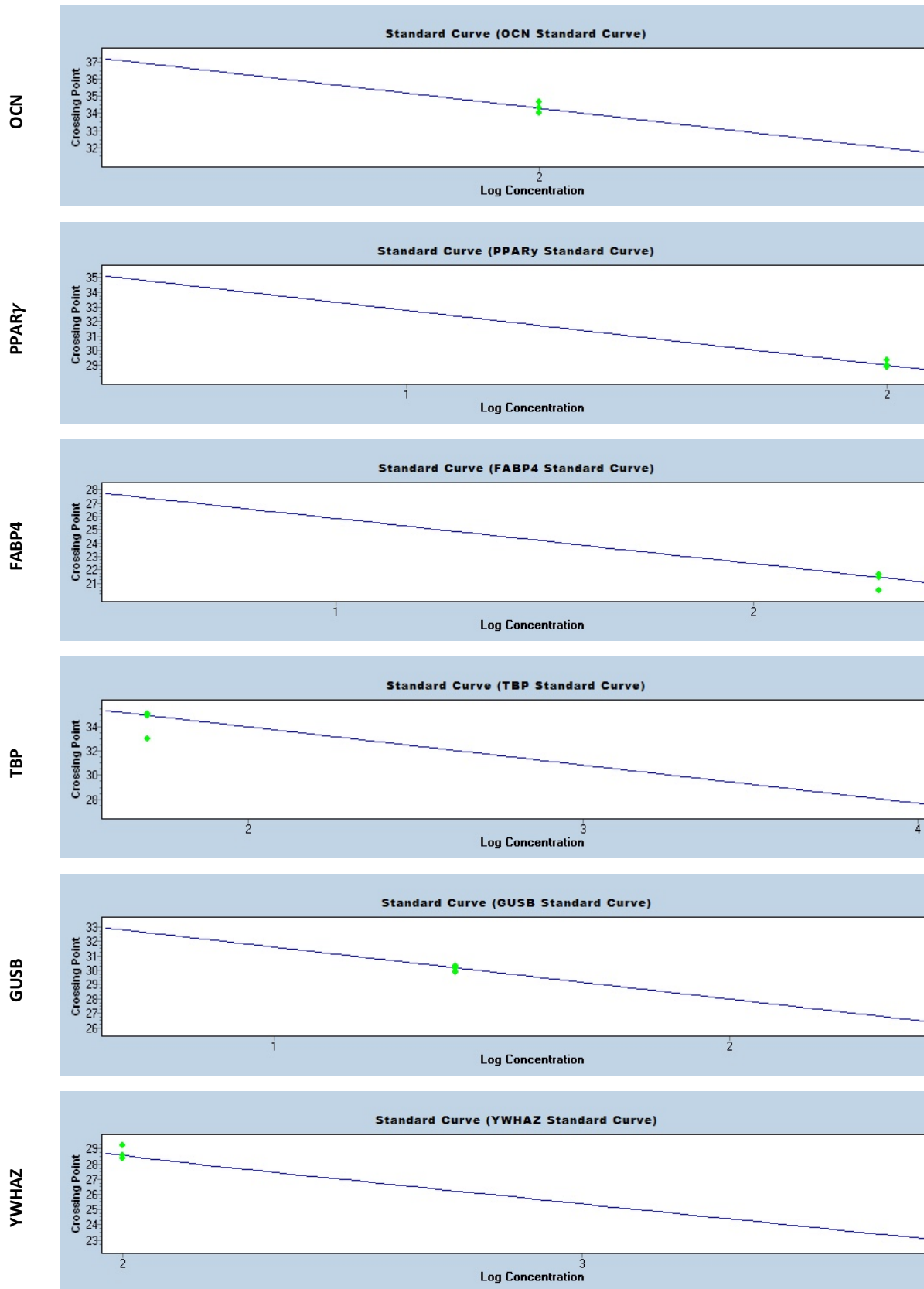


Figure G5. Standard curves for each target- and reference gene used in the study.

Standard curves were run to determine the efficiency of each primer pair which was then used to calculate the relative gene expression.





**Figure G6. Representative images of standards run on experimental plates plotted on original standard curves.**

Standards from standard curve experiments were run on each experimental plated to show that the conditions are comparable.

*Evidence for limit of detection*

Limit of detection was not performed.

*If multiplex, efficiency and LOD for each assay*

Multiplexing was not performed.

Data Analysis

*qPCR analysis program*

The LightCycler® Software (Version 1.5.1; Roche, Basel, Switzerland) was used to analyse data.

*Quantitation cycle (Cq) method determination*

The second derivative maximum method was used to determine the Cq-values (LightCycler® Software and algorithms).

*Outlier identification and disposition*

No outliers identified.

*Results of No Template Control (NTCs)*

The C<sub>q</sub>-values for the NTCs were ND (Not-detected). If at least two technical replicates amplified, the plate was re-run.

*Justification of number and choice of reference genes*

Three reference genes were used in this study: TBP, GUSB and YWHAZ. Reference genes were analysed in representative samples to determine if their expression was up or downregulated (Table G12). There was a slight up-regulation of reference genes in Day 21 samples and thus reference genes were ran at two time points (Day 7 and day 21, and the average Ct values were used for downstream analysis).

**Table G12. Summary of Mean Cp for the 3 reference genes across multiple time points indicating suitability of reference genes**

Sample number	Sample name	Condition	Day	NI	TBP (A)		GUSB (B)		YWAZ (C)		ΔCt (A vs. B)	ΔCt (A vs. C)	ΔCt (B vs. C)
					MeanCp	STD Cp	MeanCp	STD Cp	MeanCp	STD Cp			
1	A150221-01A	FBS	0		25.7301935	0.13321461	22.9911711	0.03694415	19.5133999	0.04046452	2.73902246	6.21679362	3.47777116
8	A311019-02T	FBS	7	NI	26.1618342	0.20496412	22.7886815	0.14940181	20.6394519	0.8334067	3.37315264	5.5223823	2.14922966
9	A311019-02T	FBS	7	I	24.7524797	0.52026347	21.2989017	0.28546395	19.5298356	0.87795414	3.45357796	5.22264403	1.76906606
14	A311019-02T	FBS	14	NI	25.5428227	0.08383871	22.4163528	0.15774879	19.8025726	0.04947389	3.12646985	5.74025007	2.61378023
15	A311019-02T	FBS	14	I	25.2457346	0.5989449	22.5129817	0.0804652	19.1407104	0.41671256	2.73275289	6.10502411	3.37227122
16	A150221-01A	FBS	21	NI	25.4762427	0.25043689	23.6214432	0.06633348	19.2677901	0.35056378	1.85479948	6.20845255	4.35365307
17	A150221-01A	FBS	21	I	24.647768	0.26050731	22.7503425	0.13683559	19.0669968	0.11305974	1.89742553	5.5807712	3.68334568
66	A280621-01R	pHPL	0		24.9433464	0.7625542	21.8093377	0.06557392	18.6159384	0.18297832	3.13400869	6.32740795	3.19339927
67	A311019-01A	pHPL	7	NI	27.3693712	0.70211425	25.7907888	0.06182261	22.0165805	0.67089676	1.57858245	5.35279074	3.77420828
72	A280621-01R	pHPL	7	I	24.6398627	0.36116926	22.5519129	0.14659278	19.6811131	0.41730581	2.08794976	4.9587496	2.87079985
77	A280621-01R	pHPL	14	NI	25.7202892	0.2364826	22.2404961	0.27713398	20.3478067	0.33956075	3.47979305	5.3724825	1.89268945

78	A280621-01R	pHPL	14	I	28.2892619	0.47598923	24.5349091	0.02187088	22.2080893	0.83146506	3.75435286	6.08117258	2.32681971	
83	A280621-01R	pHPL	21	NI	25.8679535	0.59156378	22.0761217	0.03985987	20.0914738	0.31824935	3.79183179	5.7764797	1.98464791	
84	A280621-01R	pHPL	21	I	29.2341469	0.8339322	26.5818049	0.26923433	24.4489757	0.23185172	2.65234205	4.78517121	2.13282917	
22	A280621-01R	PRP1	0		25.0646633	0.58924321	22.3978087	0.10779837	20.9716363	0.86081448	2.66685465	4.093027	1.42617234	
25	A280621-01R	PRP1	7	NI	24.925458	0.25081028	21.990602	0.07668699	19.7252812	0.09146504	2.934856	5.20017683	2.26532083	
26	A280621-01R	PRP1	7	I	25.0183464	0.2206534	23.9150775	0.08871236	19.7149191	0.54995028	1.10326889	5.30342726	4.20015836	
33	A311019-01A	PRP1	14	NI	25.652697	0.28837344	22.5954613	0.1497299	19.9319249	0.28025968	3.05723564	5.72077209	2.66353646	
34	A311019-01A	PRP1	14	I	31.8194397	0.93762176	27.5801104	0.03933793	25.0572069	0.81758299	4.23932923	6.76223271	2.52290347	
39	A311019-01A	PRP1	21	NI	25.1595763	0.04432224	22.5512237	0.09980989	19.9637209	0.09027012	2.60835251	5.19585537	2.58750286	
38	A280621-01R	PRP1	21	I	29.9914351	0.25787105	28.0957536	0.21261168	24.6209301	0.20812838	1.89568147	5.37050503	3.47482356	
43	A280621-01R	PRP2	0		25.1896418	0.07030338	22.5794604	0.03036281	18.9461375	0.44245394	2.6101814	6.24350429	3.63332289	
47	A280621-01R	PRP2	7	I	25.7855549	0.39615927	25.8738085	0.0527923	23.3976151	0.39607713	0.08825361	2.38793983	2.47619343	
48	A311019-01A	PRP2	7	NI	24.5323074	0.81176826	22.0515089	0.09615275	21.4468802	1.70360059	2.48079852	3.08542719	0.60462868	
52	A280621-01R	PRP2	14	NI	25.0296279	0.80968614	21.4302131	0.18175516	19.2450481	0.65114304	3.59941483	5.78457985	2.18516502	
57	A311019-02T	PRP2	14	I	24.3529326	0.36207756	22.2966009	0.16768589	19.574852	0.13960382	2.05633173	4.77808057	2.72174885	
58	A280621-01R	PRP2	21	NI	24.7573118	0.16964675	21.0730821	0.16583025	20.9221226	0.22556542	3.68422969	3.83518914	0.15095945	
59	A280621-01R	PRP2	21	I	29.8169388	1.60456121	26.8032073	0.07515569	24.1829408	0.06210276	3.01373149	5.633998	2.62026651	
85	A280621-01R	PRP3	0		28.4344303	0.2018182	24.7347779	0.003018	22.095978	0.36642374	3.69965236	6.3384523	2.63879994	
90	A311019-01A	PRP3	7	NI	27.7735829	0.61430609	24.2482344	0.05801526	22.4569116	0.39787163	3.52534849	5.31667128	1.79132278	
89	A280621-01R	PRP3	7	I	26.0785008	0.16268396	24.0131933	0.16092657	21.6378247	0.85908451	2.06530754	4.44067611	2.37536857	
94	A280621-01R	PRP3	14	NI	29.8370575	4.45850831	32.8353864	0.18317373	28.8765006	0.55283858	2.99832887	0.96055685	3.95888572	
99	A311019-02T	PRP3	14	I	26.6371015	0.14023516	23.0765297	0.07634653	22.6938426	0.2068151	3.56057183	3.94325889	0.38268706	
100	A280621-01R	PRP3	21	NI	26.3938383	0.46115834	22.2266667	0.06506407	20.8610107	0.0530632	4.16717168	5.53282769	1.36565601	
101	A280621-01R	PRP3	21	I	35.3203699	2.07358424	27.8995102	0.04315052	29.3891953	2.10454755	7.42085969	5.93117459	1.4896851	
											<b>Mean</b>	2.94662347	5.17454014	2.48941767
											<b>SD</b>	1.18132357	1.19004992	1.01978418

### *Normalization method*

Samples were first normalized to day 0 samples and then the induced samples were normalised to non-induced samples using the comparative CT method (Section 2.10).

### *Number of biological repeats*

Three ASC biological replicates were investigated. For PRP samples, three donors were also investigated against three ASC biological replicates.

### *Number and stage (RT or qPCR) of technical repeats*

Three technical repeats were included on the qPCR plate using cDNA from the same sample.

### *Repeatability (Intra assay variability)*

A SD of  $\leq 1$  between the technical replicates was considered repeatable.

### *Statistics*

Please see section 2.11.